

Formation of Terrestrial Planets

Matthew S. Clement, André Izidoro , Sean N. Raymond & Rogerio Deienno

Abstract Our understanding of the process of terrestrial planet formation has grown markedly over the past 20 years, yet key questions remain. This review begins by first addressing the critical, earliest stage of dust coagulation and concentration. While classic studies revealed how objects that grow to \sim meter sizes are rapidly removed from protoplanetary disks via orbital decay (seemingly precluding growth to larger sizes), this chapter addresses how this is resolved in contemporary, streaming instability models that favor rapid planetesimal formation via gravitational collapse of solids in over-dense regions. Once formed, planetesimals grow into Mars-Earth-sized planetary embryos by a combination of pebble- and planetesimal accretion within the lifetime of the nebular disk. After the disk dissipates, these embryos typically experience a series of late giant impacts en route to attaining their final architectures. This review also highlights three different inner Solar System formation models that can match a number of empirical constraints, and also reviews ways that one or more might be ruled out in favor of another in the near future. These include (1) the Grand Tack, (2) the Early Instability and (3) Planet Formation from Rings. Additionally, this chapter discusses formation models for the closest known analogs to our own terrestrial planets: super-Earths and terrestrial exoplanets in systems also hosting gas giants. Finally, this review lays out a chain of events that

Matthew S. Clement

Johns Hopkins APL, 11100 Johns Hopkins Rd, Laurel, MD 20723, USA e-mail: matt.clement@jhuapl.edu

André Izidoro

Department of Earth, Environmental and Planetary Sciences, MS 126, Rice University, Houston, TX 77005, USA

Sean N. Raymond

Laboratoire d'Astrophysique de Bordeaux, Univ. Bordeaux, CNRS, B18N, allée Geoffroy Saint-Hilaire, 33615 Pessac, France

Rogerio Deienno

Southwest Research Institute, 1050 Walnut St. Suite 300, Boulder, CO 80302, USA

may explain why the Solar System looks different than more than 99% of exoplanet systems.

Introduction

Over the last three decades our understanding of the formation of terrestrial planets has grown markedly. While there is no universally accepted definition of a terrestrial planet, this class of worlds is commonly understood to include smaller (radii less than around ~ 1.25 times that of the Earth) planets made mostly of silicate rocks and metals (densities greater than ~ 0.75 times that of the Earth: [Luque and Pallé 2022](#); [Margot et al. 2024](#)). On the theoretical side, these advances were in large part catalyzed by interdisciplinary scientific efforts and technological advances (e.g., faster computers, better software). Technology has also been crucial in driving observational advances as well. Although this field necessarily started within the context of our Solar System, new observational and theoretical studies have provided a push toward a more general, broadly-applicable framework. While exoplanet science has undoubtedly revolutionized our knowledge of planet formation, the Solar System offers a fantastic wealth of well-characterised physical and chemical constraints that make it an unparalleled laboratory for refining and testing models of planet growth.

Radioactive dating and the determination of various Solar System bodies' chemical compositions have led to major advances. Constraints on the ages and compositions of different planets and small bodies directly connect with models of their origins and interiors. Improvements in computational capabilities – both in hardware and software – have enabled more sophisticated and realistic numerical simulations that model a range of chemical and physical processes across all stages of planet formation. Modern planet formation theories are developed, tested and refined through interdisciplinary efforts leveraging empirical studies, geophysical and cosmochemical analyses, and dynamical simulations. Yet the formation of the terrestrial planets remains a subject of intense debate. At least three different models can explain the origins of our own inner Solar System. Each model is based on different fundamental assumptions, left to be disentangled by future research.

Low-mass, potentially terrestrial exoplanets are a hot topic in astronomy. The discovery of such planets has been a major success of planet-finding missions such as Kepler ([Borucki et al. 2010a](#)) and TESS ([Ricker et al. 2015](#)). The search for exo-terrestrial planets is especially exciting because they are potential candidates for hosting life as we know it. To date more than 5,700 exoplanets have been confirmed in over 4,000 different systems. However, these observations have elucidated how the majority of planetary systems have dynamical architectures that are strikingly different from our own. Gas giant exoplanets are relatively rare (occurring in $\lesssim 10\%$ of systems, depending on spectral type: [Petigura et al. 2018](#); [Gan et al. 2023](#); [Belezny and Kunimoto 2022](#); [Bryant et al. 2023](#)). Moreover, they are often observed on orbits very different from those of Jupiter and Saturn; either very close to their central stars or on extremely eccentric orbits (e.g. [Butler et al. 2006a](#); [Udry](#)

and Santos 2007a). Compact systems of hot super-Earths and sub-Neptunes – with sizes between 1 and 4 Earth radii; or masses between 1 and 20 Earth mass – are systematically found orbiting their stars on orbits much smaller than that of Mercury (Howard et al. 2010a; Mayor et al. 2011a). While this class of planet seems to be present around the majority of main sequence stars (e.g. Howard et al. 2012a; Fressin et al. 2013a; Petigura et al. 2013a; Chiang and Laughlin 2013; Zhu et al. 2018), no such planet exists in our inner Solar System. Given that most exoplanet systems look dramatically different than our own, it is not immediately obvious whether or not we expect those planets to have formed in the manner as our own terrestrial planets, or by completely different processes.

This article reviews terrestrial planet formation in the Solar System and around other stars. It discusses the dynamical processes that shaped the inner Solar System and expands on different formation pathways that can explain the orbital architectures of exoplanet systems. Moreover, it presents a path toward understanding how our Solar System fits in the larger context of exoplanets, and how exoplanets themselves can be used to improve our understanding of our own Solar System.

Any successful model of Solar System formation must explain why Mars and Mercury are so much smaller than the neighboring Earth and Venus. Indeed, neighboring exoplanets tend to have very similar masses and radii (Millholland et al. 2017). Additionally, the asteroid belt’s striking low mass and dynamically excited state presents a key constraint for terrestrial planet formation models. This review focuses on three well-tested models that are able to consistently explain each of these peculiar inner Solar System traits. Likewise, any successful model for the formation of super-Earths must match the observed distributions of exoplanet masses and orbital periods. This chapter also discusses the relationships between super-Earths and true ‘terrestrial planets’, and present formation models that demonstrate how the origins of the two classes of systems are likely far different than one might expect based solely on their observed sizes.

The early stages of planet formation

Planet formation starts during star formation. Protostars begin to take shape when the densest parts of a molecular cloud of gas and dust collapses under self-gravity (Shu et al. 1987; McKee and Ostriker 2007; André et al. 2014). Conservation of angular momentum turns the surrounding clump around the forming star into a circumstellar disk, the birthplace of planets (e.g. Safronov 1972). The primary empirical evidence that planets form in this manner comes from the geometry of our Solar System. The planets’ orbits are almost perfectly coplanar and orbit the Sun in a common direction. The youngest protoplanetary disks are made up of around 99% gas and 1% dust grains or ice particles (as is the case for the interstellar medium, e.g. Williams and Cieza 2011; Bae et al. 2023). Despite the two orders of magnitude difference in abundance between these two constituents, until recently little was known about the gas component as it is much harder to observe than the dust

since different gas species emit at specific wavelengths that require very high resolution spectroscopy to resolve (Najita et al. 2007; Williams and Cieza 2011; Dutrey et al. 2004; Öberg et al. 2021). For decades, the gas’s solid counterpart has been used quite successfully as a disk tracer. Infrared and submillimeter observations of dust emission, in addition to optical/near-IR scattered light imagery with coronagraphs have helped constrain the distribution of dust in rotating, pressure supported disk-like structures (e.g. Smith and Terrile 1984; Beckwith et al. 1990; O’dell and Wen 1994; Holland et al. 1998; Koerner et al. 1998; Schneider et al. 1999). Large far-infrared excesses have also been used to quantify how the thicknesses of disks increase radially (also referred to as “flaring:” Kenyon and Hartmann 1987). Recent ALMA observations have provided an unprecedented level of insight into planet forming-disks around young stars by revealing series of carved ring-type structures (van der Marel et al. 2013; Isella et al. 2013; ALMA Partnership et al. 2015; Nomura et al. 2016; Fedele et al. 2017). These features have been interpreted as signposts of planet formation in action (Dong et al. 2015; Bae et al. 2019), or dust responding to the gas via drag redistribution (e.g. Takeuchi and Artymowicz 2001; Flock et al. 2015). In contrast, molecular line emissions provides the best, and sometimes only, insight into the density, chemistry, temperature, and kinematics of the gas (e.g. Piétu et al. 2007; Qi et al. 2011). State of the art studies using ALMA are currently only capable of resolving emission lines at tens of milliarcsecond-scales, and probing the gas disk properties at regions as close as $\gtrsim 5 - 10$ au from the central star (e.g. Andrews 2020; Öberg et al. 2021).

The mass-loss rate, thermal structure and lifetime of the disk all represent key inputs and constraints for planet formation models. Observationally derived limits on these parameters are thus extremely valuable. Thermal constraints, for example, can be teased out from the fact that dust grains re-radiate stellar photons at different wavelengths depending on their temperature (e.g. Williams and Cieza 2011).

Solids orbit their central star at the nominal Keplerian speed. Contrarily gases orbit at a slightly sub-Keplerian velocity because a radial gas pressure gradient partially supports protoplanetary disks against the central star’s gravity. While the dust and gas components are well-mixed at the onset of disk formation, after just a short amount of time stellar gravity tends to force dust grains to settle into the disk mid-plane (e.g. Weidenschilling 1980; Nakagawa et al. 1986). Observations and simulations also suggest that the disk itself is in a constant state of infall towards the central stars as a consequence of radial angular momentum transport (e.g. Papaloizou and Lin 1995; Balbus 2003; Dullemond et al. 2007; Armitage 2011). As the disk loses mass onto the central star through this process (and also through photo-evaporation by ultraviolet and X-ray radiation Gorti and Hollenbach 2009), it eventually transitions from optically thick to optically thin (Alexander et al. 2014). Infra-red surveys of star-forming clusters have also been leveraged to place constraints on disk lifetimes (Haisch et al. 2001; Hernández et al. 2007; Mamajek 2009). Consistent with magnetospheric accretion models and stellar spectroscopy of gas accretion (Hillenbrand 2008), these surveys tend to conclude that the hot/inner parts of the disk do not live much longer than 10 Myr. The lifetimes of protoplanetary disks is a fundamental constraint on planet formation.

Within the framework of disk formation, evolution and eventual dissipation described above, it is convenient to divide planet formation into a series of key independent steps. Indeed, different physical and chemical processes are at play at different stages of planetary growth. For example, while the growth of micrometer-sized dust grains is driven by forces at the intermolecular level, the growth of \gtrsim km-sized bodies is dominated by gravity. In addition, the sheer number of dust particles involved in the planet formation process makes it impossible to use a single numerical simulation to study all phases of growth at all locations in the disk simultaneously. Therefore, most studies tend to focus on a specific stage of the process. The following sections briefly address each of these stages independently.

From dust to pebbles

The solids available for planet formation are not uniformly distributed across a planet-forming disk. At any given radius, only species with condensation/sublimation temperatures below the local temperature can exist as solids (Grossman and Larimer 1974). A condensation or sublimation front is a point in the disk, inside of which a given element or molecule can only be found in its gaseous form. In planet formation models, the most commonly invoked fronts are the water snowline, the CO snowline and the silicate sublimation front (e.g. Morbidelli et al. 2016, 2021; Izidoro et al. 2022a). Of course, as the disk cools, the locations of different condensation fronts sweep inward over time (e.g. Lecar et al. 2006; Dodson-Robinson et al. 2009; Hasegawa and Pudritz 2011; Martin and Livio 2012). As a result of condensation and sublimation, iron and silicates are abundant in the inner regions of the disk, while the outer regions are rich in ice and other volatiles (Lodders 2003).

The first stage of planet formation involves the growth of millimeter and cm-sized dust aggregates from micrometer-sized dust and ice particles (e.g. Lissauer 1993). This view is well supported by disk observations and analyses of chondritic meteorites. Indeed, observations of young stellar objects at millimeter and centimeter wavelengths detect dust grains at these size ranges (Testi et al. 2003; Wilner et al. 2005; Rodmann et al. 2006; Brauer et al. 2007; Natta et al. 2007; Ricci et al. 2010; Testi et al. 2014; Ansdell et al. 2017), and wave polarization in these observations has been interpreted to suggest that dust aggregates are relatively compact (Tazaki et al. 2019; Kirchschrager et al. 2019; Brunngräber and Wolf 2021). Likewise, primitive meteorites are mainly composed of millimeter-sized silicate spheres known as chondrules (Shu et al. 2001; Scott 2007) that are cemented together within a fine-grained matrix of calcium aluminum rich inclusions (CAIs), unprocessed interstellar grains and primitive organics (Scott and Taylor 1983; Scott and Krot 2014). Given a U-Pb chronometer-derived age estimate of 4.567 Gyr (Amelin et al. 2010; Connelly et al. 2012), CAIs are thought to have been the first solids to condense in the Sun's protoplanetary disk (e.g. Bouvier and Wadhwa 2010; Dauphas and Chaussidon 2011). Chondrule formation likely started around the same time CAIs were forming and continued for a few million years (Connelly et al. 2012). It is

also possible, that chondrules are actually the result of impact jets produced during planetesimal collisions (e.g. [Asphaug et al. 2011](#); [Johnson et al. 2015](#); [Wakita et al. 2017](#); [Lichtenberg et al. 2017](#)). However, most studies conclude that their properties are more consistent with being rapidly-heated aggregates of mm-sized silicate dust grains ([Desch and Connolly 2002](#); [Morris and Desch 2010](#)).

Laboratory experiments and numerical simulations also tend to conclude that the first stage of dust and ice growth is dominated by hit-and-stick collisions ([Blum and Wurm 2000](#); [Blum et al. 2000](#); [Poppe et al. 2000](#); [Güttler et al. 2010](#); [Testi et al. 2014](#)). In this early stage of accretion, Electrostatic charges, magnetic material effects ([Dominik and Nübold 2002](#); [Okuzumi 2009](#)) and adhesive van der Waals forces ([Heim et al. 1999](#); [Gundlach et al. 2011](#)) largely determine the probability that two dust particles will stick and stay joined together. Through these processes micrometer sized dust grains stick together and form larger fluffy porous aggregates ([Blum and Wurm 2008](#)), and are eventually compacted by collisions to mm or cm-sized grains ([Ormel et al. 2007](#); [Zsom et al. 2010](#); [Schräpler et al. 2022](#)). There is a general consensus that collisional growth of micrometer-sized dust grains is efficient up to mm to cm range in sufficiently dense regions of protoplanetary disks.

From pebbles to Planetesimals

Growth beyond cm-sized aggregates faces several obstacles (e.g. [Weidenschilling 1977](#); [Testi et al. 2014](#)). This subject is one of the most active current research areas in planet formation.

Numerical and laboratory experiments suggest that colliding mm and cm-sized dust grains do not grow up to meter and kilometer sized bodies ([Chokshi et al. 1993](#); [Dominik and Tielens 1997](#); [Gorti et al. 2015](#); [Krijt et al. 2016](#)). Depending on particles' sizes and impact velocities, colliding dust particles and/or aggregates may bounce off of each other instead of growing (e.g. [Wada et al. 2009](#)). This is known as the “bouncing barrier” (e.g. [Zsom et al. 2010](#); [Birnstiel et al. 2011](#); [Testi et al. 2014](#)). Because the orbital speed of nebular gas is slightly sub-Keplerian, solid particles on a Keplerian orbits essentially “feel” a headwind that can be described by a drag force ([Whipple 1972](#); [Adachi et al. 1976](#); [Weidenschilling 1977](#); [Haghighipour and Boss 2003](#)). This force causes their orbits to decay, and spiral inwards towards the central star in very short timescales. Only sufficiently small particles that are strongly coupled to the gas do not drift as consequence of this aerodynamic effect. In contrast, decimeter to meter-sized particles lie in a regime where they feel a very strong relative drag force, and spiral inwards much quicker than \gtrsim km-size objects. A 1-meter size object at ~ 1 AU in a typical disk falls toward the star in ~ 100 years (e.g. [Weidenschilling 1977](#)). The large differences in the radial speeds of inwardly migrating particles with disparate sizes thus result in high-speed collisions; leading to bouncing, fragmentation or erosion ([Krijt et al. 2015](#)) in non-turbulent disks. This problem is known as the drift-fragmentation “barrier”. In turbulent disks collisional

velocities are regulated by turbulence, which in turn determines the physical size of the fragmentation barrier (Ormel and Cuzzi 2007).

The most likely way that nature overcomes these barriers and produces macroscopic solid bodies is by bypassing the critical size for rapid particle drift and directly forming planetesimals via gravitational collapse (Goldreich and Ward 1973; Youdin and Shu 2002; Johansen et al. 2014; Lesur et al. 2023). In order for mm or cm size particles to collapse they must be highly concentrated in a particular region of the disk. As discussed previously, dust particles are expected to sediment towards the disk mid-plane. However, the collapse of a dense mid-plane layer is generally prevented by turbulent diffusion (Weidenschilling 1980; Cuzzi et al. 2008a; Johansen et al. 2009). Different mechanisms have been proposed to operate with efficiencies sufficient to concentrate particles in local regions of the gas disk and trigger direct collapse (see for example: Balbus and Hawley 1991; Kretke and Lin 2007; Lyra et al. 2008b; Brauer et al. 2008; Lyra et al. 2008a, 2009; Chambers 2010; Drazkowska et al. 2013; Squire and Hopkins 2017; Lichtenberg et al. 2021; Morbidelli et al. 2021; Izidoro et al. 2022a).

Turbulent motion of the gas can also concentrate particles in rotating substructures within the disk known as eddies (Cuzzi and Weidenschilling 2006; Chambers 2010). Instabilities such as the vertical shear instability (Nelson et al. 2013; Lin and Youdin 2015; Barker and Latter 2015; Umurhan et al. 2016) and the baroclinic instability (Lyra and Klahr 2011; Raettig et al. 2013; Barge et al. 2016; Stoll and Kley 2016) are also potential candidates for creating overly dense regions in the disk (Johansen and Lambrechts 2017). Similarly, localized high pressure regions (pressure bumps: Weidenschilling 1980; Guilera et al. 2020; Chambers 2021) can trap and concentrate drifting particles and accelerate those in the vicinity of positive pressure gradients towards super Keplerian speeds. Through this process, inward drifting particles slow down, halt, or even begin to migrate outward depending on the steepness of the local pressure gradient (e.g. Haghighipour and Boss 2003). Pressure bumps have been proposed to be consistent with high-resolution disk observations (Andrews et al. 2018; Dullemond et al. 2018), and may exist as the result of a sharp transition in the disc viscosity or due to tidal perturbations from a sufficiently large planet (for a more detailed discussion see reviews by Chiang and Youdin 2010; Johansen et al. 2014; Johansen and Lambrechts 2017). If the local density in solids increases by an order of magnitude at the pressure bump, the level of turbulence may be significantly counterbalanced, thus allowing for planetesimal formation by gravitational collapse (Youdin and Shu 2002). It is also possible for the local density of particles to be significantly increased via the delivery of slowly drifting small particles that are released as larger bodies fragment and sublime when they encounter hotter regions of the disk (Sirono 2011; Ida and Guillot 2016). This may well be the case for mm or cm-sized pebbles that form in the water and volatiles-rich outer regions of the disk and drift inwards. Similarly, if inward drifting pebbles cross the water-ice snowline, their water-content sublimates and small solid silicate/metal grains from within their interiors are released (Morbidelli et al. 2015a).

The back-reaction friction force between mm or cm-sized particles and the gas can also serve as a mechanism for aerodynamically concentrating particles (Youdin

and Goodman 2005). Because the gas is orbiting at a sub-Keplerian velocity, the back reaction of gas drag felt by a solid particle tends to accelerate the gas. If mm or cm-sized solid particles cluster sufficiently through this process, their collective back reaction becomes more pronounced. This allows individual particles from the outer regions of the disk drifting at nominal speeds to join a more slowly drifting cluster in the process of forming (Johansen and Youdin 2007). If the local dust/gas ratio subsequently meets the threshold for collapse, the cluster eventually shrinks and leads to the rapid formation of planetesimals. A more detailed physical explanation of the process can be found in Magnan et al. (2024). This process has been demonstrated to successfully form planetesimals with sizes ranging from ~ 1 to ~ 1000 Km (Johansen et al. 2007; Bai and Stone 2010; Simon et al. 2016; Schäfer et al. 2017; Carrera et al. 2017; Yang and Zhu 2021), and is typically referred to as the “streaming instability”. Streaming instabilities may be preferentially triggered outside the disk snowline where sticky ice particles form (Drazkowska and Dullemond 2014; Armitage et al. 2016a; Drazkowska and Alibert 2017). Although many questions remain (see chapters by Klahr and Armitage), this scenario represents the current consensus model for planetesimal formation.

From planetesimals to planetary embryos

Mutual gravitational interactions between large bodies plays an increasingly significant role as planetesimals continue to grow past the ~ 1 -100 km size range. At this stage planetesimals can grow larger by colliding and merging with other planetesimals, or by accreting the remaining mm or cm-sized grains in the gas disk.

Planetesimal-planetesimal growth:

Let us assume that there exists a population of planetesimals with N members and total mass Nm at 1 AU. These planetesimals have formed by a combination of the mechanisms described above, and are still embedded in the gaseous protoplanetary disk. The initial masses and physical radii of individual planetesimals are denoted m and R , respectively. This population of planetesimals will evolve through a series of collisions and gravitational scattering events. Close encounters between planetesimals increase their random velocities by increasing their orbital inclinations and eccentricities. The random velocity v_{rnd} represents the deviation of the planetesimal’s velocity from that of the Keplerian circular and planar orbit at its location:

$$v_{rnd} = \left(\frac{5}{8}e^2 + i^2\right)^{1/2}v_k, \quad (1)$$

where e and i are the planetesimal’s orbital eccentricities and inclinations (Safronov 1972; Greenberg et al. 1991). $v_k = \sqrt{\frac{GM_\odot}{r}}$ is the planetesimal’s Keplerian velocity,

where G is the gravitational constant, M_\odot is the mass of the central star, and r is the planetesimal's orbital radius.

Planetesimal growth rates are largely governed by their relative velocity with respect to one another. Of greatest importance are their random velocities, as well as the differential shear across the Hill radii of interacting bodies. The Hill radius R_H of a planetesimal orbiting a star with mass M_\odot is defined as

$$R_H = a \left(\frac{m}{3M_\odot} \right)^{1/3}, \quad (2)$$

where a and m are the planetesimal's semi-major axis and mass, respectively.

Gravitational scattering events between planetesimals are in the shear-dominated regime when $v_{rnd} < R_H \Omega$, and in the dispersion-dominated regime when $v_{rnd} > R_H \Omega$, where Ω is the local Keplerian frequency. In the shear-dominated regime, planetesimals spend a significant amount of time in close proximity to one another during a close encounter. In this case, their orbits can be gravitationally deflected fairly significantly such that their trajectories are “focused” towards each other. This increases the probability of a collision occurring, thus speeding up their growth. In the dispersion-dominated regime, however, interacting planetesimals spend much less time close to each other because of their high relative speeds. Therefore, gravitational focusing is less efficient, collisional probabilities decrease, and accretion timescales increase.

A number of dissipative effects also conspire to damp the random velocities of planetesimals. Among others, these include physical collisions (Goldreich and Tremaine 1978), gas drag (Adachi et al. 1976) and gas dynamical friction (Grishin and Perets 2015). The balance between processes that have tend to excite and those that damp orbits changes over time as the disk dissipates and planetesimals grow.

Characteristic 1-100 km-size planetesimals (Morbidelli et al. 2009a; Johansen et al. 2012b; Delbo' et al. 2017) accrete other large bodies and become Moon-Mars-mass planetary embryos and eventually planets in three different growth regimes. In the “runaway growth” regime, an initial generation of planet embryos form as the result of the fact that larger planetesimals grow faster than smaller ones. In the “orderly growth” regime large embryos grow at roughly the same rate, eventually forming planets. The “oligarchic growth” regime is an intermediate growth regime between these two scenarios.

One can write the accretion rate of a planetesimal with mass m as (Safronov 1972; Ida and Nakazawa 1989; Greenzweig and Lissauer 1990; Rafikov 2003c)

$$\frac{dm}{dt} \simeq \pi R^2 \Omega \Sigma \frac{v_{rnd}}{v_{rnd,z}} \left(1 + \frac{2Gm}{Rv_{rnd}^2} \right), \quad (3)$$

where R is the planetesimal's physical radius, Ω is its Keplerian frequency, Σ is the local planetesimal surface density, and $v_{rnd,z} \neq 0$ is the averaged planetesimal velocity's vertical component. The term $\frac{2Gm}{Rv_{rnd}^2}$ accounts for gravitational focusing and is simply the ratio of the escape velocity from the planetesimal surface to the

relative velocity of the interacting planetesimals squared. $\Sigma \approx N\bar{m}H$ quantifies the disk's vertical thickness (here N is the surface number density of planetesimals, \bar{m} is the average mass of planetesimals and $H \approx v_{rnd,z}/\Omega$). Note, however, that Eq. 3 neglects bouncing, fragmentation or erosion during collisions.

A phenomena often referred to as “dynamical friction” plays a crucial role in during the early phases of planetesimal accretion. As a result of angular momentum transfer during close-encounters with smaller bodies, the largest planetesimals in a given region of the disk tend to have their orbital eccentricities and inclinations damped. Through this process, their random velocities decrease; thus further increasing the rate at which they can accrete material through gravitational focusing. If (1) gravitational focusing is large (or planetesimal are small); (2) planetesimals' random velocities are roughly independent of their masses (v_{rnd} and $v_{rnd,z}$); and (3) growth does not strongly affect the surface density of planetesimals, Equation 3 may be simplified as (Wetherill and Stewart 1989; Kokubo and Ida 1996):

$$\frac{1}{m} \frac{dm}{dt} \approx t_{grow,run} \approx \Sigma \frac{1}{v_{rnd,z}} \frac{m^{1/3}}{v_{rnd}} \propto m^{1/3}. \quad (4)$$

In this regime the accretion rate of the most massive planetesimals tends to increase with time. This is the so called “runaway growth” regime of planetesimal accretion.

An initial population of planetary embryos is the result of runaway accretion (Kokubo and Ida 1996; Ormel et al. 2010b). At some point, gravitational perturbations between the emerging embryos have a larger effect on their dynamical evolution than interactions with smaller planetesimals, and their growth regime changes. The presence of sufficiently massive embryos increases the random velocities of planetesimals and significantly alters their local surface density (Tanaka and Ida 1997). Thus, the local velocity dispersion depends strongly on the mass of the largest embryo. As a result, the growth rate takes the form (Wetherill and Stewart 1989; Kokubo and Ida 1998):

$$\frac{1}{m} \frac{dm}{dt} \approx t_{grow,ol} \propto \Sigma \frac{1}{v_{rnd,z}} \frac{m^{-1/3}}{v_{rnd}} \propto m^{-1/3} \quad (5)$$

This so-called “Oligarchic” growth rate depends on the scaling of Σ , v_{rnd} and $v_{rnd,z}$ (Rafikov 2003c). In this regime, planetary embryos still grow faster than planetesimals, however, small planetary embryos can grow faster than larger ones. The growth of oligarchs is further accelerated in the vicinity of MMRs as a result of planetesimals concentrating and growing rapidly to intermediate masses in nearby first order resonances (Wallace and Quinn 2019; Wallace et al. 2021). According to (Ida and Makino 1993) the transition between the runaway and oligarchic regimes occurs when embryo masses are only a small fraction (a percent or so) of the total mass carried by the planetesimal population (but see Ormel et al. 2010a, for a different criterion).

The ultimate result of the oligarchic phase is a bi-modal population of planetary embryos and planetesimals. At this phase, the total mass in embryos is still much smaller than the total mass in planetesimals. Planetary embryos growing in the thick

sea of planetesimals are typically separated from one another by 5-10 mutual Hill radii (Kokubo and Ida 1995, 1998, 2000; Ormel et al. 2010b), where the mutual Hill radius of two embryos with masses m_i and m_j and semi-major axes a_i and a_j is defined as

$$R_{H,i,j} = \frac{a_i + a_j}{2} \left(\frac{m_i + m_j}{3M_\odot} \right)^{1/3}. \quad (6)$$

If the spacing between neighboring embryos decreases to less than a few mutual Hill radii, they scatter off of each other, thus bringing their orbital separation back to closer to $\sim 5R_{H,i,j}$. After embryo-embryo scattering events, dynamical friction (or gas drag) tends to re-circularize their orbits and damp their orbital inclinations provided that there is a sufficient quantity of mass in planetesimals or gas in the embryo's vicinity.

Figure 1 shows the growth of planetesimals and embryos during the oligarchic growth regime (Ormel et al. 2010b). Three snapshots in the system's evolution are shown. The particles are modeled using a Monte Carlo method that computes the collisional and dynamical evolution of the system (Ormel et al. 2010b), and tracer particles to represent the much larger swarm of small planetesimals. After 0.18 Myr, two prominent planetary embryos with radii larger than 1000 km emerge with a mutual separation of a few Hill radii.

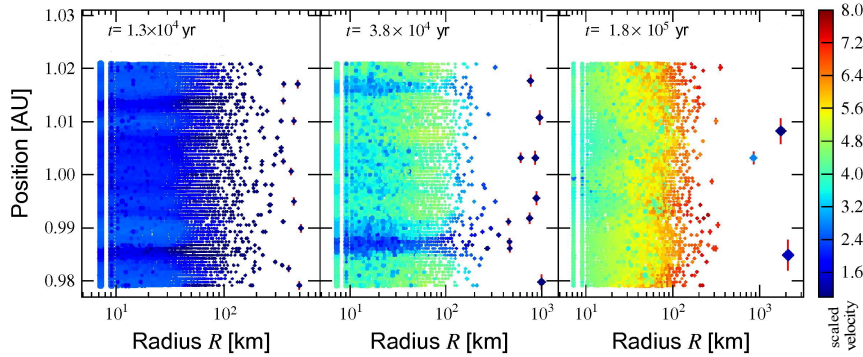


Fig. 1 Planetesimal and embryo growth in the oligarchic regime. Dots represent swarms of planetesimals which are simulated as single entity. The dot size scales with the total mass of the swarm. Individual large bodies are denoted with diamonds. The different colors represent the scaled random velocities of the bodies. The red bar intercepting the largest bodies in the system represents the respective size of their Hill radius. Figure adapted from (Ormel et al. 2010b)

Pebble Accretion: from planetesimals to planets

If planetesimals form early they may accrete dust grains and aggregates drifting inward within the disk towards the central star. The existence of such grains in planet-forming disks has been observationally confirmed (e.g. Testi et al. 2014). The accre-

tion of mm or cm-sized grains by a more massive body is commonly referred to as “pebble accretion” (Johansen and Lacerda 2010; Ormel and Klahr 2010; Lambrechts and Johansen 2012a; Morbidelli and Nesvorny 2012; Johansen et al. 2015; Xu et al. 2017).

Given appropriate conditions within the gas disk, pebble accretion can be much faster than planetesimal accretion. This may solve multiple long-standing problems, especially ones related to the formation of exoplanets and the solar system’s giant planets (for a recent review see Drazkowska et al. 2023, and references therein). In the classic, “core accretion” scenario for giant planet formation, gas giants form when their cores reach the threshold for runaway gas accretion ($\sim 10M_{\oplus}$, Mizuno 1980; Pollack et al. 1996). While this model axiomatically requires a core to form before the gaseous disk disperses, it is unclear whether the process of planetesimal accretion alone is sufficient to grow the cores of Jupiter or Saturn within a typical disk lifetime (e.g. Thommes et al. 2003; Levison et al. 2010, see also chapter by Youdin).

As discussed earlier in this chapter, millimeter- to centimeter-sized pebbles orbiting in gas disks rapidly spiral inwards due to gas drag (Adachi et al. 1976; Johansen et al. 2015). The dynamical behavior of a single drifting pebble approaching a planetesimal from a more distant orbit is determined by a competition between gas drag and its gravitational interactions with the larger body. Assuming that the planetesimal is sufficiently small such that it does not disturb the background gas disk structure (e.g. gas disk velocity and density), two end states are possible. The pebble may either cross the planetesimal orbit without being accreted, or its original orbit can be sufficiently deflected to allow for accretion.

pebble accretion can allow embryos and proto-planets to grow rapidly. However, planetesimals (or even planetary embryos) cannot grow indefinitely, even if the pebble flux is high. As an embryo grows, it gravitationally perturbs the structure of the gaseous disk. Eventually, the growing body opens a shallow gap in disk and creates a local pressure bump outside of its orbit. If the pressure bump is large enough, particles entering the bump are accelerated by the concentrated gas and stop drifting inwards. At the “Pebble isolation mass,” M_{iso} , an embryo or planet stops accreting pebbles,

$$M_{iso} = 20 \left(\frac{H_{gas}/a_p}{0.05} \right)^3 M_{\oplus}, \quad (7)$$

where H_{gas} is the gas disk scale height (Lambrechts et al. 2014; Morbidelli and Nesvorny 2012). It is worth noting that several studies have proposed that pebbles may be partially or even fully evaporated/destroyed before they can reach the accreting core. This effect may become important before the core reaches isolation mass (Alibert 2017; Brouwers et al. 2017). Further study is needed to understand exactly how this effect limits embryo growth by pebble accretion.

From planetary embryos to planets

The final stage of terrestrial planet growth is thought to occur after the protoplanetary disk’s gas dissipates; thus removing the dissipative mechanisms of gas drag and gas dynamical friction. In such an environment, gravitational focusing becomes negligible, and accretion timescales increase precipitously. Given that $v_{rnd} \approx v_{rnd,z}$ (Rafikov 2003c) Eq 3 takes the form

$$\frac{1}{m} \frac{dm}{dt} \approx t_{grow,ord} \approx \Sigma \frac{v_{rnd}}{v_{rnd,z}} m^{-1/3} \approx \Sigma m^{-1/3} \quad (8)$$

In this growth regime – termed “orderly growth” or “late stage accretion” – Σ decreases markedly with time as massive embryos accrete or scatter nearby planetesimals and open large gaps in the disk (Tanaka and Ida 1997). This stage is marked by violent giant collisions between planetary embryos, power scattering events, and ejections of macroscopic bodies. Therefore, the system’s evolution is chaotic, and the total planetesimal population decreases drastically. Assuming that 50% of the total mass in planetesimals is carried by embryos (Kenyon and Bromley 2006), the mass of an embryo at the start of orderly growth is $M_{ord} = \int_{r-\Delta r/2}^{r+\Delta r/2} 2\pi r' \Sigma(r') / 2 dr' \simeq \pi r \Delta r \Sigma$, where Δr corresponds to the width of the feeding zone of the embryo and r is the planetary embryo’s heliocentric distance (Lissauer 1987). The size of the feeding zone of an embryo typically ranges between a few to $10R_H$.

Methods and Numerical tools

A number of techniques are utilized to constrain the nature of the initial planetesimal population in the inner Solar System (i.e. its chemical, radial mass and size frequency distributions). Two and three dimensional hydrodynamical calculations including self-gravity are ubiquitously used in computational studies of the streaming instability (Youdin and Goodman 2005; Johansen and Youdin 2007; Johansen et al. 2009; Bai and Stone 2010; Johansen et al. 2012b; Simon et al. 2016). The results of these models are then parameterized, and utilized in one dimensional alpha disk models that track dust growth, disk chemistry and planetesimal formation with the aim of extracting the authentic state of the terrestrial disk around the onset of runaway growth (Birnstiel et al. 2016; Drazkowska and Dullemond 2018; Charnoz et al. 2019; Appalgren et al. 2020; Lichtenberg et al. 2021; Morbidelli et al. 2021; Izidoro et al. 2022a).

Embryo and Planetesimal accretion

Studies of the runaway and oligarchic regimes take a wide range of forms and leverage a range of computational methodologies. These includes N-body simulations (Ida and Makino 1993; Aarseth et al. 1993; Kokubo and Ida 1996, 1998, 2000; Richardson et al. 2000; Thommes et al. 2003; Barnes et al. 2009; Clement et al. 2020a; Woo et al. 2021a), analytical/semi-analytical calculations based on statistical algorithms (Greenberg et al. 1978; Wetherill and Stewart 1989; Rafikov 2003c,b,a; Goldreich et al. 2004; Kenyon and Bromley 2004; Ida and Lin 2004; Chambers 2006; Morbidelli et al. 2009a; Schlichting and Sari 2011; Schlichting et al. 2013), hybrid statistical/N-body (or N-body coagulation) codes which incorporates the two latter approaches (Spaute et al. 1991; Weidenschilling et al. 1997; Ormel et al. 2010b; Bromley and Kenyon 2011; Glaschke et al. 2014), and finally the more recently developed hybrid particle-based algorithms (Levison et al. 2012; Morishima 2015, 2017). Each tool is most optimized for modeling different specific stages of planet formation. While studies of the earlier epochs of planet formation are mostly conducted using analytical and statistical tools, the intermediate and late stages of accretion typically leverage direct N-body integrators (Lecar and Aarseth 1986; Beauge and Aarseth 1990; Chambers 2001; Kominami and Ida 2004; Raymond et al. 2009).

Statistical or semi-analytical coagulation studies model the dynamics and collisions of planetesimals in a “particle-in-a-box approximation” (Greenberg et al. 1978). This method is based on the kinetic theory of gases. It uses distribution functions to describe planetesimal orbits, and thus neglects the individual nature of the particles. This approach is routinely used to model the early stages of planet formation when the number of planetary objects is large ($\gg 10^4$). While these types of calculations give a statistical sense of the dynamics of a large population of gravitationally interacting objects, they also invoke a series of approximations which are only valid at local length scales in the protoplanetary disk (Goldreich et al. 2004). The necessity of including non-gravitational effects and collisional evolution typically leads to approaches that are not self-consistent (Leinhardt 2008).

For most applications, direct N-body numerical simulations tend to be more flexible and precise than coagulation approaches. Until recently, N-body codes could not handle more than a few thousand self-interacting bodies for long integration times (e.g. $\sim 10^8 - 10^9$ yr) without prohibitively long computational times. However, recent advances in parallel computing have made calculations as many as 10^6 particles computationally tractable (Grimm and Stadel 2014; Menon et al. 2015; Lau and Lee 2023). There are several numerical N-body integration packages available to model planetary formation and dynamics such as Mercury (Chambers 1999), Symba (Duncan et al. 1998), Rebound (Rein and Tamayo 2015; Rein and Spiegel 2015; Tamayo et al. 2020), GENGA (Grimm and Stadel 2014; Grimm et al. 2022) and PKDGRAV (Stadel 2001). Among them, Mercury and Symba are arguably the most widely used in the terrestrial planet formation literature. These codes are built on symplectic algorithms which divide the problem’s full Hamiltonian into a component describing the Keplerian motion, and a second Hamiltonian that carries all of

the terms that arise from the mutual gravitational interactions between bodies in the system (Wisdom and Holman 1991). This approach is advantageous when applied to systems where most of the total mass is carried by a single body, and they can facilitate long-term numerical integrations without the propagation and accumulation of errors (Saha and Tremaine 1994; Hernandez and Dehnen 2017; Rein et al. 2019).

Another way to simulate a system with a large number of particles is by combining direct N-body integration with super-particle approximation (Levison et al. 2012; Morishima 2015). In this approach, a large number of small particles (planetesimals) are represented by a small number of tracer particles. The tracers interact with the larger bodies through an N-body scheme. Tracer-tracer interactions (i.e., interactions among a large number of massive planetesimals represented by the tracer particles) are solved using statistical routines modelling stirring, dynamical friction and collisional evolution. The LIPAD code (Levison et al. 2012) has been used, for example, to model the formation of terrestrial planets in the Solar System from a larger number of planetesimals (Walsh and Levison 2016, 2019; Deienno et al. 2019) and also in simulations that include pebble accretion (e.g. Levison et al. 2015b).

Late stage accretion of terrestrial planets in the Solar System

This section reviews models of the late stage accretion of terrestrial planets in our own Solar System. The first series of subsections discuss the constraints on these models, and the latter subsections presents different scenarios that can match these constraints. The final text discusses strategies to distinguish or falsify these models.

Solar System Constraints

Planetary masses, orbits and number of planets

The total number of planets, their masses and orbits are typically viewed as the strongest constraints for formation models. While Mercury and Mars have moderately excited orbits ($e = 0.21$ and $i = 7^\circ$ for Mercury and $e = 0.09$ and $i = 2^\circ$ for Mars), those of Earth and Venus are quite circular. Angular Momentum Deficit (AMD) is commonly employed as a metric for quantifying the level of dynamical excitation of a planetary system (Laskar 1997; Chambers 2001). AMD measures the fraction of a planetary system's angular momentum that is missing compared to a system where the planets have the same semi-major axes but circular and coplanar orbits. AMD can thus serve as a diagnostic of how well simulated terrestrial systems match the real inner planets' level of dynamical excitation, and is defined as:

$$\text{AMD} = \frac{\sum_{j=1}^N \left[m_j \sqrt{a_j} \left(1 - \cos i_j \sqrt{1 - e_j^2} \right) \right]}{\sum_{j=1}^N m_j \sqrt{a_j}}. \quad (9)$$

where m_j and a_j are the mass and semi-major axis of the j th planet, N is the number of planets in the system, and e_j and i_j are the orbital eccentricity and inclination of each planet. The terrestrial planets' AMD is 0.0018.

Given the aforementioned excitation dichotomy in the inner Solar System (low excitation for Earth and Venus versus moderate excitation for Mercury and Mars), it can be potentially misleading to report the distribution of AMDs that result from a suite of terrestrial planet formation simulations. Indeed, a system containing an overly excited Earth analog and under-excited analogs of the other planets could potentially have the same AMD as the Solar System. For this reason, recent studies have simply used the final eccentricities and inclinations of Earth and Venus as metrics for success (Nesvorný et al. 2021; Clement et al. 2023; Lykawka and Ito 2023), as Mercury and Mars' eccentricities and inclinations are easier to reproduce, and thus tend to be less diagnostic (Brasser et al. 2009; Roig et al. 2016; Kaib and Chambers 2016)

Another useful metric is the Radial Mass Concentration (RMC) (Chambers 2001), a measure of a planetary system's degree of radial concentration. Earth and Venus contain more than 90% of the terrestrial planets' total mass in a narrow region between 0.7 and 1 AU. RMC is defined as :

$$\text{RMC} = \text{Max} \left(\frac{\sum_{j=1}^N m_j}{\sum_{j=1}^N m_j [\log_{10}(a/a_j)]^2} \right). \quad (10)$$

Higher values indicate more concentrated systems. The inner Solar System RMC is 89.9. However, much like AMD, RMC is degenerate in the sense that a large number of small planets could have the same RMC value as one with a small number of large planets. Thus, a wide range of often complex simulation success criteria have been used throughout the literature. Most of these schemes assign semi-major axis and mass limits to each planet, and consider simulations successful or marginally successful depending on how many inner planets are well reproduced (Clement et al. 2018; Lykawka and Ito 2019; Nesvorný et al. 2021). In general, planets larger than 0.5-0.7 M_{\oplus} are considered to be successful Earth and Venus analogs, 0.25-0.3 M_{\oplus} is typically used as an upper limit for Mars' mass, and Mercury analogs smaller than ~ 0.1 -0.2 M_{\oplus} are deemed satisfactory.

The Asteroid belt

Terrestrial and giant planets in our Solar System are physically separated by the asteroid belt. Unlike the reasonably circular and co-planar orbits of the planets, asteroids inhabit orbits that are quite dynamically excited. Asteroid eccentricities range from 0 to ~ 0.4 , and their orbital inclinations extend between 0° and $\sim 30^\circ$

(essentially populating all non-planet-crossing orbits in the region: Figure 2). This dichotomy is expected to be a direct result of a giant planet instability that occurred some time after nebular dispersal (Roig and Nesvorný 2015; Clement et al. 2019c, discussed in further detail later in this section).

Several regions of the belt are traversed by powerful mean motion resonances (MMRs), along with two major secular resonances (SRs) that arise from perturbations from Saturn. The most prominent MMRs overlaying the asteroid belt are associated with Jupiter’s motion; occurring when the orbital period of an asteroid is an integer multiple of Jupiter’s orbital period. In contrast, SRs occur when an asteroid and planet’s (Saturn, in the case of the main belt) precession frequencies are commensurable. As SRs overlap each of the dominant MMRs, asteroids in these regions are destabilized. This process generates the so-called Kirkwood Gaps in the belt’s radial distribution (red arrows in Figure 2). Gaps in the belt’s inclination distribution (dashed red lines in the right panel of figure 2) are largely related to the migration of these resonances early in the solar system’s history (Nagasawa et al. 2005; Walsh and Morbidelli 2011; Clement et al. 2020b). In particular, the most important SRs in terms of past sculpting of the belt and current production of near-Earth asteroids are the ν_6 (related to Saturn’s eccentricity vector precession) and ν_{16} (driven by Saturn’s nodal precession). The outer limit of the asteroid belt is often associated with the 2:1 MMR at around 3.2 au. Moreover, the distribution of objects about the major MMRs (Deienno et al. 2016) and SRs (Clement et al. 2020b) are strong diagnostic tools for constraining the past evolution of the giant planets.

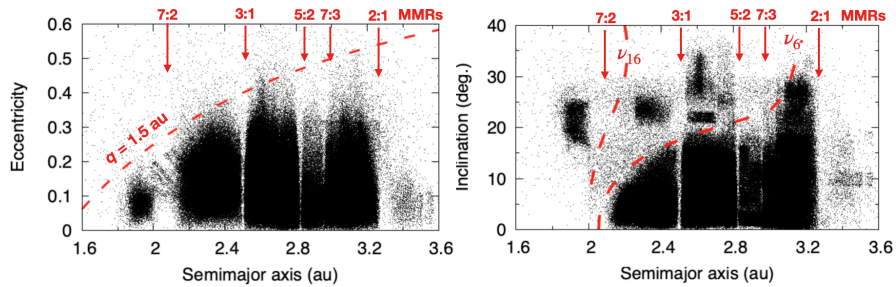


Fig. 2 Eccentricity (right) and Inclination (left) versus semi-major axis of objects with $H \leq 17.75$ ($D \approx 1$ km assuming an average geometric albedo $\langle p_v \rangle = 0.14$ taken from the MPC catalog). The red arrows at the top of the plot indicate the position of the most prominent mean motion resonances (MMRs) with Jupiter, with the 2:1 MMR roughly delimiting the asteroid belt’s outer boundary. The Curved dashed line in the left plot demarcates the perihelion distance where asteroids cross Mars’ orbit ($q = 1.5$ au) that roughly limits the inner edge of the main belt eccentricity-wise. The approximate positions of the Saturnian secular resonances (ν_{16} and ν_6) are denoted in the right panel with dashed red lines.

The asteroid belt is also quite devoid of mass when compared to the solar system’s planetary regimes (e.g. Petit et al. 2001, 2002; Morbidelli et al. 2015c). The total mass of the four terrestrial planets is about $2M_{\oplus}$. In contrast, the main asteroid belt region only contains around $5 \times 10^{-4} M_{\oplus}$ (Gradie and Tedesco 1982; DeMeo

and Carry 2013, 2014). Ceres is the most massive object in today's belt. Given the absence of large gaps in the belt's orbital structure that do not readily associate with MMRs or SRs (Raymond et al. 2009; O'Brien and Sykes 2011), it is unlikely that the belt ever hosted objects larger than the Moon. The origin of the asteroid belt's low mass is still a matter of intense debate (Morbidelli et al. 2009a; Walsh et al. 2011; Deienno et al. 2016; Raymond and Izidoro 2017a; Clement et al. 2019c). Nevertheless, the belt's extreme low mass is still one of the strongest constraints for planetesimal, terrestrial planet, and giant planet formation theories (discussed in the subsequent section).

The asteroid belt is also chemically segregated (e.g. DeMeo et al. 2015). The inner region is mostly populated by siliceous asteroids (S-type), while the outer region is dominated by carbonaceous asteroids (C-type). Thanks in part to the success of the Hayabusa and OSIRIS-REX sample return missions (Yurimoto et al. 2011; Lauretta et al. 2015; Grady et al. 2023), there is broad agreement across multiple fields that S-types are associated with non carbonaceous chondrites (NC), and C-types associate with carbonaceous chondrites (CC). While a variety of other taxonomic asteroid classes exist, S- and C-types are by far the most abundant (DeMeo and Carry 2014). Due to their large inventories of carbon and hydrates, C-type asteroids are quite dark. In contrast, S-types are moderately bright and mostly composed of rocks and iron (Grady and Tedesco 1982; DeMeo and Carry 2014). S- and C-type asteroids are expected to originate in orbits interior and exterior to that of Jupiter, respectively, and were most likely deposited in the asteroid belt region at later stages via scattering by growing terrestrial and giant planets (Raymond and Izidoro 2017a,b).

Water on Earth and other terrestrial planets

The amount of water on Earth is uncertain (e.g. Drake and Campins 2006). Estimates suggest that Earth's total water content is between ~ 1.5 and $\sim 10\text{--}40$ Earth oceans (Lécuyer et al. 1998; Marty 2012; Halliday 2013), where 1 Earth ocean is the total amount of water on Earth's surface (or 1.4×10^{24} g; this includes all lakes, ice caps, glaciers and oceans). A major fraction of this water is stranded in the Earth's mantle. Even more water may exist in Earth's core, but the true amount is much more difficult to constrain than that of the mantle (Nomura et al. 2014; Badro et al. 2014). There is also evidence for water on Mercury (Lawrence et al. 2013; Eke et al. 2017), and the high D/H ratio in Venus' atmosphere has been interpreted to strongly suggest that the planet once possessed a larger inventory of water that subsequently escaped to space (Donahue et al. 1982; Kasting and Pollack 1983; Grinspoon 1993). Similarly, the high D/H ratio of Mars' atmosphere, coupled with isotopic analyses of martian meteorites also implies that some of its primordial water was lost to space (e.g. Owen et al. 1988; Kurokawa et al. 2014). Geomorphological features on Mars indicate that the planet had ancient oceans and that a substantial amount of water is likely hidden below the surface (Baker et al. 1991). All this evidence

supports the idea that a significant amount of water was present in the inner Solar System during its formation.

Until recently, it was generally thought that asteroids in the inner region of the asteroid belt were drier than Earth. This implied that water needed to be ‘delivered’ to an otherwise-dry planet; thus stimulating studies related to how planetesimals from beyond the asteroid belt (or even beyond Jupiter and Saturn’s orbits) could have been transported to the terrestrial planet region (e.g. [Morbidity et al. 2000](#); [Raymond et al. 2004, 2007a](#); [Izidoro et al. 2013](#); [O’Brien et al. 2014](#); [Raymond and Izidoro 2017a](#); [Morbidity et al. 2012](#); [O’Brien et al. 2018](#); [Meech and Raymond 2020](#)).

Isotopic ratios in meteorites are a powerful tool that have been employed to better discriminate between water sources. CC meteorites are associated with C-type asteroids in the belt and their hydrogen and nitrogen isotopic ratios – D/H and $^{15}\text{N}/^{14}\text{N}$ – come close to matching those of Earth ([Marty and Yokochi 2006](#); [Marty 2012](#)). The D/H ratio of the solar nebula is generally inferred from Jupiter’s atmosphere, and it is estimated to be about a factor of ~ 5 -10 lower than that of CCs. Water with a D/H ratio similar to the solar value has been found in Earth’s deep mantle ([Hallis et al. 2015](#)), but in order for Earth’s water to have a primarily nebular origin one must invoke a mechanism to increase the D/H ratio of Earth’s water over the planet’s history. In principle this could be achieved if the Earth had a massive primordial hydrogen-rich atmosphere that efficiently escaped to space over a billion year timescale due to the young Sun’s very intense UV flux ([Ikoma and Genda 2006](#); [Genda and Ikoma 2008](#)). However, the solar $^{15}\text{N}/^{14}\text{N}$ ratio also does not match that of Earth ([Marty 2012](#)). Comets present a wide range of D/H ratios, which vary from terrestrial-like to several times higher ([Alexander et al. 2012](#)). Nevertheless, elemental abundances and mass balance calculations based on ^{36}Ar suggest it is unlikely that comets contributed more than a few percent of Earth’s water ([Marty et al. 2016](#)), but this same analysis also concluded that they probably contributed noble gases to Earth’s atmosphere ([Marty et al. 2016](#); [Avicé et al. 2017](#)). Therefore, until recently a consensus existed favoring CCs as the best candidates for delivering water to Earth ([Alexander et al. 2012](#)). The much higher D/H ratios of Venus and Mars probably do not represent their primordial values and the origins of their water thus remains largely unconstrained. However, any process delivering water to Earth would invariably also deliver water to the other terrestrial planets (e.g. [Morbidity et al. 2000](#); [Raymond and Izidoro 2017a](#)).

This classic paradigm of water delivery has recently begun to be reexamined in light of new isotopic measurements of meteorites with improved sensitivity (e.g. [Izidoro and Piani 2022](#)). Recent isotopic analyses have shown that Enstatite chondrite (EC) meteorites – which are thought to have accreted near Earth’s orbital distance – contain far more water than previously estimated and actually boast water contents extremely similar to that of the modern Earth ([Piani et al. 2020](#)). The D/H ratio of ECs comes about as close to matching Earth’s as CCs ([Piani et al. 2020](#)), making it difficult to disentangle the source of Earth’s water. When isotope ratios from other volatiles are taken into account – notably nitrogen and zinc – it has been argued that Earth’s volatile budget can be explained as a 70-30 mix of ECs

and CCs (Steller et al. 2022; Savage et al. 2022; Martins et al. 2023). If this was the case, given their higher concentration of volatiles, only a 5-10% contribution of CC-derived material is required to meet the constraints from the Earth's total mass budget, with the rest of the planet's mass consistent with an NC source (Steller et al. 2022; Savage et al. 2022; Martins et al. 2023).

In this new paradigm, the majority of Earth's water would have been homegrown, and incorporated along with the NC building blocks that make up the bulk of our planet's mass. Only a small fraction of Earth's bulk material originated in the outer Solar System, although it contributed a non-negligible portion of Earth's water and other volatiles. In contrast, Mars's volatiles follow a different trend, and are consistent with a much smaller contribution from CCs (Kleine et al. 2023). Future investigations into the volatile evolution of various meteorites and planetary bodies will be crucial for further pinning down the relative contributions of different reservoirs to the modern Earth's water content (e.g. Peterson et al. 2023).

Giant planet orbits and evolution

Numerical simulations and radiometric dating of materials from the Earth-Moon system demonstrate that last giant impact on Earth took place between ~ 30 and ~ 150 Myr after the formation of CAIs (Yin et al. 2002; Jacobsen 2005; Touboul et al. 2007; Allègre et al. 2008; Halliday 2008; Kleine et al. 2009; Rudge et al. 2010; Jacobson et al. 2014; Fischer and Nimmo 2018a; Zube et al. 2019). Mars, however, is probably much older than the Earth. Radiometric dating of Martian meteorites using the Hafnium-Tungsten (Hf-W) isotope system indicate that Mars reached about half of its current mass during the first 2 Myr after CAI formation (Dauphas and Pourmand 2011). However, given the scarcity of Martian samples and the fact that dating methodologies are dependent on internal differentiation models, the planet's growth history is necessarily harder to pin down than that of the Earth. Indeed, recent works have argued for a more protracted phase of accretion (Zhang et al. 2021). Nevertheless, a majority of studies in the literature generally agree that Mars formed within just a few Myr after the appearance of CAIs (Nimmo and Kleine 2007; Kruijer et al. 2017b; Costa et al. 2020). Therefore, the dichotomous nature of Earth and Mars' growth timescales presents a peculiar constraint for terrestrial planet formation models to match. Meteorites originating from Venus and Mercury have not been identified, thus making their ages unconstrained.

Even if the Moon-forming impact occurred around the earlier end of the window predicted by radiometric dating (e.g. about 30 Myr after gas disk dissipation: Kleine et al. 2009; Rudge et al. 2010; Fischer and Nimmo 2018a), it is still widely accepted that the final phase of terrestrial accretion occurred long after the giant planets were fully formed (Briceño et al. 2001; Haisch et al. 2001). Given their large gaseous envelopes (Mizuno 1980; Wetherill 1990; Lissauer 1993; Boss 1997; Guillot et al. 2004), the giant planets are constrained to have formed prior to the dispersal of the gaseous protoplanetary disk (Bodenheimer and Pollack 1986; Pollack et al. 1996; Alibert et al. 2005). Therefore, virtually all models of terrestrial planet formation

agree that giant planets play a critical role shaping the makeup of planets in the inner Solar System (e.g. [Wetherill 1978, 1986](#); [Chambers and Wetherill 1998](#); [Agnor et al. 1999](#); [Morbidelli et al. 2000](#); [Chambers 2001](#); [Raymond et al. 2006b](#); [O'Brien et al. 2006](#); [Lykawka and Ito 2013](#); [Raymond et al. 2014](#); [Izidoro et al. 2014a](#); [Fischer and Ciesla 2014](#); [Clement et al. 2018](#)). Determining where and when to include giant planets in these models is challenging because they do not currently inhabit the same orbits that they were born with ([Fernandez and Ip 1984](#); [Malhotra 1993](#); [Hahn and Malhotra 1999](#); [Masset and Snellgrove 2001](#); [Tsiganis et al. 2005](#); [Morbidelli and Crida 2007](#)).

Hydrodynamical simulations show that the giant planets' orbits probably migrated during the gas disk phase. The most likely outcome of migration is a chain of mean motion resonances between successive planets ([Masset and Snellgrove 2001](#); [Morbidelli and Crida 2007](#); [D'Angelo and Marzari 2012](#); [Pierens et al. 2014](#)). The current consensus model for the early dynamical evolution of the outer Solar System (often referred to as the Nice Model: [Gomes et al. 2005](#); [Tsiganis et al. 2005](#); [Morbidelli et al. 2005](#)) argues that a number of dynamical aspects of the outer Solar System are well explained if the giant planets were transported from their initial resonant orbits to their current ones through an epoch of dynamical instability. During the instability, the giant planets' orbits evolve rapidly ([Nesvorný 2011](#)), and they can temporarily obtain eccentricities that are much larger than their current ones ([Batygin et al. 2012](#); [Clement et al. 2021b](#)). These temporary periods of heightened excitation and rapid radial migration can strongly perturb the orbits of other planets and small bodies in the system. Among others, the Solar System qualities that seem to be consequences of this violent dynamical event include the capture of co-orbital asteroids ([Morbidelli et al. 2005](#); [Nesvorný et al. 2013](#)) and irregular satellites ([Nesvorný et al. 2007, 2014](#)) at all four giant planets, the orbital and resonant architecture's of Kuiper Belt ([Levison et al. 2008](#); [Nesvorný 2015a,b](#); [Nesvorný and Vokrouhlický 2016](#); [Kaib and Sheppard 2016](#); [Nesvorný 2021](#)) and the precise orbital excitation of the giant planet's orbits ([Morbidelli et al. 2009b](#); [Nesvorný and Morbidelli 2012](#); [Deienno et al. 2017](#); [Clement et al. 2021e,b](#)).

As originally conceived ([Gomes et al. 2005](#); [Levison et al. 2011](#)), the Nice Model was assumed to occur in conjunction with the late heavy bombardment ([Tera et al. 1974](#)); a perceived delayed spike in cratering events on the Moon evidenced by a preponderance of Apollo-sampled basins with ages of ~ 3.9 Gyr. For this reason, nearly all classic models of terrestrial planet formation assumed that the giant planets were likely in a low-eccentricity, resonant configuration during terrestrial accretion ([Raymond et al. 2006b](#); [O'Brien et al. 2006](#); [Raymond et al. 2009](#); [Izidoro et al. 2014a, 2015c, 2016](#)). However, the late instability model can be problematic in such a scenario because the giant planets' excited and chaotically evolving orbits strongly influence the terrestrial region during the instability. This can lead to planet collisions and ejections. Typically, Mercury or Mars do not survive the event ([Kaib and Chambers 2016](#)).

Over the past five years, a wide range of observational, geophysical and dynamical constraints have been interpreted to evidence the instability having occurred relatively early in the Solar System's history (within the first ~ 100 Myr: [Toliou](#)

et al. 2016; Deienno et al. 2017). While not an exhaustive list, these include an ancient binary trojan of Jupiter that would not have survived collisional evolution in the primordial trans-Neptunian region in the case of a late instability (Nesvorný et al. 2018), the distinctive inventories of HSEs (Highly Siderophile Elements) of the Earth (Becker et al. 2006; Bottke et al. 2010) and Moon (Day et al. 2007; Day and Walker 2015) that suggest a significant quantity of material was delivered to the system *after* the end of the Moon’s magma ocean phase but *before* the end of the Earth’s, cratering records in the inner Solar System (Brasser et al. 2020; Nesvorný et al. 2023), collisional families in the asteroid belt that appear to be almost as old as the Solar System (Delbo’ et al. 2017; Delbo et al. 2019) and certain properties of the Kuiper Belt’s orbital distribution (Ribeiro et al. 2020; Nesvorný 2021). Additionally, from a geochemical standpoint it is still unclear whether or not a spike in cratering on the Moon occurred 3.9 Gyr ago. Updated basin ages leveraging $^{40}\text{Ar}/^{39}\text{Ar}$ dating (Norman et al. 2006; Liu et al. 2012; Grange et al. 2013; Merle et al. 2014; Mercer et al. 2015; Boehnke and Harrison 2016) display a broader spread of dates. Additionally, newer imagery and gravity data from contemporary missions have revealed a number of older basins underlying the younger ones that were presumably sampled by the Apollo missions (Spudis et al. 2011; Evans et al. 2018). Given these new results, recent terrestrial planet formation models increasingly attempt to address the fact that the instability might have occurred at some point within the first 100 Myr after the Solar System’s birth (Clement et al. 2018, 2019b, 2021c; Nesvorný et al. 2021; DeSouza et al. 2021; Clement et al. 2023; Lykawka and Ito 2023)

Solar System Terrestrial Planet formation Models

Simulations of late stage terrestrial accretion typically start with a population of already-formed planetesimals and Moon- to Mars-mass planetary embryos. This scenario is consistent with models of the runaway and oligarchic growth regimes (Kokubo and Ida 1996, 1998, 2000; Chambers 2006; Ormel et al. 2010b,a; Carter et al. 2015; Morishima 2017; Walsh and Levison 2019; Clement et al. 2020a; Woo et al. 2021a) as well as those considering pebble accretion (Johansen et al. 2014; Moriarty and Fischer 2015; Levison et al. 2015b; Chambers 2016; Johansen and Lambrechts 2017). This initial distribution of material loosely correlates with a starting epoch around ~ 3 Myr after CAI formation (Raymond et al. 2009). Therefore, most of these simulations are initialized with fully formed giant planets and assume that the gaseous protoplanetary disk has just dissipated (e.g. Chambers and Wetherill 1998; Agnor et al. 1999).

The most important ingredient in terrestrial accretion models is simply the amount of available mass. A zeroth-order estimate of the Solar System’s starting mass comes from the “Minimum mass solar nebula model” (MMSN: Weidenschilling 1977; Hayashi 1981; Desch 2007; Crida 2009). The original MMSN model inflates the current radial mass distribution of Solar System planets to match the solar composition (adding H and He; Weidenschilling (1977); Hayashi (1981)).

These MMSN-derived models typically suggest that the primordial Solar System contained $\sim 5M_{\oplus}$ of solid material between the orbits of Mercury and Jupiter (Weidenschilling 1977).

Motivated by disk-formation simulations (e.g. Bate 2018) as well as disk observations (generally of the dust component; Andrews et al. 2010; Williams and Cieza 2011), the initial radial distribution of solids in simulations of late stage accretion typically follow power law profiles:

$$\Sigma(r) = \Sigma_1 \left(\frac{r}{1\text{AU}} \right)^{-x} \text{ g/cm}^2. \quad (11)$$

Σ_1 is the surface density of solids at 1 AU. Initial planetary embryo masses are either derived from high-resolution simulations of planetesimal accretion and runaway growth (Walsh and Levison 2019; Clement et al. 2020a; Woo et al. 2021a), or by using the semi-analytically determined isolation mass that is proportional to $r^{3(2-x)/2} \Delta^{3/2}$ (Kokubo and Ida 2002; Raymond et al. 2005). Here, x is the power-law index and Δ represents the separation of adjacent planetary embryos in mutual Hill radii (Kokubo and Ida 2000). A fraction of the disk total mass is typically distributed among equal-mass planetesimals (Raymond et al. 2004, 2006b; O’Brien et al. 2006). To improve compute times, planetesimals are often treated as “semi-interacting” particles; meaning that they can gravitationally perturb and collide with embryos but not with one another (Chambers 2001; Raymond et al. 2009). While the actual terrestrial disk’s planetesimal inventory far exceeded the $\sim 10^3$ used in most simulations of this type, studies varying the total number and individual masses of planetesimals find that they only result in lower order variations in final system outcomes (Jacobson and Morbidelli 2014a; Clement et al. 2020a). Figure 3 shows an example distribution of planetary embryos and planetesimals that follows a MMSN disk profile.

Multiple scenarios for the formation of the terrestrial planets have been proposed (Raymond et al. 2020). The subsequent sections summarize the majority of these models, and highlights three models as potentially viable evolutionary paths for the inner Solar System.

The Classic Scenario and the small-Mars problem

The classic model assumes that giant planet formation and dynamical evolution can be completely disentangled from the process of terrestrial planet formation. Classic simulations simply impose a giant planet configuration (usually considering just Jupiter and Saturn) and a distribution of terrestrial building blocks. Early simulations in this mold succeeded in producing a few planets in stable and well separated orbits, delivering water to Earth analogs from the outer terrestrial disk and in explaining a significant degree of mass depletion of the asteroid belt (Wetherill 1978, 1986, 1996; Chambers and Wetherill 1998; Agnor et al. 1999; Morbidelli et al. 2000; Chambers 2001; Raymond et al. 2004). Later, higher-resolution simulations

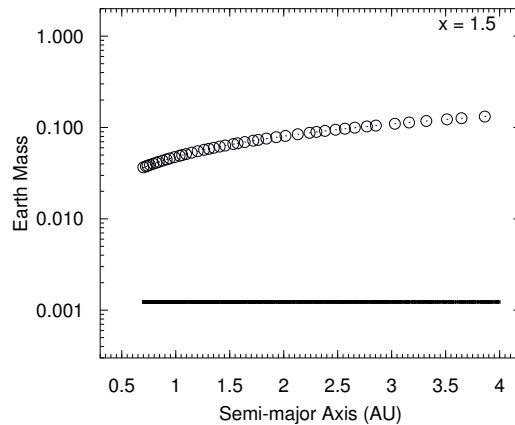


Fig. 3 Representative initial conditions for classic simulations of the late stages terrestrial planet formation using a power-law disk. In this case $x=1.5$ and $\Sigma_1 = 8\text{g/cm}^2$. The mutual separation of neighboring planetary embryos is randomly selected between 5 and 10 mutual Hill radii. Planetesimals are shown with masses of $\sim 10^{-3}$ Earth masses. The total mass carried by about 40 embryos and 1000 planetesimals is about $4.5M_{\oplus}$.

were also able to reasonably match the terrestrial planets' AMD and the timing of Earth's accretion (Raymond et al. 2006b, 2009; O'Brien et al. 2006; Morishima et al. 2008, 2010).

However, three major aspects of the systems formed in classic studies starkly contrast with the properties of the real terrestrial planets. First, Mercury analogs typically grow to masses of $\sim 0.5\text{-}1.0 M_{\oplus}$; in excess of an order of magnitude larger than the real planet. While this problem is less severe if the disk's inner edge is depleted in mass prior to the onset of the giant impact phase (Chambers and Cassen 2002; O'Brien et al. 2006; Lykawka and Ito 2017; Clement and Chambers 2021), the real Mercury mass lies at the extreme low end of the distribution of simulation-generated analog planet masses, and the majority of these worlds inhabit orbits that are too close to Venus. In the extreme case where no massive particles inhabit the region interior to Venus' current orbit at time zero it is possible to form Mercury with a mass of $\sim 0.05 M_{\oplus}$ (Hansen 2009; Lykawka and Ito 2019; Franco et al. 2022), however the proximity to Venus problem persists. Given the relative dynamical isolation of Mercury's orbit, coupled with the fact that its large core mass fraction seems to evidence its mantle having been stripped via a high-energy impact (Benz et al. 1986, 2007; Asphaug and Reufer 2014; Chau et al. 2018), certain recent models have argued that the planets' peculiar mass and other properties are the result of dynamical interactions with the migrating giant planets (Raymond et al. 2016a; Clement et al. 2021a, 2023) or terrestrial planet cores (Brož et al. 2021; Clement et al. 2021d).

In addition to their systematic shortcomings with regard to forming adequate Mercury analogs, classic terrestrial planet formation models such as those presented in Chambers and Wetherill (1998) and Raymond et al. (2006b) also tend to produce

Mars analogs with masses much closer to that of Earth than that of the real planet ($0.107 M_{\oplus}$). While issues related to Mercury have received relatively sparse attention in the recent literature, this so-called small-Mars problem has sparked a prolific output of investigations and theoretical models over the past two decades (Hansen 2009; Walsh et al. 2011; Lykawka and Ito 2013; Jacobson and Morbidelli 2014b; Izidoro et al. 2014a, 2015c; Levison et al. 2015b; Jacobson et al. 2014; Clement et al. 2018, 2019b; Brož et al. 2021; Woo et al. 2021b; Izidoro et al. 2022a; Lykawka and Ito 2023). In general, these models can be grouped into two classes: those that utilize dynamical mechanisms such as planet migration (Walsh et al. 2011) or dynamical instability (Clement et al. 2018) to gravitationally perturb and remove material from the proto-Mars region and models that investigate the planetesimal formation process itself and conclude that few large bodies originated around Mars' modern orbit to begin with (Johansen et al. 2021; Morbidelli et al. 2021; Izidoro et al. 2022a). While all of these published models are capable of reproducing Mars' mass in a reasonable fraction of realizations, only a smaller subset have been scrutinized against a range of dynamical and cosmochemical constraints, and thus represent potentially viable formation models for the inner Solar System. Perhaps the most critical of these constraints that is not matched in classic accretion models is the extremely rapid nature of Mars' formation timescale relative to that of the Earth (Dauphas and Pourmand 2011; Kruijjer et al. 2017b; Costa et al. 2020). This leaves a relatively small window of opportunity for models using dynamical events to reshape the Mars region. This review focuses on three models that have been validated against a number of constraints. One of these models falls in to the class of models where the regions around Mars and the asteroid belt is initially *depleted*, and the other two scenarios argue that the region was once full of material and subsequently *emptied*.

The final persistent problem with classic terrestrial planet formation models is the propensity for ~ 0.1 - $0.4 M_{\oplus}$ planets to form in the asteroid belt (Chambers and Wetherill 2001). Unlike the still mysterious case of Mercury's origin, it is fairly obvious that issues pertaining to the mass budgets of Mars and the asteroid belt are inextricably linked (Izidoro et al. 2015c). While it is certainly plausible that planetary-mass objects could have formed in the asteroid belt and been subsequently lost, the process would be problematic for the belt's orbital architecture. Indeed, the fact that no significant gaps in the belt's a/e and a/i distributions that are not attributable to mean motion or secular resonances implies an upper limit on the mass of any object that could have ever formed in the asteroid belt of around a Lunar mass (O'Brien and Sykes 2011).

It is natural to seek out models where a single mechanism is responsible for either removing excessive material that would be responsible for forming an overly massive Mars along and unnecessary planets in the asteroid belt, or preventing the material from ever existing in the first place. The models discussed in the subsequent sections all adopt this approach of treating the Mars and asteroid belt mass deficiencies as facets of a common, fundamental problem with the classic model (Wetherill 1978; Chambers and Wetherill 1998).

The Grand Tack scenario

Once planets grow large enough to exchange angular momentum with the gas disk (somewhere between the masses of Mars and the Earth, depending on disk parameters: [Papaloizou and Larwood 2000](#); [Tanaka et al. 2002](#); [Tanaka and Ward 2004](#)) their semi-major axes can evolve inward or outward via Type-I or Type-II migration. In the former, lower-mass regime, a combination of torques that arise from the interactions between the star, disk and planet drive migration ([Goldreich and Tremaine 1980](#); [Ward 1986](#); [Paardekooper and Mellema 2006](#); [Kley and Crida 2008](#); [Paardekooper et al. 2011](#); [Benítez-Llambay et al. 2015](#)). In the latter case of Type-II evolution, planets massive enough to carve gaps in the nebular disk experience slower migration that is largely regulated by the radial gas flow within the disk ([Dürmann and Kley 2015](#); [Ida et al. 2018](#)). While the particular migration scheme experienced by a particular system is essentially impossible to determine as it is a complex function of a number of unconstrained properties of the primordial disk, many peculiar aspects of exoplanet demographics have been interpreted to strongly suggest that large-scale orbital migration has sculpted the majority of systems' dynamical architectures (e.g. [Ogihara and Ida 2009](#); [Lega et al. 2015](#); [Ogihara et al. 2015](#); [Izidoro et al. 2017](#); [Bitsch et al. 2019](#); [Lambrechts et al. 2019](#); [Izidoro et al. 2021, 2022b](#)).

Jupiter and Saturn's orbital migration can strongly perturb the orbits of objects in the inner solar system ([Nagasawa et al. 2005](#); [Thommes et al. 2008](#); [Minton and Malhotra 2011](#)). In the absence of clear constraints on the giant planet's actual birth location (see [Chambers 2021](#); [D'Angelo et al. 2021](#), for recent papers that reach conflicting results), dynamical evolutionary models must consider each of four possibilities: (1) the gas giants formed close to their present locations, (2) they formed closer to the Sun and migrated out, (3) they formed further from the Sun and migrated in, and (4) migration was bidirectional. While subsequent, post-disk evolution requires the giant planets roughly obtain semi-major axes close to their current ones around the time of gas dissipation ([Tsiganis et al. 2005](#); [Deienno et al. 2017](#); [Clement et al. 2021e](#)), there are currently no strong constraints definitively ruling out any of these possibilities prior to disk dispersal ([Masset and Snellgrove 2001](#); [Pierens and Nelson 2008](#); [Pierens and Raymond 2011](#); [Morbidelli and Raymond 2016](#)).

The Grand Tack invokes bidirectional migration to remove mass from the proto-Mars and asteroid belt regions ([Walsh et al. 2011, 2012](#); [Raymond and Morbidelli 2014](#); [Jacobson et al. 2014](#); [Brasser et al. 2016](#); [Deienno et al. 2016](#); [Walsh and Levison 2016](#); [Allibert et al. 2023](#); [Ogihara et al. 2023](#)). In essence, the model posits that Jupiter and Saturn followed a very specific inward-outward migration scheme that consequently sculpts the mass and compositional distribution of objects in the asteroid belt, while also truncating the terrestrial disk into a narrow annulus with an outer edge around ~ 1.0 au. In successful simulations of the latter stages of giant impacts in the inner solar system, Mars is typically scattered out of the annulus and stranded on its modern orbit ([Agnor et al. 1999](#); [Hansen 2009](#)). This formation avenue for Mars also serves to limit the probability of large, late giant impacts on

the planet; in good agreement with Hf-W constraints on its formation timescale (Dauphas and Pourmand 2011).

Figure 4 demonstrates how the Grand Tack model provides a compelling explanation for the belt's diminutive mass, dynamically excited state, and observed radial mixing of S- and C-types (Walsh et al. 2012; Deienno et al. 2016). When Jupiter first encounters the inner planetesimal disk during its initial inward migration phases, it immediately disperses primordial asteroid belt planetesimals (red points in figure 4) throughout the solar system. Some objects are shepherded inward via smoothly migrating interior resonances with Jupiter, and others are scattered onto more distant orbits. Thus, after Saturn's inward migration is complete, the present day asteroid belt region is largely empty, and the outer solar system possesses a mixture of material originally derived from the inner and outer solar system (S- and C-type objects). When the two gas giants reverse the direction of their migration, or "tack," they encounter this sea of scattered planetesimals. The majority of these objects are further scattered onto more distant and more eccentric orbits, however a small fraction survive on stable orbits in the modern asteroid belt and some deliver water to the growing terrestrial planets through impacts (O'Brien et al. 2014, 2018).

Deienno et al. (2016) used high-resolution numerical simulations to investigate the consequences of the combined effects of Jupiter's migration through the terrestrial disk, the outer solar system's subsequent epoch of dynamical instability (Tsiganis et al. 2005; Nesvorný and Morbidelli 2012), and the ensuing ~ 4.0 Gyr of evolution on the asteroid belt's eccentricity and inclination distributions. In general, the distribution of modeled asteroid eccentricities provided a reasonable match to the real one. However the inclination distribution of the inner main belt was overly excited. A possible remedy for this deficiency might be the removal of excessive high-inclination objects during Jupiter and Saturn's post-instability migration as a result to resonance cycling caused by their conspicuous proximity to the 5:2 comensurability (Clement et al. 2020b).

In addition to its success when measured against constraints related to Mars and the asteroid belt, internal structure models of Earth's growth and differentiation (Rubie et al. 2015) have demonstrated that the model can also match Earth's internal composition and the mantle's inventory of water in broad strokes. These studies (see also Ogihara et al. 2023, for a more recent investigation) also predict a substantial fraction of water being incorporated into the core of the growing Earth; and thus provide a potential explanation for the apparent under-density of its core (Birch 1952).

The Early Instability scenario

Jupiter need not physically traverse the terrestrial region to deplete planetesimals in the asteroid belt and proto-Mars regions. Indeed, simply altering a classic terrestrial planet formation simulation (Chambers and Wetherill 1998) by placing Jupiter and Saturn on their modern orbits with eccentricities equal to double their current values

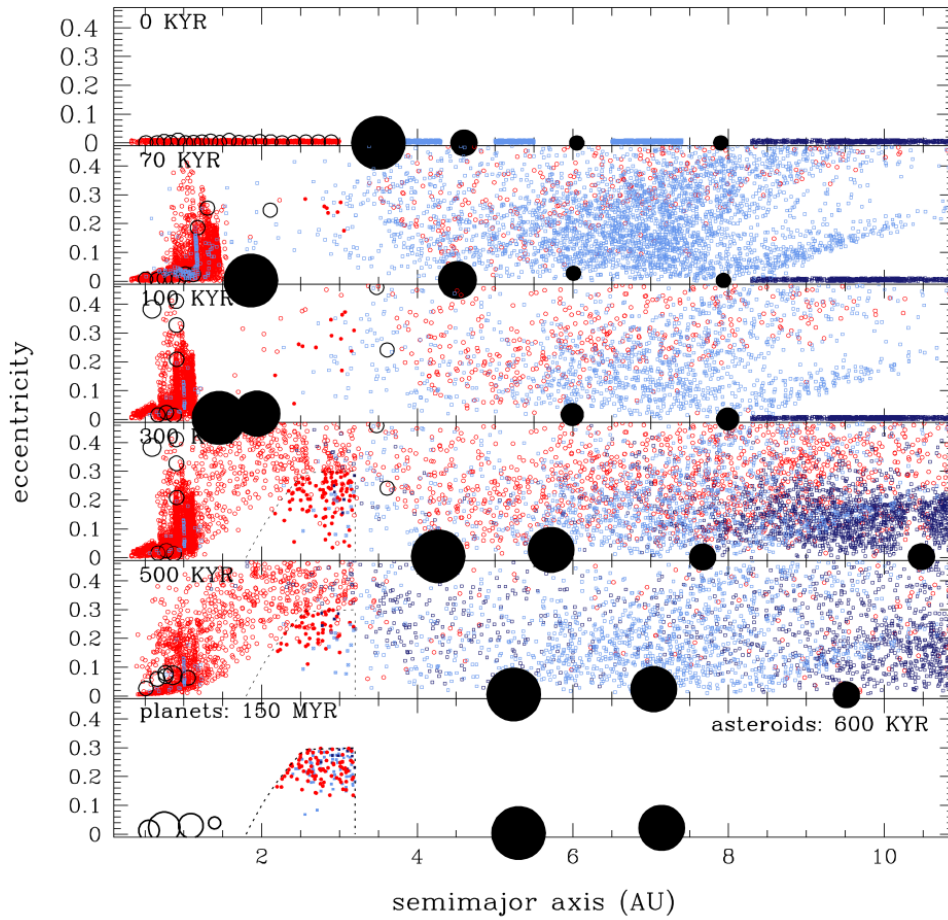


Fig. 4 Snapshots showing the dynamical evolution of the Solar System in the Grand Tack model. The four gas giants are represented by the black filled circles. Jupiter starts fully formed while the other giants planets grow. Terrestrial planetary embryos are represented by open circles. Water-rich and water-poor planetesimals/asteroids are shown by blue and red small dots, respectively. During the inward migration phase Jupiter shepherds planetesimals and planetary embryos, thus creating a confined disk around 1 AU. Saturn encounters Jupiter and both planets start to migrate outwards at about 100 kyr. During the outward migration phase the giant planets scatter planetesimals inward and repopulate the previously depleted belt with a mix of asteroids originated from different regions. Figure reproduced from [Walsh et al. \(2011\)](#).

regularly yield Mars analogs of the appropriate mass (Raymond et al. 2009). Multiple studies (Nagasawa et al. 2005; Bromley and Kenyon 2017; Woo et al. 2021a) have also demonstrated that, if the giant planets attain non-zero eccentricities during the gas disk phase (Pierens et al. 2014; Clement et al. 2021e), the locations of their secular resonance sweep across the asteroid belt and inner Solar System during the disk's photoevaporation phase; thereby depleting the region and limiting the mass of Mars and the asteroid belt. Moreover, Lykawka and Ito (2013) found that a small Mars can be formed if Jupiter and Saturn migrate smoothly with elevated eccentricities from their formation configuration (presumably the 3:2 mean motion resonance: Morbidelli and Crida 2007; Nesvorný and Morbidelli 2012) to their modern orientation with respect to one another. These three results demonstrate the extreme sensitivity of planetesimals in the terrestrial region to changes in the giant planets' eccentricities and spacing.

The Early Instability model attempts to circumvent a late instability's harmful effects on the fully formed terrestrial planets (Brasser et al. 2009; Agnor and Lin 2012; Brasser et al. 2013; Kaib and Chambers 2016) by taking advantage of a wealth of recent constraints that convincingly pin the instability's occurrence down to the first 100 or so Myr after the Solar System's birth (discussed in the previous section). Clement et al. (2018) investigated a range of possible timings within this window and found that, if the event occurs within the first 1-10 Myr after gas dispersal, resonant perturbations from the excited giant planets conspire to remove material from the region around Mars' orbit and the asteroid belt. In addition to providing a resolution to the small Mars problem, this particular timing also fits in well with meteoritic constraints on Mars' formation timescale (Dauphas and Pourmand 2011; Kruijer et al. 2017b). If the instability occurs too early, while the terrestrial region is still abundantly populated with small planetesimals, the disk that was truncated by the giant planets' excited orbits has a tendency to re-spread and produce under-mass Earth and Venus analogs and overly massive Mars analogs (Clement et al. 2018). Contrarily, if the instability occurs too late, Mars has already grown beyond its modern mass, and the final planetary systems are similar to those formed in classic terrestrial planet formation models (Nesvorný et al. 2021). Thus, as far as the terrestrial planets are concerned, late instabilities ($t > 10$ Myr) would only be viable if the regions around Mars and asteroid belt were already at least partially depleted in mass prior to the instability's onset (Nesvorný et al. 2021; Lykawka and Ito 2023). An instability at $t \simeq 50$ -100 Myr would also occur around the same time as the Moon-forming impact (Kleine et al. 2009), and could potentially trigger the event (DeSouza et al. 2021).

An early giant planet instability is a rather effective mechanism for removing a substantial amount of mass from a primordially massive asteroid belt (Deienno et al. 2018). Clement et al. (2019c) noted that depletion in the belt scales as a function of Jupiter's eccentricity excitation. When Jupiter's eccentricity is excited all the way to its modern value (a constraint that itself is challenging to match in instability models, see Nesvorný and Morbidelli 2012; Clement et al. 2021e, for a more detailed explanation), the belt can be depleted by 2-3 orders of magnitudes. However, this depletion factor is higher than what has been found in more recent studies ($\sim 90\%$

depletion) using controlled instability evolutions (Deienno et al. 2018; Nesvorný et al. 2021). If the primordial terrestrial disk indeed possessed a smooth surface density profile (as considered in Clement et al. 2018), it would have possessed approximately 10,000 times more mass initially than it does today. Post-instability chaotic evolution and resonant interactions over ~ 4 Gyr is only expected to deplete the belt by $\sim 50\%$ (Minton and Malhotra 2010). This leaves three options for explaining the belt’s present mass of $\sim 5.0 \times 10^{-4} M_{\oplus}$, all of which are potentially compatible with the Early Instability as an explanation for Mars’ mass. First, the asteroid belt could have been born massive (consistent with a uniform surface density profile in the inner Solar System and the MMSN: Weidenschilling 1977). This would require a rather strong instability as proposed in Clement et al. (2019c) to deplete the belt by around three orders of magnitude, however such a massive primordial belt is likely incompatible with constraints from the belt’s SFD (Deienno et al. 2024). Second, the asteroid belt could have been partially depleted prior to the instability, perhaps by a Grand Tack-like migration of the giant planets (not necessarily as radially extensive as proposed in Walsh et al. 2011). A more mild instability like the one modeled in Deienno et al. (2018) could have then subsequently depleted the remainder of excessive mass in the region. Finally, the asteroid belt could have been born with very little mass (Raymond and Izidoro 2017b), and the instability was not responsible for its depletion at all (note that these last two options have not been explicitly tested, however more simplified models presented in Clement et al. 2019b; Nesvorný et al. 2021, suggest that they are reasonable).

The dynamical excitation of the giant planets during the instability provides a mechanism that significantly mixes material between different radial bins (Clement et al. 2019c) in the asteroid belt (Clement et al. 2019c), and simultaneously scatters distant, icy planetesimals inward onto trajectories that allow for water delivery to Earth (Clement et al. 2018). Therefore, provided an alternative mechanism for implanting C-type objects (for instance, through aerodynamical destabilization during Jupiter and Saturn’s growth phase Raymond and Izidoro 2017a), the model is fully consistent with the asteroid belt’s modern radial distribution of taxonomic classes.

Recent work on the Early Instability model has demonstrated its compatibility with Earth’s core and mantle compositions (Gu et al. 2023), as well potentially viable formation avenues for Mercury (Clement et al. 2023). In particular, the excited giant planets’ orbits’ dynamical perturbations in the inner Solar System facilitate high-velocity collisions that are capable of stripping Mercury’s primordial mantle and reproducing the planets’ large inferred core mass fraction (Hauck et al. 2013).

Planet Formation from Rings and the primordially empty/low-mass asteroid belt

While the first two models discussed here suggest that the asteroid belt was born massive and *emptied* via dynamical perturbations from, or the physical presence of Jupiter and Saturn, it has also been proposed that the belt did not contain a sub-

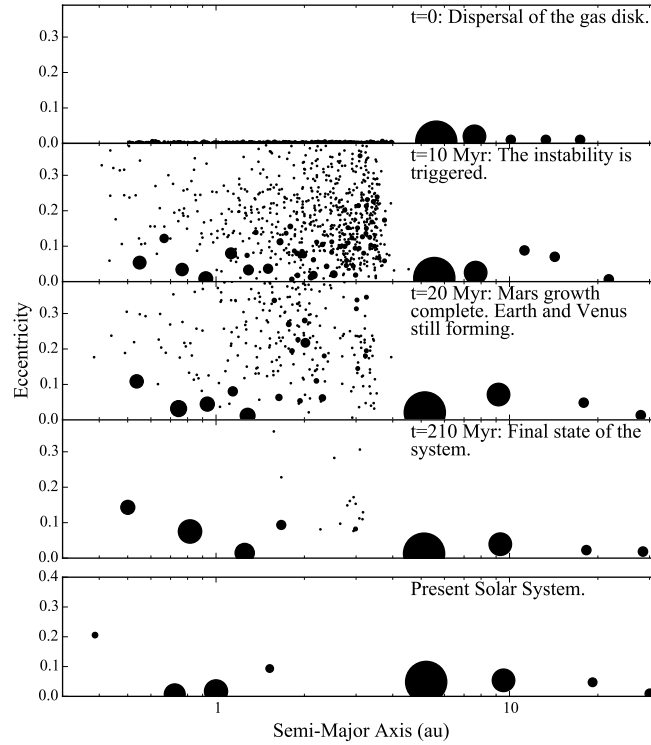


Fig. 5 Example successful evolution of the Early Instability model (reproduced from [Clement et al. 2018](#)). The second panel shows the onset of the giant planet instability around ~ 10 Myr after the dispersal of the gas disk ([Clement et al. 2019b, 2021c](#); [Nesvorný et al. 2021](#), note that more recent works have experimented with alternative timings with mixed results). Perturbations from Jupiter and Saturn's excited orbits destabilize and remove material from the proto-Mars and asteroid belt regions, excite the orbits of asteroids that do survive ([Deienno et al. 2018](#); [Clement et al. 2019c](#)), while leaving Earth and Venus' formation largely undisturbed (panels 3 and 4).

stantial population of planetesimals to begin with. The simplest explanation for how this might have happened is by Jupiter's core blocking the inward pebble flux and thus starving much of the inner solar system of the raw materials needed to form large bodies ([Lambrechts and Johansen 2014](#); [Morbidelli et al. 2015b](#)). Indeed, recent high-resolution ALMA observations of ring-like features within protoplanetary disks ([Huang et al. 2018](#)) seem to indicate that the radial structures of actual young planet-forming regions are anything but smooth (e.g. [Hayashi 1981](#)). Additional evidence for large-scale structure early in the solar system's history comes from the disparate compositions of NC and CC meteorites (the so-called NC/CC

dichotomy) when measured using a number of different isotope systems (Budde et al. 2016). These distinctive inferred formation ages and compositions have been interpreted to imply that two distinctive regions of planetesimals were physically separated early in the solar system’s history (Kruijer et al. 2017a). Several explanations for this separation of reservoirs have been proposed, including the rapid formation of Jupiter’s core (Kruijer et al. 2017a) and a primordial pressure maximum in the vicinity of Jupiter’s modern orbit caused by an ALMA disk-like ring feature (Brasser and Mojzsis 2020).

Returning to the aforementioned issues with terrestrial planet formation models, it is noteworthy that the terrestrial planet’s orbits are extremely well reproduced when the initial distribution of planetesimals and embryos is confined within a narrow annulus between ~ 0.7 - 1.0 au (Agnor et al. 1999; Hansen 2009; Levison et al. 2015b; Izidoro et al. 2015c; Kaib and Cowan 2015; Raymond and Izidoro 2017b; Lykawka and Ito 2019). Until the observation of ring-like features in protoplanetary disks, the lack of an *explanation* for the origin of a such a narrow radial feature was the biggest weakness of these so-called “annulus” models. Given the plethora of ALMA observations of ring-like structures, in tandem with the inferred NC/CC dichotomy in the solar system, the challenge for contemporary modelers has shifted to finding an explanation for the formation of rings in very specific locations of the solar nebula.

Planetesimal formation is well known to be highly sensitive to the local disk properties (Simon et al. 2016; Yang et al. 2017; Yang and Zhu 2021). Indeed, dust coagulation and pebble accretion models have demonstrated that, given the correct selection of disk parameters, large concentrations of planetesimals can form around 1 au, but not elsewhere in the terrestrial region (Moriarty and Fischer 2015; Drazkowska et al. 2016). Izidoro et al. (2015c) systematically studied the formation of terrestrial planets in disks with different radial mass distributions (i.e. in shallow and steep surface density profiles, see also: Raymond et al. 2005; Kokubo et al. 2006). This study identified an important trade-off between Mars’ mass and the asteroid belt’s level of excitation: shallow disks produce overly massive Mars analogs and properly excited asteroid belts while steeper disks typically yield good Mars analogs and under-excited asteroids. The latter is a result of inefficient gravitational self-stirring in models of a severely depleted primordial belt, however this issue is resolved if the giant planet instability occurs earlier within the process of terrestrial planet formation (Izidoro et al. 2016; Deienno et al. 2018, although not necessarily as early or within as specific a window as required in the Early Instability model).

Subsequent work on this scenario demonstrated that it is entirely possible no modern asteroids actually formed in the asteroid belt. Terrestrial planet formation simulations that are initialized with a narrow annulus of embryos and planetesimals naturally implant a small fraction of planetesimals from the terrestrial region into the asteroid belt (in excess of the current total mass of S-types: Raymond and Izidoro 2017b; Woo et al. 2022). During the chaotic sequence of giant impacts that unfolds during the terrestrial accretion process planetesimals are scattered onto high-eccentricity, belt-crossing orbits. A fraction of these are subsequently scattered by rogue embryos onto lower-eccentricity orbits beyond 2 AU, preferentially in the

inner main belt. Thus, if the number of primordial asteroids that form in the belt is less than the present day region's constituency of S-types, it would imply that the majority of modern S-types are "refugees" from the $a < 2.0$ au region of the disk.

A different process is likely responsible for implanting C-type asteroids native to the outer solar system into the belt. During the phase of giant planet growth where Jupiter and Saturn rapidly accrete gas directly from the nebula, the orbits of nearby planetesimals are perturbed and gravitationally scattered onto eccentric orbits. Given the dissipative nature of gas drag (Adachi et al. 1976), the eccentricity of inwardly-scattered planetesimals are subsequently damped; leading to their capture onto stable orbits in the outer main belt (see Figure 6). A fraction of these scattered bodies are not implanted into the belt region and instead acquire eccentricities that are large enough to allow their trajectories to cross those of the growing terrestrial planets and deliver water (Raymond and Izidoro 2017a). In contrast with other models (e.g., the Grand Tack), this mechanism is an *unavoidable* consequence of giant planet formation that would operate in any proposed terrestrial planet formation scenario.

Originally referred to as the "low-mass asteroid belt" model (Raymond and Izidoro 2017b), a number of recent studies have designed extremely detailed models that investigate the combined effects of disk chemistry, gas dynamics, pebble accretion and post-disk dynamics, and attempt to comprehensively link the earliest formation of ring-like structures with the solar system's modern architecture. Lichtenberg et al. (2021) developed a one-dimensional disk model and argued that, under a reasonable set of assumptions, the migration of the water-ice snowline can proceed in a manner such that planetesimal formation occurs in two distinctive bursts, at disparate locations and times. In successful simulations, the inner region contains roughly an Earth-mass worth of planetesimals, and the total mass of large bodies in the outer reservoir is around that of Jupiter. However, certain distinctive compositional properties of NC and CC meteorites (for example, their dissimilar isotopic ratios, oxidation states and Fe/Ni ratios, e.g.: Spitzer et al. 2021) are challenging to reconcile in a model where their parent bodies form under similar conditions (i.e.: at the snow-line) but at different locations and times.

Morbidelli et al. (2021) used a similar numerical approach as Lichtenberg et al. (2021) and found that, if turbulent diffusion is low, it is possible to trigger planetesimal formation within the first ~ 500 kyr of evolution via dust pile-ups at both the snowline (around ~ 5 au) and the silicate sublimation line (closer to ~ 1 au). Most recently, Izidoro et al. (2022a) used a one-dimensional disk model accounting for dust coagulation, fragmentation, and turbulent mixing to show that, assuming the solar nebula contained a set of minor, primordial pressure bumps (top panel of figure 7) at the locations of the silicate sublimation line, water snow-line and CO snow-line, planetesimal formation proceeds via dust pile-ups in highly localized regions (second panel of figure 7). Presumably, these pressure bumps would be the result of disk opacity (Müller et al. 2021; Charnoz et al. 2021) or zonal flows (Pinilla et al. 2021). With only these assumptions, the "ring" model is able to generate the narrow annulus of terrestrial disk material (Hansen 2009) needed to reproduce the masses and formation histories of the terrestrial planets (Raymond et al. 2020), an appro-

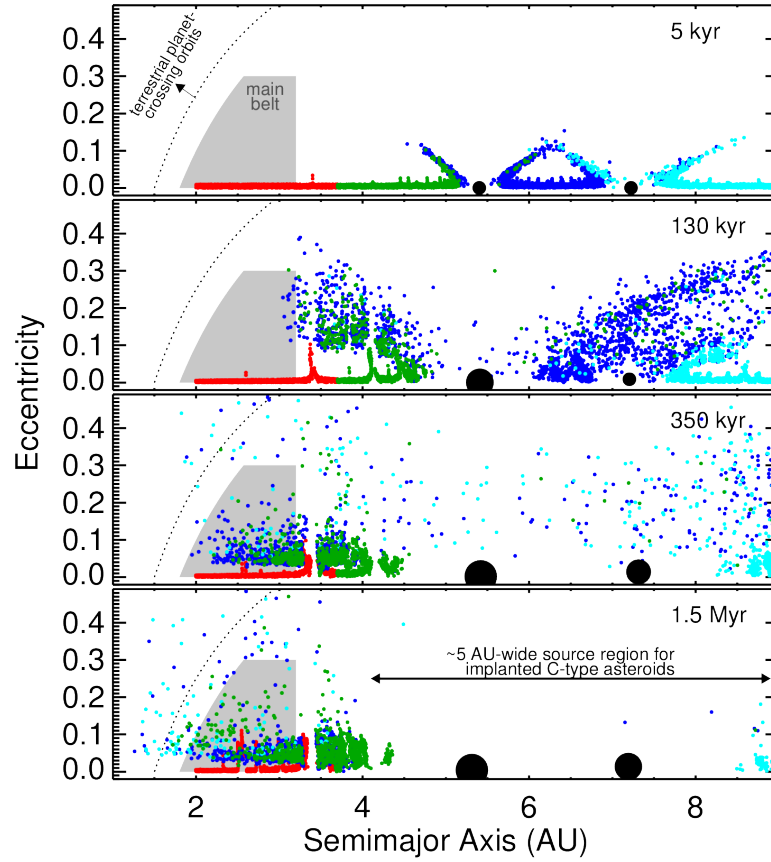


Fig. 6 Implantation of asteroids in the belt during the epoch of rapid gas accretion onto Jupiter and Saturn (reproduced from [Raymond and Izidoro 2017a](#)). The gas giants are represented by the growing filled circles. Planetesimals are color-coded to reflect their original locations. The gray shaded region delimits the asteroid belt. In the depicted simulation, Jupiter grows linearly from a $3M_{\oplus}$ core to its current mass between 100 and 200 ky, while Saturn’s runaway accretion takes place between 300 to 400 kyr.

appropriate quantity of planetesimals in the outer disk to form the giant planets and the Kuiper belt (third panel of figure 7), and the correct total masses and compositional dichotomy of S- and C-types in the asteroid belt (bottom panel of figure 7: [DeMeo and Carry 2013](#)). [Izidoro et al. \(2022a\)](#) also performed a series of N-body, late-stage accretion simulations to demonstrate the model’s compatibility with multiple other inner solar system qualities such as the dissimilar isotopic compositions of Earth (predominantly EC: [Dauphas 2017](#)) and Mars (mostly Ordinary Chondrites: [Tang and Dauphas 2014](#)). While additional work will be required to verify the model’s compatibility with dynamical constraints from the asteroid belt’s eccentricity and

inclination distributions, it is reasonable to assume that it will be largely consistent with other studies that find the subsequent Nice Model instability primarily sculpts these properties (Roig and Nesvorný 2015; Deienno et al. 2016; Clement et al. 2020b).

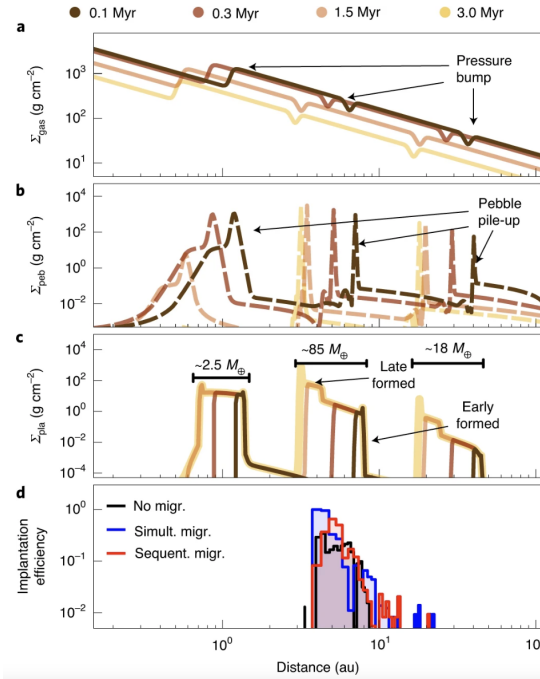


Fig. 7 Example evolution where snow-line driven ring-like structures in the solar nebula sculpt the gas and solid radial surface density profiles into concentrated segments that match the present-day system’s peculiar mass distribution (reproduced from Izidoro et al. 2022a). The top panel shows the assumed disk gas surface density profile at various times in the simulation (different shades of brown and yellow lines corresponding to 0.1, 0.3, 1.5 and 3.0 Myr). The three primordial pressure bumps are linked to the locations of the Silicate sublimation ($T \simeq 1,400$ K), the water snow-line ($T \simeq 170$ K) and the CO snow-line ($T \simeq 30$ K). The features’ affect on the solid pebble population is depicted in the second panel, and is ultimately responsible for triggering planetesimal formation in highly localized, ring-like regions.

Models for the formation of Mercury

As discussed in the previous section on solar system constraints, a successful model for Mercury’s origin must simultaneously explain why its mass is only 5-6% that of Earth and Venus, why its orbit is dynamically detached from those of the other terrestrial planets, and the reason for formation of its anomalously large core mass

fraction (CMF: [Hauck et al. 2013](#)). Of these three issues, the latter has arguably received the greatest attention in the recent literature. Specifically, there are two possible explanations for Mercury’s CMF of ~ 0.7 - 0.8 . In the first class of models (“chaotic:” [Benz et al. 1988](#); [Ebel and Stewart 2017](#)), proto-Mercury is hypothesized to be the victim of an extremely violent collision between two objects initially possessing Earth-like CMFs of ~ 0.3 . As a result of the collision, Mercury’s primordial mantle is stripped and the final planet is comprised mostly of the original object’s core material. In the second paradigm (“orderly:” [Morgan and Anders 1980](#); [Ebel and Stewart 2017](#)), the planetesimals in the proto-Mercury region already possessed boosted iron contents prior to the onset of the giant impact phase. While both scenarios can occasionally replicate other aspects of Mercury (specifically its size and orbit), in contrast to the aforementioned models that explain Mars’ low mass and rapid formation timescale, no model currently exists that can consistently match constraints for Mercury’s CMF, mass and orbit, as well as other broad dynamical constraints for the rest of the inner Solar System.

Chaotic Models

Similar to studies of the Moon-forming impact (e.g. [Cameron 1985](#); [Benz et al. 1986](#); [Canup 2004](#)), investigations of the giant impact hypothesis for Mercury’s origin typically leverage hydrodynamical models with the aim of uncovering impact geometries (initial masses and velocity vectors of the target and projectile) that can reproduce Mercury’s current mass and CMF. In addition to the planet’s internal structure, these studies are motivated by the fact that Mercury’s crust and mantle are highly reduced and depleted in volatiles ([Weider et al. 2015](#); [Ebel and Stewart 2017](#), however, the MESSENGER mission revealed that Mercury’s inventory of less volatile lithophile elements like Si, Ca, Al, and Mg is similar to that of the other terrestrial planets). Within this class of models, two general possibilities exist: proto-Mercury as the target being struck by a smaller projectile ([Benz et al. 2007](#)) or proto-Mercury being the projectile and colliding with a larger proto-planet ([Asphaug and Reufer 2014](#)). In the latter scenario, the obvious targets would be proto-Earth or proto-Venus. These possibilities therefore require a mechanism for dynamically detaching Mercury’s orbit from those of the other terrestrial planets. Orbital migration has been proposed as a potential avenue for isolating Mercury’s orbit ([Brož et al. 2021](#); [Clement et al. 2021d](#)), however this idea has not been robustly tested in conjunction with the impact scenario of [Asphaug and Reufer \(2014\)](#). It is also possible that Mercury’s mantle was incrementally tidally stripped as the result of repeated close encounters with Venus ([Deng 2020](#); [Fang and Deng 2020](#)), however this scenario carries with it many of the same drawbacks as models requiring an actual collision.

Given the amount of mantle material that must be redistributed to replicate Mercury’s modern CMF, the collisional velocities involved in either scenario are necessarily high (approaching six times the mutual escape velocity for oblique impacts). Such extreme events are outside of the spectrum of collisional outcomes that occur

in transitional N-body studies of terrestrial planet formation (Jackson et al. 2018; Clement et al. 2019a). However, the region around Mercury’s modern orbit is also home to a number of strong orbital resonances (Michel and Froeschlé 1997; Batygin and Laughlin 2015) that can drive chaotic evolution of proto-planets in the region and even trigger extremely high-velocity impacts (Clement et al. 2021a). Thus, if a chain of embryos or planets formed inside the modern orbit of Mercury (in contrast to how terrestrial planet formation models typically treat the region, Volk and Gladman 2015), energetic, mantle-stripping events might be quite common. However, studies of this scenario tend to form Mercury at extremely low semi-major axes (Clement et al. 2021a). Excessive velocities can also be avoided if Mercury’s mantle is stripped incrementally through a series of multiple hit-and-run events (Chau et al. 2018; Franco et al. 2022). Indeed, N-body simulations incorporating collisional fragmentation do find that high-CMF planets can form with somewhat regularity as a result of fortuitous chains of imperfect accretion events that happen to transpire during the highly stochastic giant impact phase (Chambers 2013; Clement et al. 2019b, 2023). This possibility disentangles Mercury’s mass and CMF from its specific location in the Solar System by arguing that Mercury-like planets should be rather common in the cosmos. Indeed, exoplanet surveys have recently begun to reveal a number of Super-Earths with densities that might be indicative of a Mercury-like internal structure (Rodríguez Martínez et al. 2023; Mah and Bitsch 2023).

Aside from the aforementioned challenges related to replicating Mercury’s dynamical offset from Venus, perhaps the largest problem for chaotic hypotheses to overcome is the high likelihood of debris and disrupted volatile re-accretion (Benz et al. 2007; Gladman and Coffey 2009; Crespi et al. 2021). As hydrodynamical simulations typically find that a large quantity of the material ejected from giant impacts is in the form of dust, it is possible that the majority of the ground-up mantle material that was removed via Poynting–Robertson drag (Melis et al. 2012) or interactions with the young Sun’s strong wind (Spalding and Adams 2020).

Orderly Models

Early models attempting to explain Mercury’s curious composition and internal structure argued that silicates in the region around proto-Mercury were evaporated as a result of heightened stellar activity during the pre-Main Sequence phase (Morgan and Anders 1980). However, such a scenario is inconsistent with MESSENGER’s findings that less volatile, lithophile elements in Mercury’s crust have roughly chondritic abundances. While a number of models for preferential iron-enrichment of Mercury’s planetesimal precursors have been proposed since MESSENGER, it is important to note that these scenarios axiomatically require Mercury grow within a separate reservoir of material than Earth and Venus. In order to match constraints for Mercury’s mass and orbit, this innermost component of the inner disk must be significantly depleted in mass relative to the outer disk component, and also possess a distinctive surface density profile (equation 11: Lykawka and Ito 2017; Clement and Chambers 2021; Lykawka and Ito 2023). While such a structure

is necessarily contrived and inconsistent with planetesimal formation and accretion models (Boley et al. 2014), convergent (Brož et al. 2021) or outward (Clement et al. 2021d) migration of terrestrial embryos have been proposed as dynamical mechanisms for re-sculpting the inner component of the terrestrial disk.

One process potentially responsible for iron enrichment of Mercury’s planetesimal precursors is the photophoretic effect (Wurm et al. 2013). When \sim mm-scale particles in a gaseous disk are exposed to non-isotropic solar radiation, they can migrate substantially. The extent of this migration varies based off the local thermal gradient and the size of the particles themselves (Krauss and Wurm 2005). Through this process particles can be size sorted, although it is still unclear how efficient this mechanism is in the opaque mid-plane of protoplanetary disks (Cuzzi et al. 2008b). Nevertheless, advanced disk chemistry models incorporating effects such as this have demonstrated the formation of a compositionally distinct inner region of the terrestrial disk (e.g. Moriarty et al. 2014; Pignatale et al. 2016).

Magnetic aggregation has also been proposed as a mechanism for iron-enrichment of planetesimals in the inner terrestrial disk (Kruss and Wurm 2020). Laboratory experiments have shown that suspended magnetized particles within ferromagnetic fluids generate chain-like structures as a result of their behaving like dipoles (Kruss and Wurm 2018; Jungmann et al. 2022). If the magnetic field in the region of the disk around proto-Mercury is sufficiently strong, it is possible that these long iron-rich chains can be preferentially incorporated into planetesimals formed via the streaming instability.

Another idea for altering the chemistry of planetesimals in the neighborhood of the forming Mercury comes from high temperature experiments with pre-solar interplanetary dust particles in carbon-rich, oxygen-depleted environments. Ebel and Alexander (2011) showed that these conditions favor the formation of condensates with Fe/Si ratios half that of the bulk Mercury. Indeed, anhydrous chondritic interplanetary dust particles have Carbon abundances that are an order of magnitude more than those of CI chondrites (Ebel and Alexander 2005). However, the efficiency of this mechanism is highly dependent on the unconstrained chemical structure of the disk mid-plane in the vicinity of proto-Mercury.

Recently, Johansen and Dorn (2022) developed a model that relies on the high surface tension of iron (Ozawa et al. 2011) relative to silicates (Lümmen and Kraska 2005). Iron particles nucleate homogeneously only under very supersaturated conditions, thus promoting the depositional growth of a small population of nucleated iron particles embedded in a large distribution of iron pebbles. Contrarily, while silicates nucleate under similar conditions they also obtain smaller sizes than iron particles (Kashchiev 2006). This dichotomy in turn promotes the growth iron-rich, silicate-poor planetesimals via the streaming instability (Youdin and Goodman 2005).

Substantial investigation is still required to better understand whether any of these “orderly” enrichment processes played a role in Mercury’s growth, and if so to what degree. While more sophisticated planetesimal formation, disk chemistry and dynamical formation models will surely shed additional light on the potential source of Mercury’s high CMF, the subsequent section details ways in which ex-

oplanet demographics might help break degeneracies between the “orderly” and “chaotic” hypotheses in the future.

Constraining and distinguishing formation scenarios

A number of models for the late stage accretion of terrestrial planets in the Solar System have been proposed over the past decade. Among others, recently proposed models that still require additional study include the convergent migration scenario of [Brož et al. \(2021\)](#), the pebble accretion models of [Levison et al. \(2015b\)](#) and [Johansen et al. \(2021\)](#), and the chaotic excitation scheme proposed by [Lykawka and Ito \(2023\)](#). This review focused on three specific models that are not only consistent with the masses and orbits of the terrestrial planets (RMC and AMD), the structure of the asteroid belt and the origins of water in the inner Solar System ([Walsh et al. 2011](#); [Clement et al. 2018](#); [Izidoro et al. 2022a](#)); but perhaps more importantly are self-consistent with envisioned dynamical ([Tsiganis et al. 2005](#); [Morbideilli and Crida 2007](#); [Nesvorný and Morbidelli 2012](#)) and cosmochemical ([Kleine et al. 2009](#); [Dauphas and Pourmand 2011](#); [Kruijjer et al. 2017a](#); [Dauphas 2017](#)) models of global Solar System evolution. While numerical simulations of each of these models seems to produce “good” terrestrial analogs systems with similar regularity, only one of them is potentially correct. So how can we hope to distinguish between them?

Empirical tests to discriminate between these models in the future may be based on space observations of Solar System minor bodies ([Morbideilli and Raymond 2016](#)), or high precision isotopic measurements of different planetary objects (e.g. [Tang and Dauphas 2014](#); [Dauphas 2017](#); [Dauphas et al. 2024](#)). On the theoretical side, models may be ruled out or bolstered by more sophisticated numerical simulations with superior treatments of various physical mechanisms like pebble accretion and planetary migration [Izidoro et al. \(2016\)](#), or through approaches that blend dynamical and disk chemistry models ([Lichtenberg et al. 2021](#); [Morbideilli et al. 2021](#); [Izidoro et al. 2022a](#)).

The Grand Tack model requires a very specific large-scale giant planet migration sequence. One of the main loose ends of the Grand Tack is that it is not clear if the required inward-then-outward large scale migration is possible when gas accretion onto Jupiter and Saturn is self-consistently computed ([Raymond and Morbidelli 2014](#)). Unfortunately, our understanding of gas accretion onto cores is still incomplete. Indeed, hydrodynamical simulations of the growth and migration of Jupiter and Saturn typically invoke a series of simplifications considering the challenge in performing high-resolution self-consistent simulations of this process (e.g. [Zhang and Zhou 2010](#); [Pierens et al. 2014](#)).

The major drawback of the Early Instability model is the very specific timing (<10 Myr, and possibly within the limited window of 1-5 Myr as found in [Clement et al. 2019b, 2021c](#)). Indeed, while many Solar System constraints pin the instability’s occurrence down to the first 100 Myr after disk dispersal, a number of these (e.g. [Nesvorný 2015a](#); [Morbideilli et al. 2018](#); [Nesvorný et al. 2023](#)) fit in best with

an instability that occurs in the latter half of this window. Moreover, the Earth's atmospheric inventory of Xenon appears to have a cometary signature that is missing in the mantle (Marty et al. 2017); suggesting a substantial delivery of volatiles from comets (presumably dispersed via the instability) *after* core closure. However, recent work by Joiret et al. (2023) found that cometary bombardment can occur over a more prolonged window of tens of Myr after the onset of the instability. Therefore, it is at least plausible that the instability could have occurred quite early and still delivered cometary Xenon to Earth well after its formation (note, there are dynamical reasons to favor an extremely Early Instability as well Quarles and Kaib 2019; Liu et al. 2022).

The Achilles' heel of the rings model lies in the assumed initial condition of primordial pressure bumps. If no such structure existed in the Solar System, or planetesimal formation was in fact efficient beyond 1-1.5 au, another mechanism must have been responsible for limiting Mars' mass (Morbidelli and Raymond 2016). Moreover, while the proposition of highly-localized planetesimal formation (Drazkowska et al. 2016; Raymond and Izidoro 2017b; Lichtenberg et al. 2021) is indeed a powerful explanation for the NC/CC dichotomy (Kruijer et al. 2017a), it is worth considering the diversity of ages and compositions (see, for example: Alexander 2022) of the various members of the highly diverse set of sub-classes within each major chondrite groups. Moreover, certain ungrouped meteorites have been interpreted to evidence very early mixing of NC and CC-derived materials (Spitzer et al. 2022). Thus, from a meteorites perspective, the full story of planetesimal formation is likely to be far more complicated than assumed in any terrestrial planet formation model.

Strong tests aiming to disentangle these models may also emerge from more complex multidisciplinary approaches combining the accretion history of Earth produced in N-body simulations with models of core-mantle differentiation and geochemical models (see, for example: Rubie et al. 2015, 2016; Fischer and Nimmo 2018b; Zube et al. 2019; Gu et al. 2023). Analyses such as these may eventually be the key to distinguishing between the various terrestrial planet formation scenarios.

Exoplanet demographics can also provide valuable insights into the spectrum of processes that potentially played roles in the formation of our own Solar System. For instance, additional "super-Mercuries" will undoubtedly be discovered in the near future through more precise density measurements facilitated by next generation telescopes. If such planets occur with similar regularity at different positions in multi-planet systems, it would support the idea that Mercury formed as the result of a series of mantle-stripping impacts (Mah and Bitsch 2023). Contrarily, if super-Mercuries are over-represented in the subset of planets that are the closest to their system's central star, it would appear more likely that Mercury formed from a population of iron-rich planetesimals.

Terrestrial planet formation in the context of exoplanets

If we understand terrestrial planet formation in the Solar System (at least to some degree), then we can hopefully extrapolate this knowledge to terrestrial planet formation in a more general setting. The thousands of known exoplanets – many of which are close to Earth-sized – offer an excellent testbed for our models. The difficulty is in knowing which exoplanets are truly analogous to our own terrestrial planets and which are entirely different beasts.

As of 2023 there are more than 5,000 confirmed exoplanets (Christiansen 2022). The bulk were discovered either by radial velocity surveys using Doppler spectroscopy (Fischer et al. 2014) or by transit surveys; notably NASA’s *Kepler* mission (Borucki et al. 2010b). It is now known that at least a few percent (and perhaps even $\gtrsim 10\%$) of Sun-like stars host gas giant planets (Mayor et al. 2011b; Howard et al. 2012b; Petigura et al. 2018; Gan et al. 2023; Beleznyay and Kunitomo 2022; Bryant et al. 2023) but that hot Jupiters exist around only $\sim 1\%$ (Wright et al. 2012; Howard et al. 2010b). While most gas giants are found on orbits beyond 0.5–1 AU (Butler et al. 2006b; Udry and Santos 2007b), the population is dominated by planets on eccentric orbits. True Jupiter ‘analogs’ – with orbital radii larger 2 AU and eccentricities smaller than 0.1 – exist around only $\sim 1\%$ of stars like the Sun (Martin and Livio 2015; Morbidelli and Raymond 2016). This is thus an upper limit on the occurrence rate of potential true Solar System analogs. While analogs of individual planets like Venus or Uranus may be more common, bulk system architectures like ours cannot be.

At first glance, “hot super-Earths” and “sub-Neptunes” – often defined as being smaller than $4R_{\oplus}$ or $20M_{\oplus}$ with orbits shorter than ~ 100 days – seem tantalizingly similar to the solar system’s terrestrial planets. Super-Earths have been shown to orbit at least half of all main sequence stars, including both Sun-like (Mayor et al. 2011b; Howard et al. 2012b; Fressin et al. 2013b; Petigura et al. 2013b; Zhu et al. 2018) and low-mass stars (Bonfils et al. 2013; Mulders et al. 2015). Many systems have been found to host multiple super-Earths. These so-called “multiples” tend to have compact orbital configurations and similar-sized planets (Lissauer et al. 2011a,b; Millholland et al. 2017; Weiss et al. 2018). Extensive radial velocity monitoring of *Kepler* super-Earths has also revealed a noteworthy dichotomy: smaller planets (radii $\lesssim 1.5 R_{\oplus}$) have high densities and are indeed rocky (super-Earths) whereas larger planets (sub-Neptunes with $1.5 \lesssim R \lesssim 4 R_{\oplus}$) tend to have lower densities and likely more like the solar system’s ice giants than its terrestrial planets (Weiss et al. 2013; Marcy et al. 2014; Weiss and Marcy 2014). The division between super-Earths and mini-Neptunes appears to lie close to $1.5R_{\oplus}$ (Weiss and Marcy 2014; Lopez and Fortney 2014; Rogers 2015; Wolfgang et al. 2016; Chen and Kipping 2017).

This section begins with a discussion of various models for the origin of super-Earths (broadly-defined to include all planets smaller than $4R_{\oplus}$), and then concludes with an overview of how terrestrial planet formation may proceed in systems with gas giants on orbits very different from Jupiter’s.

Origin of super-Earth systems

The observed population of super-Earths is rich enough to provide quantitative constraints on formation models:

1. Their occurrence rate ($\sim 50\%$ around main sequence stars; [Mayor et al. 2011b](#); [Fressin et al. 2013b](#); [Petigura et al. 2013b](#); [Dong and Zhu 2013](#)).
2. Their multiplicity distribution. Indeed, it is easier to precisely determine the masses and orbits of planets in systems with multiple planets, for instance through transit-timing variations offer ([Lissauer et al. 2011b](#)). However, the observed population of exoplanets has more single super-Earth systems than multiple systems, which is sometimes referred to as the “Kepler dichotomy” ([Fang and Margot 2012](#); [Tremaine and Dong 2012](#); [Johansen et al. 2012a](#)).
3. The distribution of orbital period ratios of adjacent planets in multiple planet systems ([Lissauer et al. 2011b](#); [Fabrycky et al. 2014](#)). Of particular curiosity is the fact that the distribution is not preferentially peaked at first order MMRs (as Type-1 migration models would predict) *and* is also not particularly uniform ([Fabrycky et al. 2014](#)).
4. The division between rocky super-Earths and gas-rich mini-Neptunes at $\sim 1.5 R_{\oplus}$ ([Weiss and Marcy 2014](#); [Lopez and Fortney 2014](#); [Rogers 2015](#); [Wolfgang et al. 2016](#); [Chen and Kipping 2017](#)).

Many models have been proposed to explain the origin of super-Earths. Before almost any super-Earths were known, [Raymond et al. \(2008\)](#) proposed six potential formation pathways for their formation and laid out a simple framework to use observations of system architecture and planet bulk density to differentiate between them. Several of those pathways were quickly disproven because they did not match observations; for instance, one mechanism proposed that super-Earths form from material shepherd inward by a migrating giant planet ([Fogg and Nelson 2005, 2007](#); [Raymond et al. 2006a](#); [Mandell et al. 2007](#)). It was quickly shown that there is no correlation between close-in gas giants and super-Earths – to the contrary, there is generally an anti-correlation between hot Jupiters and other close-in planets ([Latham et al. 2011](#); [Steffen et al. 2012](#)).

At the time of the writing of this chapter, two models remain viable: the *migration* and *drift* models. Nevertheless, it is still worth explaining why simple, in-situ growth of super-Earths is not a viable formation mechanism. In-situ growth of super-Earths was first proposed by [Raymond et al. \(2008\)](#), and immediately discarded because of the prohibitively large disk masses required. It was re-proposed by [Hansen and Murray \(2012, 2013\)](#) and [Chiang and Laughlin \(2013\)](#), and was again refuted for both dynamical and disk-related reasons ([Raymond and Cossou 2014](#); [Schlichting 2014](#); [Schlaufman 2014](#); [Inamdar and Schlichting 2015](#); [Ogihara et al. 2015](#)). The simplest argument against in-situ growth is as follows. If super-Earths form in-situ then they must grow extremely quickly because in extremely dense disks possessing many Earth-masses worth of material extremely close to the central star. However, if planets form that quickly in massive gas disks, they must migrate. In fact, the disks required to build super-Earths close-in are so dense that aerodynamic drag acts on

full-grown planets on a shorter timescale than the disk dissipation timescale (Inamdar and Schlichting 2015). Thus, in-situ growth implies that planets must migrate. If they migrate then their orbits change and thus they cannot truly form “in-situ”.

The drift model proposes that planets form sequentially in concentric, gravitationally unstable rings that form as dust drifts inward. Dust is indeed expected to coagulate and drift inward (e.g. Birnstiel et al. 2012) and if there exists a trap in its route towards the central star, a fraction of the mass in drifting pebbles can be captured. Chatterjee and Tan (2014) proposed that, once a pebble ring attains a high enough density, it can directly collapse into a full-sized planet. The inner edge of the dead-zone (the region where collapse can occur) subsequently retreats, thus shifting the formation location of the next super-Earth. This model is promising and the subject of a series of papers (Chatterjee and Tan 2014, 2015; Boley et al. 2014; Hu et al. 2016, 2017). However, additional work is still required to comprehensively address each of the constraints listed above.

The migration model proposes that planetary embryos grow far from the central star, and subsequently move inward via Type-I migration (see example in Fig. 8; Goldreich and Tremaine 1980; Ward 1986; Tanaka et al. 2002). Given that disks have magnetically-truncated inner edges (e.g. Romanova et al. 2003, 2004), inward migrating embryos may be caught at so-called planet traps (Lyra et al. 2010; Hasegawa and Pudritz 2011, 2012; Horn et al. 2012; Bitsch et al. 2014; Alessi et al. 2017) before eventually reaching the inner edge where a strong torque prevents them from falling onto the star (Masset et al. 2006). Systems of migrating embryos thus pile up into chains of mean motion resonances anchored at the inner edge of the disk (Cresswell et al. 2007; Terquem and Papaloizou 2007; Ogihara and Ida 2009; McNeil and Nelson 2010; Cossou et al. 2014; Izidoro et al. 2014b). While collisions are common during this phase, they only temporarily destabilize the resonant chain before it is quickly reconstituted. Short lived gaseous disks (e.g. Hasegawa and Pudritz 2011; Bitsch et al. 2015; Alessi et al. 2017) or reduced gas accretion rates (Lambrechts and Lega 2017) have been proposed as potential mechanisms for preventing these embryos from growing further and becoming gas giant planets before they have a chance to migrate inward. When the disk dissipates, eccentricities and inclinations of the resonant planets are no longer damped (Tanaka and Ward 2004; Cresswell et al. 2007; Bitsch and Kley 2010). This causes most resonant chains to become unstable, and triggers a late phase of giant collisions in a gas-free (or at least, very low gas density) environment (Terquem and Papaloizou 2007; Ogihara and Ida 2009; Cossou et al. 2014; Izidoro et al. 2017, 2021). Assuming that 5-10% of systems remain stable after the disk dissipates, the surviving systems in simulations of this process provide a quantitative match to both the observed super-Earth period ratio and multiplicity distributions (Izidoro et al. 2017, 2021). In this manner, the Kepler dichotomy is an observational artifact generated by the bimodal inclination distribution of super-Earths, a few of which have very low mutual inclinations (and thus a high probability of being discovered as multiple systems), however the majority have significant mutual inclinations that are the consequence of these late instabilities (Izidoro et al. 2017). The model also necessarily explains the existence of super-Earths in resonant chains like Kepler-223 (Mills et al. 2016).

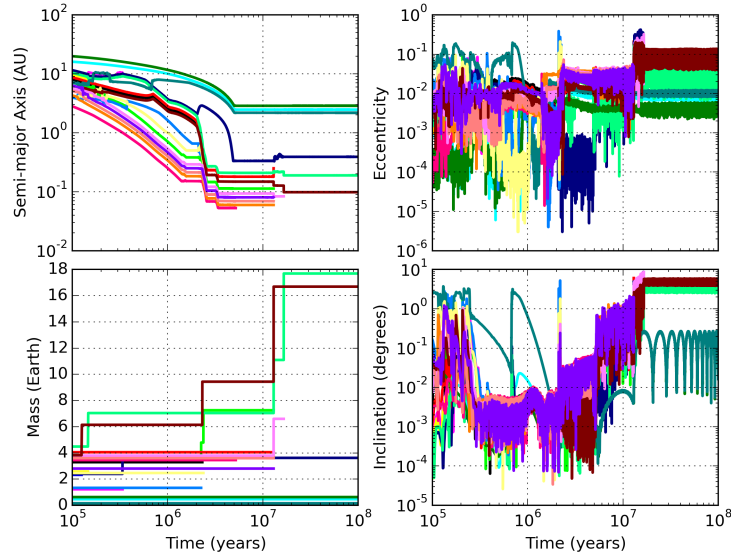


Fig. 8 Mass and orbital evolution of a system forming close-in super-Earths, reproduced from [Izidoro et al. \(2017\)](#). A set of \sim Earth-mass planetary embryos are initialized beyond the snowline and subsequently migrate inward (undergoing occasional collisions as they do) to create a long resonant chain. In the plotted case, 10 super-Earths initially reside in a chain of resonances interior to 0.5 AU. When the gas disk dissipates at 5 Myr, the system remained quasi-stable for a few Myr before eventually undergoing a large scale instability that leads to a phase of late collisions. The final system consists of just three (relatively massive) super-Earths with modest eccentricities and a large enough mutual inclinations to preclude the transit detection of all three planets.

How can we hope to use observations to differentiate between the drift and migration models? In its current form the migration model is built on the assumption that embryos large enough to migrate should preferentially form far from their stars, past the snowline. In the Solar System it is indeed thought that large embryos formed in the outer Solar System and became the cores of the giant planets, whereas small embryos formed in the inner Solar System and became the building blocks of the terrestrial planets ([Morbidelli et al. 2015b](#)). Given their distant formation zones, the migration model thus predicts that super-Earths should be predominantly water-rich with correspondingly low densities ([Raymond et al. 2008](#)). In contrast, inward migrating pebbles in the drift model should have time to devolatilize before they collapse into proto-planets, and the resulting accretion super-Earths should be predominantly rocky. However, this difference depends strongly on where the first planetesimals form, as these serve as the seeds for embryo growth. This question is unresolved: some studies find that planetesimals first form at ~ 1 AU ([Drazkowska et al. 2016](#)) whereas others find that planetesimals first form past the snowline ([Armitage et al. 2016b](#); [Drazkowska and Alibert 2017](#); [Carrera et al. 2017](#)).

The transition between super-Earths and sub-Neptunes is thought to be a result of a competition between accretion and erosion (Ginzburg et al. 2016; Lee and Chiang 2016, see also chapter by Schlichting). Growing planetary embryos accrete primitive atmospheres from the disk (e.g. Lee et al. 2014; Inamdar and Schlichting 2015), but accretion is slowed by heating associated with small impacts (Hubickyj et al. 2005), and also eroded by large impacts (Inamdar and Schlichting 2016) during the disk's dissipation (Ikoma and Hori 2012; Ginzburg et al. 2016). Photo-evaporation of close-in planets may also play an important role by preferentially stripping the atmospheres of low-mass, highly-irradiated planets (Owen and Wu 2013, 2017; Lopez and Rice 2016). Planets located in the “photo-evaporation valley” – the region of very close-in orbits where any atmospheres should have been stripped from low-mass planets – appear to be mostly rocky (Lopez 2017; Jin and Mordasini 2018). Of course, this only applies for the closest-in planets, which can be plausibly built from rocky material shepherded inward by migrating, volatile-rich planets in the migration model (Izidoro et al. 2014b). However, it is extremely difficult to accurately determine the compositions of more distant planets because they can be derived from at least three different types of building blocks: rock, water and Hydrogen (Selsis et al. 2007; Adams et al. 2008). Thus, only the most extreme densities can provide useful insights (e.g., very high density planets are likely to have little water or Hydrogen).

Terrestrial planet forming in systems with giant exoplanets

The dynamical evolution of such systems is thought to be quite different than that of Jupiter and Saturn. Indeed, the median eccentricity of giant exoplanets is 0.25 (Butler et al. 2006b; Udry and Santos 2007b), five times larger than that of Jupiter and Saturn. Although observational biases preclude a clear determination, most giant exoplanets are also located somewhat closer to their stars than the solar system's gas giants (typically at 1-2 AU: Cumming et al. 2008; Mayor et al. 2011b; Rowan et al. 2016; Wittenmyer et al. 2016).

Two key processes are thought to be responsible for shaping the orbital distribution of giant exoplanets: type II inward migration and planet-planet scattering. While Jupiter and Saturn certainly migrated, the extent of migration remains unclear. Similarly, a wide range of migration schemes are possible for exoplanets. Indeed, some may have migrated all the way to the inner edge of the disk to become hot Jupiters (Lin and Papaloizou 1986; Lin et al. 1996). The high eccentricities of giant exoplanets are easily explained if the observed planets are the survivors of system-wide instabilities during which giant planets scattered repeatedly off of each other during close passages inside each others' Hill spheres (Rasio and Ford 1996; Weidenschilling and Marzari 1996; Lin and Ida 1997; Adams and Laughlin 2003; Moorhead and Adams 2005; Ford et al. 2003; Chatterjee et al. 2008a; Ford and Rasio 2008a; Raymond et al. 2008, 2010a). This phase of planet-planet scattering typically concludes with the ejection of one or more planets. In some cases scat-

tering can push planets to sufficiently high eccentricities that they pass very close to their stars at pericenter; thus allowing tidal dissipation to circularize and shrink their orbits. This has been proposed as an alternate channel for the formation of hot Jupiters (Nagasawa et al. 2008; Beaugé and Nesvorný 2012).

It is natural to question how giant planet migration and scattering affect the growth and evolution of potential terrestrial planets. Giant planet migration has been shown to be much less destructive to would-be terrestrial planets than was generally assumed in the late 1990s and early 2000s (Gonzalez et al. 2001; Lineweaver et al. 2004). An inward-migrating gas giant does not simply collide with the material in its path (except in rare circumstances; Tanaka and Ida 1999). Rather, strong inner mean motion resonances acting in concert with gas drag shepherd material inward, often helping to catalyze the formation of planets interior to the giant planets' final orbits (Fogg and Nelson 2005, 2007; Raymond et al. 2006a; Mandell et al. 2007). Moreover, a significant amount of the material undergoing close encounters with the migrating giant planet is scattered outward and stranded on eccentric and inclined orbits. This material can subsequently re-accumulate into a generation of terrestrial planets that tend to have extremely wide feeding zones and are thus very volatile-rich (Raymond et al. 2006a; Mandell et al. 2007).

The eccentricity distribution of eccentric giant planets can be matched by planet-planet scattering models (e.g. Chatterjee et al. 2008b; Jurić and Tremaine 2008; Ford and Rasio 2008b; Raymond et al. 2010b). In contrast to giant planet migration, giant planet scattering is typically very harmful to the process of terrestrial planet formation. When gas giants destabilize they scatter each other onto eccentric orbits, and any small bodies (planetesimals, planetary embryos or planets) in their path are typically destroyed (Veras and Armitage 2005, 2006; Raymond et al. 2011, 2012; Matsumura et al. 2013; Marzari 2014; Carrera et al. 2016). Objects that are closer-in than the gas giants are preferentially driven onto such eccentric orbits that they collide with the host star, whereas more distant objects are typically ejected (Raymond et al. 2011, 2017; Marzari 2014).

Putting our Solar System in context

How can we understand our Solar System in a larger context? What are the key processes that make our system different than most?

Jupiter is likely the Solar System's primary architect. Let us consider its potential effects on the greater system at different phases of its growth. Jupiter's core was perhaps seeded by an early generation of planetesimals that then grew by pebble accretion (Ormel et al. 2010b; Lambrechts and Johansen 2012b, 2014; Chambers 2021). It is unclear *where* this took place. Studies have covered the full spectrum of possibilities, from distant formation followed by inward migration (Bitsch et al. 2015; Deienno et al. 2022) to in-situ growth (Levison et al. 2015a) to close-in formation followed by outward migration (Raymond et al. 2016b). Nonetheless, once its core reached $\sim 20 M_{\oplus}$ it likely created a pressure bump exterior to its orbit that

blocked the inward pebble flux (Lambrechts et al. 2014; Kruijer et al. 2017a). This acted to starve the inner Solar System of the raw materials needed to form super-Earths or giant planets (Morbidelli et al. 2015b; Lambrechts et al. 2019; Izidoro et al. 2022a; Chambers 2023).

Although the direction, duration and speed are uncertain, Jupiter's core subsequently migrated; thereby shepherding any nearby cores and planetesimals (Izidoro et al. 2014b). When Jupiter underwent rapid gas accretion it strongly perturbed the orbits nearby small bodies, scattering them across the Solar System (and implanting some in the inner Solar System Raymond and Izidoro 2017a). It carved a gap in the disk and transitioned to slower, Type-II migration (Lin and Papaloizou 1986; Ward 1997; Crida et al. 2006). Jupiter now served as a strong barrier for more distant planetary embryos that would otherwise migrate inward to become close-in super-Earths (Terquem and Papaloizou 2007; Ogihara and Ida 2009; Izidoro et al. 2015b). Blocked by Jupiter and Saturn, these embryos instead continued to accrete embryos in-place and became the ice giants (Jakubík et al. 2012; Izidoro et al. 2015a; Chau et al. 2021). Once the disk dissipated, Jupiter's dynamical influence played a key role in the late-stage accretion of the terrestrial planets and the dynamical sculpting of the asteroid belt (particularly during the epoch of giant planet instability, Raymond et al. 2014; Deienno et al. 2018; Clement et al. 2018).

There are thus two potential ways that Jupiter may explain why the Solar System is different, specifically our lack of super-Earths. The first is by blocking the pebble flux and starving the growing terrestrial planetary embryos. The second is by blocking the inward migration of large cores (Izidoro et al. 2015a).

Considering only the Sun and Jupiter, exoplanet statistics tell us that the Solar System is already at best a 1% outlier (and more like 0.1% when considering all stellar types: Petigura et al. 2018; Gan et al. 2023; Belezny and Kunimoto 2022; Bryant et al. 2023). Yet it is likely that Earth-sized planets on Earth-like orbits may be far more common. The Drake equation parameter η_{Earth} – the fraction of stars that host a roughly Earth-mass or Earth-sized planet in the habitable zone – has been directly measured for low-mass stars to be tens of percent (Bonfils et al. 2013; Kopparapu 2013; Dressing and Charbonneau 2015; Bergsten et al. 2023). Yet how 'Earth-like' are such planets? Without Jupiter, would a planet at Earth's distance still look like our own Earth?

When viewed through the lens of planet formation, two of Earth's characteristics are unusual: its water content and formation timescale. The building blocks of planets tend to either be very dry (possessing only a fraction of a percent of water like non-carbonaceous chondrites) or very wet ($\sim 10\%$ water like carbonaceous chondrites, or $\sim 50\%$ water like comets). In contrast, Earth's composition can be explained by having grown mostly from dry material with only a sprinkling of wet material (Marty 2012; Dauphas 2017; Dauphas et al. 2024). A simple explanation for this mixture is that, even though Jupiter's formation provided a sprinkling of water-rich material (Raymond and Izidoro 2017a), once the giant planets grew large enough they blocked all subsequent water delivery (e.g. Morbidelli et al. 2016; Sato et al. 2016). Without Jupiter it stands to reason that Earth should either be completely dry or, more likely, much wetter.

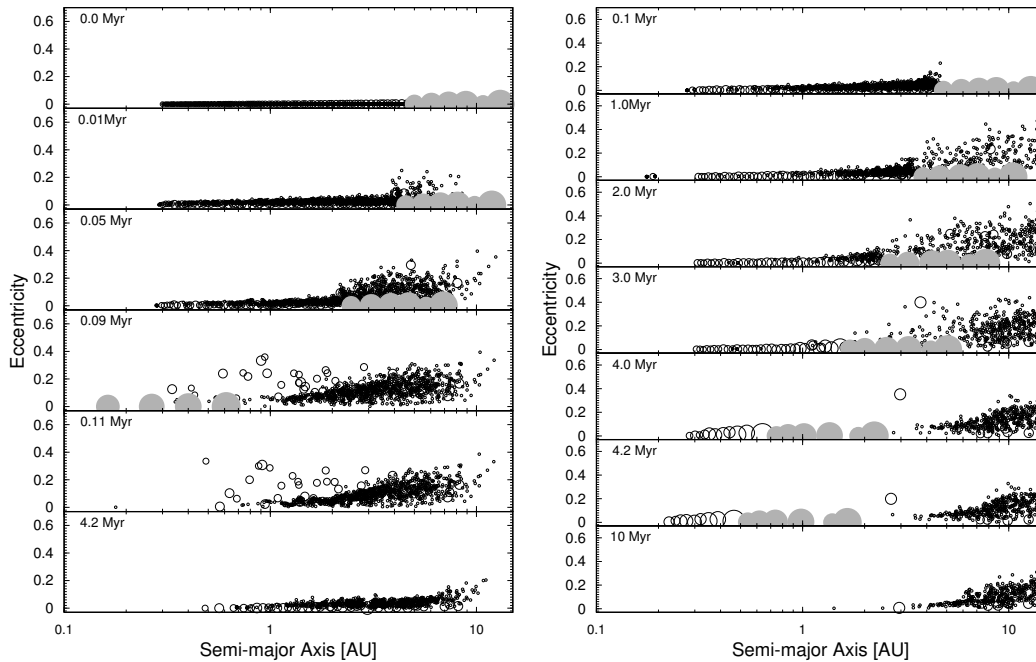


Fig. 9 Snapshots of the dynamical evolution of a population of planetesimal and planetary embryos in the presence of migrating super-Earths. The gray filled circles represent the super-Earths. Planetary embryos and planetesimals are shown by open circles and small dots, respectively. The super-Earth system is composed of six super-Earths with masses roughly similar to those of the Kepler 11 system (e.g. [Lissauer et al. 2013](#)). The left-panel shows a simulation where the system of super-Earths migrate fast, in a short timescale of about 100 kyr. The right-panel represents a simulation where the system of super-Earths migrate slowly, in a timescale comparable to the disk lifetime. Figure adapted from ([Izidoro et al. 2014b](#))

Earth’s last giant impact is constrained not to have happened earlier than ~ 40 Myr after CAIs ([Touboul et al. 2007](#); [Kleine et al. 2009](#); [Avice et al. 2017](#)). However, most ‘Earth-like’ planets probably form much faster. Super-Earths typically complete their formation shortly after dispersal of the gaseous disk ([Izidoro et al. 2017](#); [Alessi et al. 2017](#)). Accretion in the terrestrial planet zone of low-mass stars is similarly fast whether or not migration is accounted for ([Raymond et al. 2007b](#); [Lissauer 2007](#); [Ogihara and Ida 2009](#); [Clement et al. 2022](#)). The geophysical consequences of fast accretion remain to be further explored, but it stands to reason that fast-growing planets are likely to be hotter and may thus lose more of their water compared with slower-growing planets like Earth. This could in principle counteract our previous assertion that most terrestrial planets should be wetter than Earth.

While other Earths remain a glamorous target for exoplanet searches, developing a more comprehensive understanding of the ways in which exoplanets are similar to, and different than the worlds of our own Solar System is also an extremely compelling line of inquiry. For instance, constraining the abundance and configuration of

ice giants on orbits exterior to gas giants will significantly bolster our understanding of orbital migration and dynamical instabilities. Likewise, the radial ordering of systems with different-sized planets at different orbital distances will constrain models of pebble accretion.

Summary

This chapter reviewed the current paradigm of terrestrial planet formation; from dust-coagulation to planetesimal formation to late stage accretion. It discussed the classic scenario of terrestrial planet formation, its well-documented shortcomings, and recently proposed alternatives that resolve these issues such as the Grand-Tack model, Early Instability model and the Planet Formation from Rings scenario. It also discussed the origins of hot super-Earths, placed the Solar System in the context of exoplanets and discussed terrestrial planet formation in exoplanetary systems. The following bullets summarize key advances the study of planet formation, and outstanding questions that continue to drive future investigation:

- The streaming instability stands as a promising mechanism for explaining how mm- to cm-sized particles grow to 100 km-scale planetesimals. Yet the streaming instability require specific conditions to operate. This implies that planetesimals may form in preferential locations (e.g., just beyond the snowline) that will in turn strongly influence the further formation of the system.
- Planetesimals grow into planetary embryos (or giant planet cores) by accreting planetesimals or pebbles (or a combination of both). Simulations of planetesimal accretion struggle to grow giant planet cores within the lifetime of protoplanetary disks. pebble accretion may solve this long-standing timescale conflict, but many key aspects of pebble accretion remain largely unexplored.
- Three models of the late stage of accretion of terrestrial planet can explain the structure of the inner Solar System: the Grand-Tack, an early giant planet instability and Planet Formation from Rings. A clear future step in planet formation is to differentiate between these models. Combining N-body simulations with geochemical models will undoubtedly be a powerful tool in this pursuit.
- Of the Solar System's planets, the origin of Mercury is the most mysterious. In particular, it remains unclear whether the small planet acquired its high iron-content and relatively large core through a giant impact or by forming from a population of chemically distinct planetesimals. The discovery of additional exoplanets with Mercury-like densities (super-Mercuries) might help to break degeneracies between these scenarios in the future.
- Hot super-Earths cannot form by pure in-situ accretion. Super-Earths forming in-situ would grow extremely fast because of the large solid masses required in the inner regions and the corresponding short dynamical timescales. If super-Earths form rapidly in the gaseous disk, they must migrate and not form 'in-situ'.
- Close-in super-Earths may have formed farther from their stars and migrated inward. Migration creates resonant chains anchored at the inner edge of the disk,

most of which destabilize when the disk dissipates. Simulations of this process have been used to quantitatively match the orbital architectures of known super-Earths-hosting systems. No system of super-Earths is likely to have formed in the Solar System simply because it should still exist today (given that disks have inner edges that prevent planets from migrating onto their stars).

- The Solar System is quantifiably unusual in its lack of super-Earths and in having a wide-orbit gas giant on a low-eccentricity orbit (a $\lesssim 1\%$ rarity among Sun-like stars). These two characteristics may be linked, as Jupiter may have prevented Uranus and Neptune's proto-planet precursors from invading the inner Solar System. Additionally, the fortuitous lack of close encounters between Jupiter and Saturn during the Solar System's instability likely prevented the destruction of the terrestrial planets.
- Future exoplanet surveys providing data on the occurrence of planets at moderate distances from the host star and more refined constraints on the bulk composition of transiting low-mass planets will shed light on the deep mysteries of terrestrial planet formation.

Acknowledgements We acknowledge a large community of colleagues whose contributions made this review possible. M.S.C. is supported by NASA Emerging Worlds grant 80NSSC23K0868 and NASA's CHAMPs team, supported by NASA under Grant No. 80NSSC21K0905 issued through the Interdisciplinary Consortia for Astrobiology Research (ICAR) program. S.N.R. thanks the CNRS's Programme Nationale de Planetologie (PNP) and MITI/80PRIME program for support. The work of R.D. was supported by the NASA Emerging Worlds program, grant 80NSSC21K0387.

References

- Aarseth SJ, Lin DNC Palmer PL (1993) Evolution of Planetesimals. II. Numerical Simulations. *ApJ*403:351
- Adachi I, Hayashi C Nakazawa K (1976) The gas drag effect on the elliptical motion of a solid body in the primordial solar nebula. *Progress of Theoretical Physics* 56:1756–1771
- Adams ER, Seager S Elkins-Tanton L (2008) Ocean Planet or Thick Atmosphere: On the Mass-Radius Relationship for Solid Exoplanets with Massive Atmospheres. *ApJ*673:1160–1164
- Adams FC Laughlin G (2003) Migration and dynamical relaxation in crowded systems of giant planets. *Icarus* 163:290–306
- Agnor CB Lin DNC (2012) On the Migration of Jupiter and Saturn: Constraints from Linear Models of Secular Resonant Coupling with the Terrestrial Planets. *ApJ*745:143
- Agnor CB, Canup RM Levison HF (1999) On the Character and Consequences of Large Impacts in the Late Stage of Terrestrial Planet Formation. *Icarus*142:219–237
- Alessi M, Pudritz RE Cridland AJ (2017) On the formation and chemical composition of super Earths. *MNRAS*464:428–452
- Alexander CMO (2022) An exploration of whether Earth can be built from chondritic components, not bulk chondrites. *Geochim Cosmochim Acta*318:428–451
- Alexander CMO, Bowden R, Fogel ML et al. (2012) The Provenances of Asteroids, and Their Contributions to the Volatile Inventories of the Terrestrial Planets. *Science* 337:721
- Alexander R, Pascucci I, Andrews S, Armitage P Cieza L (2014) The Dispersal of Protoplanetary Disks. *Protostars and Planets VI* pp 475–496

- Alibert Y (2017) Maximum mass of planetary embryos that formed in core-accretion models. *A&A*606:A69
- Alibert Y, Mordasini C, Benz W, Winisdoerffer C (2005) Models of giant planet formation with migration and disc evolution. *A&A*434:343–353
- Allègre CJ, Manhès G, Göpel C (2008) The major differentiation of the Earth at ~ 4.45 Ga. *Earth and Planetary Science Letters* 267:386–398
- Allibert L, Siebert J, Charnoz S, Jacobson SA, Raymond SN (2023) The effect of collisional erosion on the composition of Earth-analog planets in Grand Tack models: Implications for the formation of the Earth. *Icarus*391:115325
- ALMA Partnership, Brogan CL, Pérez LM et al. (2015) The 2014 ALMA Long Baseline Campaign: First Results from High Angular Resolution Observations toward the HL Tau Region. *ApJ*808:L3
- Amelin Y, Kaltenbach A, Iizuka T et al. (2010) U-Pb chronology of the Solar System's oldest solids with variable $^{238}\text{U}/^{235}\text{U}$. *Earth and Planetary Science Letters* 300(3-4):343–350
- André P, Di Francesco J, Ward-Thompson D et al. (2014) From Filamentary Networks to Dense Cores in Molecular Clouds: Toward a New Paradigm for Star Formation. *Protostars and Planets VI* pp 27–51
- Andrews SM (2020) Observations of Protoplanetary Disk Structures. *ARA&A*58:483–528
- Andrews SM, Wilner DJ, Hughes AM, Qi C, Dullemond CP (2010) Protoplanetary Disk Structures in Ophiuchus. II. Extension to Fainter Sources. *ApJ*723:1241–1254
- Andrews SM, Huang J, Pérez LM et al. (2018) The Disk Substructures at High Angular Resolution Project (DSHARP). I. Motivation, Sample, Calibration, and Overview. *ApJ*869(2):L41
- Ansdell M, Williams JP, Manara CF et al. (2017) An ALMA Survey of Protoplanetary Disks in the σ Orionis Cluster. *AJ*153:240
- Appelgren J, Lambrechts M, Johansen A (2020) Dust clearing by radial drift in evolving protoplanetary discs. *A&A*638:A156
- Armitage PJ (2011) Dynamics of Protoplanetary Disks. *ARA&A*49:195–236
- Armitage PJ, Eisner JA, Simon JB (2016a) Prompt Planetesimal Formation beyond the Snow Line. *ApJ*828:L2
- Armitage PJ, Eisner JA, Simon JB (2016b) Prompt Planetesimal Formation beyond the Snow Line. *ApJ*828:L2
- Asphaug E, Reufer A (2014) Mercury and other iron-rich planetary bodies as relics of inefficient accretion. *Nature Geoscience* 7:564–568
- Asphaug E, Jutzi M, Movshovitz N (2011) Chondrule formation during planetesimal accretion. *Earth and Planetary Science Letters* 308:369–379
- Avice G, Marty B, Burgess R (2017) The origin and degassing history of the Earth's atmosphere revealed by Archean xenon. *Nature Communications* 8:15455
- Badro J, Côté AS, Brodholt JP (2014) A seismologically consistent compositional model of Earth's core. *Proceedings of the National Academy of Science* 111:7542–7545
- Bae J, Zhu Z, Baruteau C et al. (2019) An Ideal Testbed for Planet-Disk Interaction: Two Giant Protoplanets in Resonance Shaping the PDS 70 Protoplanetary Disk. *ApJ*884(2):L41
- Bae J, Isella A, Zhu Z et al. (2023) Structured Distributions of Gas and Solids in Protoplanetary Disks. In: Inutsuka S, Aikawa Y, Muto T, Tomida K, Tamura M (eds) *Astronomical Society of the Pacific Conference Series, Astronomical Society of the Pacific Conference Series*, vol 534, p 423
- Bai XN, Stone JM (2010) Dynamics of Solids in the Midplane of Protoplanetary Disks: Implications for Planetesimal Formation. *ApJ*722:1437–1459
- Baker VR, Strom RG, Gulick VC, Kargel JS, Komatsu G (1991) Ancient oceans, ice sheets and the hydrological cycle on Mars. *Nature*352:589–594
- Balbus SA (2003) Enhanced Angular Momentum Transport in Accretion Disks. *ARA&A*41:555–597
- Balbus SA, Hawley JF (1991) A powerful local shear instability in weakly magnetized disks. I - Linear analysis. II - Nonlinear evolution. *ApJ*376:214–233

- Barge P, Richard S Le Dizès S (2016) Vortices in stratified protoplanetary disks. From baroclinic instability to vortex layers. *A&A*592:A136
- Barker AJ Latter HN (2015) On the vertical-shear instability in astrophysical discs. *MNRAS*450:21–37
- Barnes R, Quinn TR, Lissauer JJ Richardson DC (2009) N-Body simulations of growth from 1 km planetesimals at 0.4 AU. *Icarus*203:626–643
- Bate MR (2018) On the diversity and statistical properties of protostellar discs. *MNRAS*
- Batygin K Laughlin G (2015) Jupiter’s decisive role in the inner Solar System’s early evolution. *Proceedings of the National Academy of Science* 112:4214–4217
- Batygin K, Brown ME Betts H (2012) Instability-driven Dynamical Evolution Model of a Primordially Five-planet Outer Solar System. *ApJ*744:L3
- Beauge C Aarseth SJ (1990) N-body simulations of planetary formation. *MNRAS*245:30–39
- Beaugé C Nesvorný D (2012) Multiple-planet Scattering and the Origin of Hot Jupiters. *ApJ*751:119
- Becker H, Horan MF, Walker RJ et al. (2006) Highly siderophile element composition of the Earth’s primitive upper mantle: Constraints from new data on peridotite massifs and xenoliths. *Geochim Cosmochim Acta*70(17):4528–4550
- Beckwith SVW, Sargent AL, Chini RS Guesten R (1990) A survey for circumstellar disks around young stellar objects. *AJ*99:924–945
- Beleznyay M Kunimoto M (2022) Exploring the dependence of hot Jupiter occurrence rates on stellar mass with TESS. *MNRAS*516(1):75–83
- Benítez-Llambay P, Masset F, Koenigsberger G Szulágyi J (2015) Planet heating prevents inward migration of planetary cores. *Nature*520(7545):63–65
- Benz W, Slattery WL Cameron AGW (1986) The origin of the moon and the single-impact hypothesis I. *Icarus*66(3):515–535
- Benz W, Slattery WL Cameron AGW (1988) Collisional stripping of Mercury’s mantle. *Icarus*74:516–528
- Benz W, Anic A, Horner J Whitby JA (2007) The Origin of Mercury. *Space Sci Rev*132:189–202
- Bergsten GJ, Pascucci I, Hardegree-Ullman KK et al. (2023) No Evidence for More Earth-sized Planets in the Habitable Zone of Kepler’s M versus FGK Stars. *arXiv e-prints arXiv:2310.11613*
- Birch F (1952) Elasticity and Constitution of the Earth’s Interior. *J Geophys Res*57(2):227–286
- Birnstiel T, Ormel CW Dullemond CP (2011) Dust size distributions in coagulation/fragmentation equilibrium: numerical solutions and analytical fits. *A&A*525:A11
- Birnstiel T, Klahr H Ercolano B (2012) A simple model for the evolution of the dust population in protoplanetary disks. *A&A*539:A148
- Birnstiel T, Fang M Johansen A (2016) Dust Evolution and the Formation of Planetesimals. *Space Sci Rev*205(1-4):41–75
- Bitsch B Kley W (2010) Orbital evolution of eccentric planets in radiative discs. *A&A*523:A30
- Bitsch B, Morbidelli A, Lega E Crida A (2014) Stellar irradiated discs and implications on migration of embedded planets. II. Accreting-discs. *A&A*564:A135
- Bitsch B, Lambrechts M Johansen A (2015) The growth of planets by pebble accretion in evolving protoplanetary discs. *A&A*582:A112
- Bitsch B, Izidoro A, Johansen A et al. (2019) Formation of planetary systems by pebble accretion and migration: growth of gas giants. *A&A*623:A88
- Blum J Wurm G (2000) Experiments on Sticking, Restructuring, and Fragmentation of Preplanetary Dust Aggregates. *Icarus*143:138–146
- Blum J Wurm G (2008) The Growth Mechanisms of Macroscopic Bodies in Protoplanetary Disks. *ARA&A*46:21–56
- Blum J, Wurm G, Kempf S et al. (2000) Growth and Form of Planetary Seedlings: Results from a Microgravity Aggregation Experiment. *Physical Review Letters* 85:2426–2429
- Bodenheimer P Pollack JB (1986) Calculations of the accretion and evolution of giant planets The effects of solid cores. *Icarus*67:391–408

- Boehneke P Harrison TM (2016) Illusory Late Heavy Bombardments. *Proceedings of the National Academy of Science* 113:10,802–10,806
- Boley AC, Morris MA Ford EB (2014) Overcoming the Meter Barrier and the Formation of Systems with Tightly Packed Inner Planets (STIPs). *ApJ*792:L27
- Bonfils X, Delfosse X, Udry S et al. (2013) The HARPS search for southern extra-solar planets. XXXI. The M-dwarf sample. *A&A*549:A109
- Borucki WJ, Koch D, Basri G et al. (2010a) Kepler Planet-Detection Mission: Introduction and First Results. *Science* 327:977
- Borucki WJ, Koch D, Basri G et al. (2010b) Kepler Planet-Detection Mission: Introduction and First Results. *Science* 327:977–
- Boss AP (1997) Giant planet formation by gravitational instability. *Science* 276:1836–1839
- Bottke WF, Walker RJ, Day JMD, Nesvorný D Elkins-Tanton L (2010) Stochastic Late Accretion to Earth, the Moon, and Mars. *Science* 330(6010):1527
- Bouvier A Wadhwa M (2010) The age of the Solar System redefined by the oldest Pb-Pb age of a meteoritic inclusion. *Nature Geoscience* 3:637–641
- Brasser R Mojzsis SJ (2020) The partitioning of the inner and outer Solar System by a structured protoplanetary disk. *Nature Astronomy* 4:492–499
- Brasser R, Morbidelli A, Gomes R, Tsiganis K Levison HF (2009) Constructing the secular architecture of the solar system II: the terrestrial planets. *A&A*507:1053–1065
- Brasser R, Walsh KJ Nesvorný D (2013) Constraining the primordial orbits of the terrestrial planets. *MNRAS*433:3417–3427
- Brasser R, Matsumura S, Ida S, Mojzsis SJ Werner SC (2016) Analysis of Terrestrial Planet Formation by the Grand Tack Model: System Architecture and Tack Location. *ApJ*821:75
- Brasser R, Werner S Mojzsis S (2020) Impact bombardment chronology of the terrestrial planets from 4.5 ga to 3.5 ga. *Icarus* 338:113,514, URL <http://www.sciencedirect.com/science/article/pii/S0019103519302982>
- Brauer F, Dullemond CP, Johansen A et al. (2007) Survival of the mm-cm size grain population observed in protoplanetary disks. *A&A*469:1169–1182
- Brauer F, Henning T Dullemond CP (2008) Planetesimal formation near the snow line in MRI-driven turbulent protoplanetary disks. *A&A*487:L1–L4
- Briceño C, Vivas AK, Calvet N et al. (2001) The CIDA-QUEST Large-Scale Survey of Orion OB1: Evidence for Rapid Disk Dissipation in a Dispersed Stellar Population. *Science* 291:93–97
- Bromley BC Kenyon SJ (2011) A New Hybrid N-body-coagulation Code for the Formation of Gas Giant Planets. *ApJ*731:101
- Bromley BC Kenyon SJ (2017) Terrestrial Planet Formation: Dynamical Shake-up and the Low Mass of Mars. *AJ*153:216
- Brouwers MG, Vazan A Ormel CW (2017) How cores grow by pebble accretion I. Direct core growth. *ArXiv e-prints*
- Brož M, Chrenko O, Nesvorný D Dauphas N (2021) Early terrestrial planet formation by torque-driven convergent migration of planetary embryos. *Nature Astronomy*
- Brunngräber R Wolf S (2021) Self-scattering on large, porous grains in protoplanetary disks with dust settling. *A&A*648:A87
- Bryant EM, Bayliss D Van Eylen V (2023) The occurrence rate of giant planets orbiting low-mass stars with TESS. *MNRAS*521(3):3663–3681
- Budde G, Burkhardt C, Brennecke GA et al. (2016) Molybdenum isotopic evidence for the origin of chondrules and a distinct genetic heritage of carbonaceous and non-carbonaceous meteorites. *Earth and Planetary Science Letters* 454:293–303
- Butler RP, Wright JT, Marcy GW et al. (2006a) Catalog of Nearby Exoplanets. *ApJ*646:505–522
- Butler RP, Wright JT, Marcy GW et al. (2006b) Catalog of Nearby Exoplanets. *ApJ*646:505–522
- Cameron AGW (1985) Formation of the prelunar accretion disk. *Icarus*62(2):319–327
- Canup RM (2004) Simulations of a late lunar-forming impact. *Icarus*168(2):433–456
- Carrera D, Davies MB Johansen A (2016) Survival of habitable planets in unstable planetary systems. *MNRAS*463:3226–3238

- Carrera D, Gorti U, Johansen A, Davies MB (2017) Planetesimal Formation by the Streaming Instability in a Photoevaporating Disk. *ApJ*839:16
- Carter PJ, Leinhardt ZM, Elliott T, Walter MJ, Stewart ST (2015) Compositional Evolution during Rocky Protoplanet Accretion. *ApJ*813(1):72
- Chambers J (2006) A semi-analytic model for oligarchic growth. *Icarus*180:496–513
- Chambers J (2021) Rapid Formation of Jupiter and Wide-orbit Exoplanets in Disks with Pressure Bumps. *ApJ*914(2):102
- Chambers J (2023) Making the Solar System. *ApJ*944(2):127
- Chambers JE (1999) A hybrid symplectic integrator that permits close encounters between massive bodies. *MNRAS*304:793–799
- Chambers JE (2001) Making More Terrestrial Planets. *Icarus*152:205–224
- Chambers JE (2010) Planetesimal formation by turbulent concentration. *Icarus*208:505–517
- Chambers JE (2013) Late-stage planetary accretion including hit-and-run collisions and fragmentation. *Icarus*224(1):43–56
- Chambers JE (2016) Pebble Accretion and the Diversity of Planetary Systems. *ApJ*825:63
- Chambers JE, Cassen P (2002) The effects of nebula surface density profile and giant-planet eccentricities on planetary accretion in the inner solar system. *Meteoritics and Planetary Science* 37:1523–1540
- Chambers JE, Wetherill GW (1998) Making the Terrestrial Planets: N-Body Integrations of Planetary Embryos in Three Dimensions. *Icarus*136:304–327
- Chambers JE, Wetherill GW (2001) Planets in the asteroid belt. *MaPS*36(3):381–399
- Charnoz S, Pignatale FC, Hyodo R et al. (2019) Planetesimal formation in an evolving protoplanetary disk with a dead zone. *A&A*627:A50
- Charnoz S, Avicé G, Hyodo R, Pignatale FC, Chausson M (2021) Forming pressure traps at the snow line to isolate isotopic reservoirs in the absence of a planet. *A&A*652:A35
- Chatterjee S, Tan JC (2014) Inside-out Planet Formation. *ApJ*780:53
- Chatterjee S, Tan JC (2015) Vulcan Planets: Inside-out Formation of the Innermost Super-Earths. *ApJ*798:L32
- Chatterjee S, Ford EB, Matsumura S, Rasio FA (2008a) Dynamical Outcomes of Planet-Planet Scattering. *ApJ*686:580–602
- Chatterjee S, Ford EB, Matsumura S, Rasio FA (2008b) Dynamical Outcomes of Planet-Planet Scattering. *ApJ*686:580–602
- Chau A, Reinhardt C, Helled R, Stadel J (2018) Forming Mercury by Giant Impacts. *ApJ*865(1):35
- Chau A, Reinhardt C, Izidoro A, Stadel J, Helled R (2021) Could Uranus and Neptune form by collisions of planetary embryos? *MNRAS*502(2):1647–1660
- Chen J, Kipping D (2017) Probabilistic Forecasting of the Masses and Radii of Other Worlds. *ApJ*834:17
- Chiang E, Laughlin G (2013) The minimum-mass extrasolar nebula: in situ formation of close-in super-Earths. *MNRAS*431:3444–3455
- Chiang E, Youdin AN (2010) Forming Planetesimals in Solar and Extrasolar Nebulae. *Annual Review of Earth and Planetary Sciences* 38:493–522
- Chokshi A, Tielens AGGM, Hollenbach D (1993) Dust coagulation. *ApJ*407:806–819
- Christiansen JL (2022) Five thousand exoplanets at the NASA Exoplanet Archive. *Nature Astronomy* 6:516–519
- Clement MS, Chambers JE (2021) Dynamical avenues for mercury’s origin. II. in situ formation in the inner terrestrial disk. *The Astronomical Journal* 162(1):3, URL <https://doi.org/10.3847/1538-3881/abfb6c>
- Clement MS, Kaib NA, Raymond SN, Walsh KJ (2018) Mars’ growth stunted by an early giant planet instability. *Icarus*311:340–356
- Clement MS, Kaib NA, Chambers JE (2019a) Dynamical Constraints on Mercury’s Collisional Origin. *AJ*157(5):208
- Clement MS, Kaib NA, Raymond SN, Chambers JE, Walsh KJ (2019b) The early instability scenario: Terrestrial planet formation during the giant planet instability, and the effect of collisional fragmentation. *Icarus*321:778–790

- Clement MS, Raymond SN Kaib NA (2019c) Excitation and Depletion of the Asteroid Belt in the Early Instability Scenario. *AJ*157:38
- Clement MS, Kaib NA Chambers JE (2020a) Embryo Formation with GPU Acceleration: Reevaluating the Initial Conditions for Terrestrial Accretion. *The Planetary Science Journal* 1(1):18
- Clement MS, Morbidelli A, Raymond SN Kaib NA (2020b) A record of the final phase of giant planet migration fossilized in the asteroid belt's orbital structure. *MNRAS*492(1):L56–L60
- Clement MS, Chambers JE Jackson AP (2021a) Dynamical Avenues for Mercury's Origin. I. The Lone Survivor of a Primordial Generation of Short-period Protoplanets. *AJ*161(5):240
- Clement MS, Deienno R, Kaib NA et al. (2021b) Born extra-eccentric: A broad spectrum of primordial configurations of the gas giants that match their present-day orbits. *Icarus*367:114556
- Clement MS, Kaib NA, Raymond SN Chambers JE (2021c) The early instability scenario: Mars' mass explained by Jupiter's orbit. *Icarus*367:114585
- Clement MS, Raymond SN Chambers JE (2021d) Mercury as the Relic of Earth and Venus Outward Migration. *ApJ*923(1):L16
- Clement MS, Raymond SN, Kaib NA et al. (2021e) Born eccentric: Constraints on Jupiter and Saturn's pre-instability orbits. *Icarus*355:114122
- Clement MS, Quintana EV Quarles BL (2022) Habitable Planet Formation around Low-mass Stars: Rapid Accretion, Rapid Debris Removal, and the Essential Contribution of External Giants. *ApJ*928(1):91
- Clement MS, Chambers JE, Kaib NA, Raymond SN Jackson AP (2023) Mercury's formation within the early instability scenario. *Icarus*394:115445
- Connelly JN, Bizzarro M, Krot AN et al. (2012) The Absolute Chronology and Thermal Processing of Solids in the Solar Protoplanetary Disk. *Science* 338:651
- Cossou C, Raymond SN, Hersant F Pierens A (2014) Hot super-Earths and giant planet cores from different migration histories. *A&A*569:A56
- Costa MM, Jensen NK, Bouvier LC et al. (2020) The internal structure and geodynamics of mars inferred from a 4.2-gyr zircon record. *Proceedings of the National Academy of Sciences* 117(49):30,973–30,979, URL <https://www.pnas.org/content/117/49/30973>
- Crespi S, Dobbs-Dixon I, Georgakarakos N et al. (2021) Protoplanet collisions: Statistical properties of ejecta. *MNRAS*508(4):6013–6022
- Cresswell P, Dirksen G, Kley W Nelson RP (2007) On the evolution of eccentric and inclined protoplanets embedded in protoplanetary disks. *A&A*473:329–342
- Crida A (2009) Minimum Mass Solar Nebulae and Planetary Migration. *ApJ*698:606–614
- Crida A, Morbidelli A Masset F (2006) On the width and shape of gaps in protoplanetary disks. *Icarus* 181:587–604
- Cumming A, Butler RP, Marcy GW et al. (2008) The Keck Planet Search: Detectability and the Minimum Mass and Orbital Period Distribution of Extrasolar Planets. *PASP*120:531–554
- Cuzzi JN Weidenschilling SJ (2006) Particle-Gas Dynamics and Primary Accretion, pp 353–381
- Cuzzi JN, Hogan RC Shariff K (2008a) Toward Planetesimals: Dense Chondrule Clumps in the Protoplanetary Nebula. *ApJ*687:1432–1447
- Cuzzi JN, Hogan RC Shariff K (2008b) Toward Planetesimals: Dense Chondrule Clumps in the Protoplanetary Nebula. *ApJ*687(2):1432–1447
- D'Angelo G Marzari F (2012) Outward Migration of Jupiter and Saturn in Evolved Gaseous Disks. *ApJ*757:50
- D'Angelo G, Weidenschilling SJ, Lissauer JJ Bodenheimer P (2021) Growth of Jupiter: Formation in disks of gas and solids and evolution to the present epoch. *Icarus*355:114087
- Dauphas N (2017) The isotopic nature of the Earth's accreting material through time. *Nature*541:521–524
- Dauphas N Chaussidon M (2011) A Perspective from Extinct Radionuclides on a Young Stellar Object: The Sun and Its Accretion Disk. *Annual Review of Earth and Planetary Sciences* 39:351–386
- Dauphas N Pourmand A (2011) Hf-W-Th evidence for rapid growth of Mars and its status as a planetary embryo. *Nature*473:489–492

- Dauphas N, Hopp T Nesvorný D (2024) Bayesian inference on the isotopic building blocks of Mars and Earth. *Icarus*408:115805
- Day JMD Walker RJ (2015) Highly siderophile element depletion in the Moon. *Earth and Planetary Science Letters* 423:114–124
- Day JMD, Pearson DG Taylor LA (2007) Highly Siderophile Element Constraints on Accretion and Differentiation of the Earth-Moon System. *Science* 315(5809):217
- Deienno R, Gomes RS, Walsh KJ, Morbidelli A Nesvorný D (2016) Is the Grand Tack model compatible with the orbital distribution of main belt asteroids? *Icarus*272:114–124
- Deienno R, Morbidelli A, Gomes RS Nesvorný D (2017) Constraining the Giant Planets' Initial Configuration from Their Evolution: Implications for the Timing of the Planetary Instability. *AJ*153:153
- Deienno R, Izidoro A, Morbidelli A et al. (2018) Excitation of a Primordial Cold Asteroid Belt as an Outcome of Planetary Instability. *ApJ*864:50
- Deienno R, Walsh KJ, Kretke KA Levison HF (2019) Energy Dissipation in Large Collisions—No Change in Planet Formation Outcomes. *ApJ*876(2):103
- Deienno R, Izidoro A, Morbidelli A, Nesvorný D Bottke WF (2022) Implications of Jupiter Inward Gas-driven Migration for the Inner Solar System. *ApJ*936(2):L24
- Deienno R, Nesvorný D, Clement MS et al. (2024) Accretion and Uneven Depletion of the Main Asteroid Belt. *PSJ*5(5):110
- Delbo M, Walsh K, Bolin B, Avdellidou C Morbidelli A (2017) Identification of a primordial asteroid family constrains the original planetesimal population. *Science* 357(6355):1026–1029
- Delbo M, Avdellidou C Morbidelli A (2019) Ancient and primordial collisional families as the main sources of X-type asteroids of the inner main belt. *A&A*624:A69
- DeMeo FE Carry B (2013) The taxonomic distribution of asteroids from multi-filter all-sky photometric surveys. *Icarus*226:723–741
- DeMeo FE Carry B (2014) Solar System evolution from compositional mapping of the asteroid belt. *Nature*505:629–634
- DeMeo FE, Alexander CMO, Walsh KJ, Chapman CR Binzel RP (2015) The Compositional Structure of the Asteroid Belt, pp 13–41. DOI 10.2458/azu_uapress_9780816532131-ch002
- Deng H (2020) Hypothetical Hyperbolic Encounters between Venus and Proto-Mercury that Partially Stripped Away Proto-Mercury's Mantle. *ApJ*888(1):L1
- Desch SJ (2007) Mass Distribution and Planet Formation in the Solar Nebula. *ApJ*671:878–893
- Desch SJ Connolly HC Jr (2002) A model of the thermal processing of particles in solar nebula shocks: Application to the cooling rates of chondrules. *Meteoritics and Planetary Science* 37:183–207
- DeSouza SR, Roig F Nesvorný D (2021) Can a jumping-Jupiter trigger the Moon's formation impact? *MNRAS*507(1):539–547
- Dodson-Robinson SE, Willacy K, Bodenheimer P, Turner NJ Beichman CA (2009) Ice lines, planetesimal composition and solid surface density in the solar nebula. *Icarus*200:672–693
- Dominik C Nübold H (2002) Magnetic Aggregation: Dynamics and Numerical Modeling. *Icarus*157:173–186
- Dominik C Tielens AGGM (1997) The Physics of Dust Coagulation and the Structure of Dust Aggregates in Space. *ApJ*480:647–673
- Donahue TM, Hoffman JH, Hodges RR Watson AJ (1982) Venus was wet - A measurement of the ratio of deuterium to hydrogen. *Science* 216:630–633
- Dong R, Zhu Z Whitney B (2015) Observational Signatures of Planets in Protoplanetary Disks I. Gaps Opened by Single and Multiple Young Planets in Disks. *ApJ*809:93
- Dong S Zhu Z (2013) Fast Rise of "Neptune-size" Planets (4–8 R_{\oplus}) from $P \sim 10$ to ~ 250 Days – Statistics of Kepler Planet Candidates up to ~ 0.75 AU. *ApJ*778:53
- Drake MJ Campins H (2006) Origin of water on the terrestrial planets. In: Daniela L, Sylvio Ferraz M Angel FJ (eds) *Asteroids, Comets, Meteors*, IAU Symposium, vol 229, pp 381–394, DOI 10.1017/S1743921305006861
- Draskowska J Alibert Y (2017) Planetesimal formation starts at the snow line. *A&A*608:A92

- Drazkowska J Dullemond CP (2014) Can dust coagulation trigger streaming instability? *A&A*572:A78
- Drazkowska J Dullemond CP (2018) Planetesimal formation during protoplanetary disk buildup. *A&A*614:A62
- Drazkowska J, Windmark F Dullemond CP (2013) Planetesimal formation via sweep-up growth at the inner edge of dead zones. *A&A*556:A37
- Drazkowska J, Alibert Y Moore B (2016) Close-in planetesimal formation by pile-up of drifting pebbles. *A&A*594:A105
- Drazkowska J, Bitsch B, Lambrechts M et al. (2023) Planet Formation Theory in the Era of ALMA and Kepler: from Pebbles to Exoplanets. In: Inutsuka S, Aikawa Y, Muto T, Tomida K Tamura M (eds) *Protostars and Planets VII*, Astronomical Society of the Pacific Conference Series, vol 534, p 717, DOI 10.48550/arXiv.2203.09759
- Dressing CD Charbonneau D (2015) The Occurrence of Potentially Habitable Planets Orbiting M Dwarfs Estimated from the Full Kepler Dataset and an Empirical Measurement of the Detection Sensitivity. *ApJ*807:45
- Dullemond CP, Hollenbach D, Kamp I D'Alessio P (2007) Models of the Structure and Evolution of Protoplanetary Disks. *Protostars and Planets V* pp 555–572
- Dullemond CP, Birnstiel T, Huang J et al. (2018) The Disk Substructures at High Angular Resolution Project (DSHARP). VI. Dust Trapping in Thin-ringed Protoplanetary Disks. *ApJ*869(2):L46
- Duncan MJ, Levison HF Lee MH (1998) A Multiple Time Step Symplectic Algorithm for Integrating Close Encounters. *AJ*116:2067–2077
- Dürmann C Kley W (2015) Migration of massive planets in accreting disks. *A&A*574:A52
- Dutrey A, Lecavelier Des Etangs A Augereau JC (2004) The observation of circumstellar disks: dust and gas components, pp 81–95
- Ebel DS Alexander CMO (2005) Condensation from Cluster-IDP Enriched Vapor Inside the Snow Line: Implications for Mercury, Asteroids, and Enstatite Chondrites. In: Mackwell S Stansbery E (eds) *36th Annual Lunar and Planetary Science Conference, Lunar and Planetary Science Conference*, p 1797
- Ebel DS Alexander CMO (2011) Equilibrium condensation from chondritic porous IDP enriched vapor: Implications for Mercury and enstatite chondrite origins. *Planet Space Sci*59(15):1888–1894
- Ebel DS Stewart ST (2017) The Elusive Origin of Mercury. *ArXiv e-prints*
- Eke VR, Lawrence DJ Teodoro LFA (2017) How thick are Mercury's polar water ice deposits? *Icarus*284:407–415
- Evans AJ, Andrews-Hanna JC, Head JW et al. (2018) Reexamination of Early Lunar Chronology With GRAIL Data: Terranes, Basins, and Impact Fluxes. *Journal of Geophysical Research (Planets)* 123(7):1596–1617
- Fabrycky DC, Lissauer JJ, Ragozzine D et al. (2014) Architecture of Kepler's Multi-transiting Systems. II. New Investigations with Twice as Many Candidates. *ApJ*790:146
- Fang J Margot JL (2012) Architecture of Planetary Systems Based on Kepler Data: Number of Planets and Coplanarity. *ApJ*761:92
- Fang T Deng H (2020) Extreme close encounters between proto-Mercury and proto-Venus in terrestrial planet formation. *MNRAS*496(3):3781–3785
- Fedele D, Tazzari M, Booth R et al. (2017) ALMA continuum observations of the protoplanetary disk AS 209. Evidence of multiple gaps opened by a single planet. *ArXiv e-prints*
- Fernandez JA Ip WH (1984) Some dynamical aspects of the accretion of Uranus and Neptune - The exchange of orbital angular momentum with planetesimals. *Icarus*58:109–120
- Fischer DA, Howard AW, Laughlin GP et al. (2014) Exoplanet Detection Techniques. *Protostars and Planets VI* pp 715–737
- Fischer RA Ciesla FJ (2014) Dynamics of the terrestrial planets from a large number of N-body simulations. *Earth and Planetary Science Letters* 392:28–38

- Fischer RA Nimmo F (2018a) Effects of core formation on the Hf-W isotopic composition of the Earth and dating of the Moon-forming impact. *Earth and Planetary Science Letters* 499:257–265
- Fischer RA Nimmo F (2018b) Effects of core formation on the Hf-W isotopic composition of the Earth and dating of the Moon-forming impact. *Earth and Planetary Science Letters* 499:257–265
- Flock M, Ruge JP, Dzyurkevich N et al. (2015) Gaps, rings, and non-axisymmetric structures in protoplanetary disks. From simulations to ALMA observations. *A&A*574:A68
- Fogg MJ Nelson RP (2005) Oligarchic and giant impact growth of terrestrial planets in the presence of gas giant planet migration. *A&A*441:791–806
- Fogg MJ Nelson RP (2007) On the formation of terrestrial planets in hot-Jupiter systems. *A&A*461:1195–1208
- Ford EB Rasio FA (2008a) Origins of Eccentric Extrasolar Planets: Testing the Planet-Planet Scattering Model. *ApJ*686:621–636
- Ford EB Rasio FA (2008b) Origins of Eccentric Extrasolar Planets: Testing the Planet-Planet Scattering Model. *ApJ*686:621–636
- Ford EB, Rasio FA Yu K (2003) Dynamical Instabilities in Extrasolar Planetary Systems. In: D Deming & S Seager (ed) *Scientific Frontiers in Research on Extrasolar Planets*, Astronomical Society of the Pacific Conference Series, vol 294, pp 181–188
- Franco P, Izidoro A, Winter OC, Torres KS Amarante A (2022) Explaining mercury via a single giant impact is highly unlikely. *MNRAS*515(4):5576–5586
- Fressin F, Torres G, Charbonneau D et al. (2013a) The False Positive Rate of Kepler and the Occurrence of Planets. *ApJ*766:81
- Fressin F, Torres G, Charbonneau D et al. (2013b) The False Positive Rate of Kepler and the Occurrence of Planets. *ApJ*766:81
- Gan T, Wang SX, Wang S et al. (2023) Occurrence Rate of Hot Jupiters Around Early-type M Dwarfs Based on Transiting Exoplanet Survey Satellite Data. *AJ*165(1):17
- Genda H Ikoma M (2008) Origin of the ocean on the Earth: Early evolution of water D/H in a hydrogen-rich atmosphere. *Icarus*194:42–52
- Ginzburg S, Schlichting HE Sari R (2016) Super-Earth Atmospheres: Self-consistent Gas Accretion and Retention. *ApJ*825:29
- Gladman B Coffey J (2009) Mercurian impact ejecta: Meteorites and mantle. *MaPS*44(2):285–291
- Glaschke P, Amaro-Seoane P Spurzem R (2014) Hybrid methods in planetesimal dynamics: description of a new composite algorithm. *MNRAS*445:3620–3649
- Goldreich P Tremaine S (1980) Disk-satellite interactions. *ApJ*241:425–441
- Goldreich P Tremaine SD (1978) The velocity dispersion in Saturn’s rings. *Icarus*34:227–239
- Goldreich P Ward WR (1973) The Formation of Planetesimals. *ApJ*183:1051–1062
- Goldreich P, Lithwick Y Sari R (2004) Planet Formation by Coagulation: A Focus on Uranus and Neptune. *ARA&A*42:549–601
- Gomes R, Levison HF, Tsiganis K Morbidelli A (2005) Origin of the cataclysmic Late Heavy Bombardment period of the terrestrial planets. *Nature*435:466–469
- Gonzalez G, Brownlee D Ward P (2001) The Galactic Habitable Zone: Galactic Chemical Evolution. *Icarus*152:185–200
- Gorti U Hollenbach D (2009) Photoevaporation of Circumstellar Disks By Far-Ultraviolet, Extreme-Ultraviolet and X-Ray Radiation from the Central Star. *ApJ*690:1539–1552
- Gorti U, Hollenbach D Dullemond CP (2015) The Impact of Dust Evolution and Photoevaporation on Disk Dispersal. *ApJ*804:29
- Gradie J Tedesco E (1982) Compositional structure of the asteroid belt. *Science* 216:1405–1407
- Grady MM, Abernethy FAJ, Anand M et al. (2023) UV-Vis Spectroscopy of Hayabusa 2 Grains: Comparison with Carbonaceous Chondrites and Asteroid (162173) Ryugu. In: *LPI Contributions*, LPI Contributions, vol 2806, p 2907
- Grange ML, Nemchin AA Pidgeon RT (2013) The effect of 1.9 and 1.4 Ga impact events on 4.3 Ga zircon and phosphate from an Apollo 15 melt breccia. *Journal of Geophysical Research (Planets)* 118(10):2180–2197

- Greenberg R, Hartmann WK, Chapman CR Wacker JF (1978) Planetesimals to planets - Numerical simulation of collisional evolution. *Icarus*35:1–26
- Greenberg R, Bottke WF, Carusi A Valsecchi GB (1991) Planetary accretion rates - Analytical derivation. *Icarus*94:98–111
- Greenzweig Y Lissauer JJ (1990) Accretion rates of protoplanets. *Icarus*87:40–77
- Grimm SL Stadel JG (2014) The GENGA Code: Gravitational Encounters in N-body Simulations with GPU Acceleration. *ApJ*796:23
- Grimm SL, Stadel JG, Brasser R, Meier MMM Mordasini C (2022) GENGA. II. GPU Planetary N-body Simulations with Non-Newtonian Forces and High Number of Particles. *ApJ*932(2):124
- Grinspoon DH (1993) Implications of the high D/H ratio for the sources of water in Venus' atmosphere. *Nature*363:428–431
- Grishin E Perets HB (2015) Application of Gas Dynamical Friction for Planetesimals. I. Evolution of Single Planetesimals. *ApJ*811:54
- Grossman L Larimer JW (1974) Early chemical history of the solar system. *Reviews of Geophysics and Space Physics* 12:71–101
- Gu JT, Fischer RA, Brennan MC et al. (2023) Comparisons of the core and mantle compositions of earth analogs from different terrestrial planet formation scenarios. *Icarus*394:115425
- Guilera OM, Sándor Z, Ronco MP, Venturini J Miller Bertolami MM (2020) Giant planet formation at the pressure maxima of protoplanetary disks. II. A hybrid accretion scenario. *A&A*642:A140
- Guillot T, Stevenson DJ, Hubbard WB Saumon D (2004) The interior of Jupiter, pp 35–57
- Gundlach B, Kilias S, Beitz E Blum J (2011) Micrometer-sized ice particles for planetary-science experiments - I. Preparation, critical rolling friction force, and specific surface energy. *Icarus*214:717–723
- Güttler C, Blum J, Zsom A, Ormel CW Dullemond CP (2010) The outcome of protoplanetary dust growth: pebbles, boulders, or planetesimals?. I. Mapping the zoo of laboratory collision experiments. *A&A*513:A56
- Haghighipour N Boss AP (2003) On Gas Drag-Induced Rapid Migration of Solids in a Nonuniform Solar Nebula. *ApJ*598:1301–1311
- Hahn JM Malhotra R (1999) Orbital Evolution of Planets Embedded in a Planetesimal Disk. *AJ*117:3041–3053
- Haisch KE Jr, Lada EA Lada CJ (2001) Disk Frequencies and Lifetimes in Young Clusters. *ApJ*553:L153–L156
- Halliday AN (2008) A young Moon-forming giant impact at 70–110 million years accompanied by late-stage mixing, core formation and degassing of the Earth. *Philosophical Transactions of the Royal Society of London Series A* 366:4163–4181
- Halliday AN (2013) The origins of volatiles in the terrestrial planets. *Geochim Cosmochim Acta*105:146–171
- Hallis LJ, Huss GR, Nagashima K et al. (2015) Evidence for primordial water in Earth's deep mantle. *Science* 350:795–797
- Hansen BMS (2009) Formation of the Terrestrial Planets from a Narrow Annulus. *ApJ*703:1131–1140
- Hansen BMS Murray N (2012) Migration Then Assembly: Formation of Neptune-mass Planets inside 1 AU. *ApJ*751:158
- Hansen BMS Murray N (2013) Testing in Situ Assembly with the Kepler Planet Candidate Sample. *ApJ*775:53
- Hasegawa Y Pudritz RE (2011) The origin of planetary system architectures - I. Multiple planet traps in gaseous discs. *MNRAS*417:1236–1259
- Hasegawa Y Pudritz RE (2012) Evolutionary Tracks of Trapped, Accreting Protoplanets: The Origin of the Observed Mass-Period Relation. *ApJ*760:117
- Hauck SA, Margot JL, Solomon SC et al. (2013) The curious case of Mercury's internal structure. *Journal of Geophysical Research (Planets)* 118(6):1204–1220
- Hayashi C (1981) Structure of the Solar Nebula, Growth and Decay of Magnetic Fields and Effects of Magnetic and Turbulent Viscosities on the Nebula. *Progress of Theoretical Physics Supplement* 70:35–53

- Heim LO, Blum J, Preuss M Butt HJ (1999) Adhesion and Friction Forces between Spherical Micrometer-Sized Particles. *Physical Review Letters* 83:3328–3331
- Hernandez DM Dehnen W (2017) A study of symplectic integrators for planetary system problems: error analysis and comparisons. *MNRAS* 468(3):2614–2636
- Hernández J, Hartmann L, Megeath T et al. (2007) A Spitzer Space Telescope Study of Disks in the Young σ Orionis Cluster. *ApJ* 662(2):1067–1081
- Hillenbrand LA (2008) Disk-dispersal and planet-formation timescales. *Physica Scripta Volume T* 130(1):014024
- Holland WS, Greaves JS, Zuckerman B et al. (1998) Submillimetre images of dusty debris around nearby stars. *Nature* 392:788–791
- Horn B, Lyra W, Mac Low MM Sándor Z (2012) Orbital Migration of Interacting Low-mass Planets in Evolutionary Radiative Turbulent Models. *ApJ* 750:34
- Howard AW, Marcy GW, Johnson JA et al. (2010a) The Occurrence and Mass Distribution of Close-in Super-Earths, Neptunes, and Jupiters. *Science* 330:653
- Howard AW, Marcy GW, Johnson JA et al. (2010b) The Occurrence and Mass Distribution of Close-in Super-Earths, Neptunes, and Jupiters. *Science* 330:653–
- Howard AW, Marcy GW, Bryson ST et al. (2012a) Planet Occurrence within 0.25 AU of Solar-type Stars from Kepler. *ApJS* 201:15
- Howard AW, Marcy GW, Bryson ST et al. (2012b) Planet Occurrence within 0.25 AU of Solar-type Stars from Kepler. *ApJS* 201:15
- Hu X, Zhu Z, Tan JC Chatterjee S (2016) Inside-out Planet Formation. III. Planet-Disk Interaction at the Dead Zone Inner Boundary. *ApJ* 816:19
- Hu X, Tan JC, Zhu Z et al. (2017) Inside-Out Planet Formation. IV. Pebble Evolution and Planet Formation Timescales. *ArXiv e-prints*
- Huang J, Andrews SM, Dullemond CP et al. (2018) The Disk Substructures at High Angular Resolution Project (DSHARP). II. Characteristics of Annular Substructures. *ApJ* 869(2):L42
- Hubickyj O, Bodenheimer P Lissauer JJ (2005) Accretion of the gaseous envelope of Jupiter around a 5–10 Earth-mass core. *Icarus* 179:415–431
- Ida S Guillot T (2016) Formation of dust-rich planetesimals from sublimated pebbles inside of the snow line. *A&A* 596:L3
- Ida S Lin DNC (2004) Toward a Deterministic Model of Planetary Formation. I. A Desert in the Mass and Semimajor Axis Distributions of Extrasolar Planets. *ApJ* 604:388–413
- Ida S Makino J (1993) Scattering of planetesimals by a protoplanet - Slowing down of runaway growth. *Icarus* 106:210
- Ida S Nakazawa K (1989) Collisional probability of planetesimals revolving in the solar gravitational field. III. *A&A* 224:303–315
- Ida S, Tanaka H, Johansen A, Kanagawa KD Tanigawa T (2018) Slowing Down Type II Migration of Gas Giants to Match Observational Data. *ApJ* 864(1):77
- Ikoma M Genda H (2006) Constraints on the Mass of a Habitable Planet with Water of Nebular Origin. *ApJ* 648:696–706
- Ikoma M Hori Y (2012) In Situ Accretion of Hydrogen-rich Atmospheres on Short-period Super-Earths: Implications for the Kepler-11 Planets. *ApJ* 753:66
- Inamdar NK Schlichting HE (2015) The formation of super-Earths and mini-Neptunes with giant impacts. *MNRAS* 448:1751–1760
- Inamdar NK Schlichting HE (2016) Stealing the Gas: Giant Impacts and the Large Diversity in Exoplanet Densities. *ApJ* 817:L13
- Isella A, Pérez LM, Carpenter JM et al. (2013) An Azimuthal Asymmetry in the LkH α 330 Disk. *ApJ* 775:30
- Izidoro A Piani L (2022) Origin of Water in the Terrestrial Planets: Insights from Meteorite Data and Planet Formation Models. *Elements* 18(3):181–186
- Izidoro A, de Souza Torres K, Winter OC Haghhighipour N (2013) A Compound Model for the Origin of Earth's Water. *ApJ* 767:54

- Izidoro A, Haghighipour N, Winter OC Tsuchida M (2014a) Terrestrial Planet Formation in a Protoplanetary Disk with a Local Mass Depletion: A Successful Scenario for the Formation of Mars. *ApJ*782:31
- Izidoro A, Morbidelli A Raymond SN (2014b) Terrestrial Planet Formation in the Presence of Migrating Super-Earths. *ApJ*794:11
- Izidoro A, Morbidelli A, Raymond SN, Hersant F Pierens A (2015a) Accretion of Uranus and Neptune from inward-migrating planetary embryos blocked by Jupiter and Saturn. *A&A*582:A99
- Izidoro A, Raymond SN, Morbidelli A, Hersant F Pierens A (2015b) Gas Giant Planets as Dynamical Barriers to Inward-Migrating Super-Earths. *ApJ*800:L22
- Izidoro A, Raymond SN, Morbidelli A Winter OC (2015c) Terrestrial planet formation constrained by Mars and the structure of the asteroid belt. *MNRAS*453:3619–3634
- Izidoro A, Raymond SN, Pierens A et al. (2016) The Asteroid Belt as a Relic from a Chaotic Early Solar System. *ApJ*833:40
- Izidoro A, Ogihara M, Raymond SN et al. (2017) Breaking the chains: hot super-Earth systems from migration and disruption of compact resonant chains. *MNRAS*470:1750–1770
- Izidoro A, Bitsch B, Raymond SN et al. (2021) Formation of planetary systems by pebble accretion and migration. Hot super-Earth systems from breaking compact resonant chains. *A&A*650:A152
- Izidoro A, Dasgupta R, Raymond SN et al. (2022a) Planetesimal rings as the cause of the Solar System's planetary architecture. *Nature Astronomy* 6:357–366
- Izidoro A, Schlichting HE, Isella A et al. (2022b) The Exoplanet Radius Valley from Gas-driven Planet Migration and Breaking of Resonant Chains. *ApJ*939(2):L19
- Jackson AP, Gabriel TSJ Asphaug EI (2018) Constraints on the pre-impact orbits of Solar system giant impactors. *MNRAS*474(3):2924–2936
- Jacobsen SB (2005) The Hf-W Isotopic System and the Origin of the Earth and Moon. *Annual Review of Earth and Planetary Sciences* 33:531–570
- Jacobson SA Morbidelli A (2014a) Lunar and terrestrial planet formation in the Grand Tack scenario. *Philosophical Transactions of the Royal Society of London Series A* 372:0174
- Jacobson SA Morbidelli A (2014b) Lunar and terrestrial planet formation in the Grand Tack scenario. *Philosophical Transactions of the Royal Society of London Series A* 372:0174
- Jacobson SA, Morbidelli A, Raymond SN et al. (2014) Highly siderophile elements in Earth's mantle as a clock for the Moon-forming impact. *Nature*508:84–87
- Jakubík M, Morbidelli A, Neslušan L Brasser R (2012) The accretion of Uranus and Neptune by collisions among planetary embryos in the vicinity of Jupiter and Saturn. *A&A*540:A71
- Jin S Mordasini C (2018) Compositional Imprints in Density–Distance–Time: A Rocky Composition for Close-in Low-mass Exoplanets from the Location of the Valley of Evaporation. *ApJ*853:163
- Johansen A Dorn C (2022) Nucleation and growth of iron pebbles explains the formation of iron-rich planets akin to Mercury. *A&A*662:A19
- Johansen A Lacerda P (2010) Prograde rotation of protoplanets by accretion of pebbles in a gaseous environment. *MNRAS*404:475–485
- Johansen A Lambrechts M (2017) Forming Planets via Pebble Accretion. *Annual Review of Earth and Planetary Sciences* 45:359–387
- Johansen A Youdin A (2007) Protoplanetary Disk Turbulence Driven by the Streaming Instability: Nonlinear Saturation and Particle Concentration. *ApJ*662:627–641
- Johansen A, Oishi JS, Mac Low MM et al. (2007) Rapid planetesimal formation in turbulent circumstellar disks. *Nature*448:1022–1025
- Johansen A, Youdin A Mac Low MM (2009) Particle Clumping and Planetesimal Formation Depend Strongly on Metallicity. *ApJ*704:L75–L79
- Johansen A, Davies MB, Church RP Holmelin V (2012a) Can Planetary Instability Explain the Kepler Dichotomy? *ApJ*758:39
- Johansen A, Youdin AN Lithwick Y (2012b) Adding particle collisions to the formation of asteroids and Kuiper belt objects via streaming instabilities. *A&A*537:A125

- Johansen A, Blum J, Tanaka H et al. (2014) The Multifaceted Planetesimal Formation Process. *Protostars and Planets VI* pp 547–570
- Johansen A, Mac Low MM, Lacerda P Bizzarro M (2015) Growth of asteroids, planetary embryos, and Kuiper belt objects by chondrule accretion. *Science Advances* 1:1500109
- Johansen A, Ronnet T, Bizzarro M et al. (2021) A pebble accretion model for the formation of the terrestrial planets in the Solar System. *Science Advances* 7(8):eabc0444
- Johnson BC, Minton DA, Melosh HJ Zuber MT (2015) Impact jetting as the origin of chondrules. *Nature* 517:339–341
- Joiret S, Raymond SN, Avicé G et al. (2023) A race against the clock: Constraining the timing of cometary bombardment relative to earth’s growth. *Icarus* 406:115,754, URL <https://www.sciencedirect.com/science/article/pii/S0019103523003317>
- Jungmann F, Kruss M, Teiser J Wurm G (2022) Aggregation of sub-mm particles in strong electric fields under microgravity conditions. *Icarus* 373:114766
- Jurić M Tremaine S (2008) Dynamical Origin of Extrasolar Planet Eccentricity Distribution. *ApJ* 686:603–620
- Kaib NA Chambers JE (2016) The fragility of the terrestrial planets during a giant-planet instability. *MNRAS* 455:3561–3569
- Kaib NA Cowan NB (2015) The feeding zones of terrestrial planets and insights into Moon formation. *Icarus* 252:161–174
- Kaib NA Sheppard SS (2016) Tracking Neptune’s Migration History through High-perihelion Resonant Trans-Neptunian Objects. *AJ* 152(5):133
- Kashchiev D (2006) Analysis of experimental data for the nucleation rate of water droplets. *J Chem Phys* 125(4):044,505–044,505
- Kasting JF Pollack JB (1983) Loss of water from Venus. I - Hydrodynamic escape of hydrogen. *Icarus* 53:479–508
- Kenyon SJ Bromley BC (2004) Collisional Cascades in Planetesimal Disks. II. Embedded Planets. *AJ* 127:513–530
- Kenyon SJ Bromley BC (2006) Terrestrial Planet Formation. I. The Transition from Oligarchic Growth to Chaotic Growth. *AJ* 131:1837–1850
- Kenyon SJ Hartmann L (1987) Spectral energy distributions of T Tauri stars - Disk flaring and limits on accretion. *ApJ* 323:714–733
- Kirchschlager F, Bertrang GHM Flock M (2019) Intrinsic polarization of elongated porous dust grains. *MNRAS* 488(1):1211–1219
- Kleine T, Touboul M, Bourdon B et al. (2009) Hf-W chronology of the accretion and early evolution of asteroids and terrestrial planets. *Geochim Cosmochim Acta* 73:5150–5188
- Kleine T, Steller T, Burkhardt C Nimmo F (2023) An inner solar system origin of volatile elements in Mars. *Icarus* 397:115519
- Kley W Crida A (2008) Migration of protoplanets in radiative discs. *A&A* 487:L9–L12
- Koerner DW, Ressler ME, Werner MW Backman DE (1998) Mid-Infrared Imaging of a Circumstellar Disk around HR 4796: Mapping the Debris of Planetary Formation. *ApJ* 503:L83–L87
- Kokubo E Ida S (1995) Orbital evolution of protoplanets embedded in a swarm of planetesimals. *Icarus* 114:247–257
- Kokubo E Ida S (1996) On Runaway Growth of Planetesimals. *Icarus* 123:180–191
- Kokubo E Ida S (1998) Oligarchic Growth of Protoplanets. *Icarus* 131:171–178
- Kokubo E Ida S (2000) Formation of Protoplanets from Planetesimals in the Solar Nebula. *Icarus* 143:15–27
- Kokubo E Ida S (2002) Formation of Protoplanet Systems and Diversity of Planetary Systems. *ApJ* 581:666–680
- Kokubo E, Kominami J Ida S (2006) Formation of Terrestrial Planets from Protoplanets. I. Statistics of Basic Dynamical Properties. *ApJ* 642:1131–1139
- Kominami J Ida S (2004) Formation of terrestrial planets in a dissipating gas disk with Jupiter and Saturn. *Icarus* 167:231–243
- Kopparapu RK (2013) A Revised Estimate of the Occurrence Rate of Terrestrial Planets in the Habitable Zones around Kepler M-dwarfs. *ApJ* 767:L8

- Krauss O Wurm G (2005) Photophoresis and the Pile-up of Dust in Young Circumstellar Disks. *ApJ*630(2):1088–1092
- Kretke KA Lin DNC (2007) Grain Retention and Formation of Planetesimals near the Snow Line in MRI-driven Turbulent Protoplanetary Disks. *ApJ*664:L55–L58
- Krijt S, Ormel CW, Dominik C Tielens AGGM (2015) Erosion and the limits to planetesimal growth. *A&A*574:A83
- Krijt S, Ormel CW, Dominik C Tielens AGGM (2016) A panoptic model for planetesimal formation and pebble delivery. *A&A*586:A20
- Kruijer TS, Burkhardt C, Budde G Kleine T (2017a) Age of Jupiter inferred from the distinct genetics and formation times of meteorites. *Proceedings of the National Academy of Science* 114:6712–6716
- Kruijer TS, Kleine T, Borg LE et al. (2017b) The early differentiation of Mars inferred from Hf-W chronometry. *Earth and Planetary Science Letters* 474:345–354
- Kruss M Wurm G (2018) Seeding the Formation of Mercurys: An Iron-sensitive Bouncing Barrier in Disk Magnetic Fields. *ApJ*869(1):45
- Kruss M Wurm G (2020) Composition and Size Dependent Sorting in Preplanetary Growth: Seeding the Formation of Mercury-like Planets. *PSJ*1(1):23
- Kurokawa H, Sato M, Ushioda M et al. (2014) Evolution of water reservoirs on Mars: Constraints from hydrogen isotopes in martian meteorites. *Earth and Planetary Science Letters* 394:179–185
- Lambrechts M Johansen A (2012a) Rapid growth of gas-giant cores by pebble accretion. *A&A*544:A32
- Lambrechts M Johansen A (2012b) Rapid growth of gas-giant cores by pebble accretion. *A&A*544:A32
- Lambrechts M Johansen A (2014) Forming the cores of giant planets from the radial pebble flux in protoplanetary discs. *A&A*572:A107
- Lambrechts M Lega E (2017) Reduced gas accretion on super-Earths and ice giants. *A&A*606:A146
- Lambrechts M, Johansen A Morbidelli A (2014) Separating gas-giant and ice-giant planets by halting pebble accretion. *A&A*572:A35
- Lambrechts M, Morbidelli A, Jacobson SA et al. (2019) Formation of planetary systems by pebble accretion and migration. How the radial pebble flux determines a terrestrial-planet or super-Earth growth mode. *A&A*627:A83
- Laskar J (1997) Large scale chaos and the spacing of the inner planets. *A&A*317:L75–L78
- Latham DW, Rowe JF, Quinn SN et al. (2011) A First Comparison of Kepler Planet Candidates in Single and Multiple Systems. *ApJ*732:L24
- Lau TCH Lee MH (2023) Parallelization of the Symplectic Massive Body Algorithm (SyMBA) N-body Code. *Research Notes of the American Astronomical Society* 7(4):74
- Lauretta DS, Bartels AE, Barucci MA et al. (2015) The OSIRIS-REx target asteroid (101955) Bennu: Constraints on its physical, geological, and dynamical nature from astronomical observations. *MaPS*50(4):834–849
- Lawrence DJ, Feldman WC, Goldsten JO et al. (2013) Evidence for Water Ice Near Mercury's North Pole from MESSENGER Neutron Spectrometer Measurements. *Science* 339:292
- Lecar M Aarseth SJ (1986) A numerical simulation of the formation of the terrestrial planets. *ApJ*305:564–579
- Lecar M, Podolak M, Sasselov D Chiang E (2006) On the Location of the Snow Line in a Protoplanetary Disk. *ApJ*640:1115–1118
- Lécuyer C, Gillet P Robert F (1998) The hydrogen isotope composition of seawater and the global water cycle. *Chemical Geology* 145:249–261
- Lee EJ Chiang E (2016) Breeding Super-Earths and Birthing Super-puffs in Transitional Disks. *ApJ*817:90
- Lee EJ, Chiang E Ormel CW (2014) Make Super-Earths, Not Jupiters: Accreting Nebular Gas onto Solid Cores at 0.1 AU and Beyond. *ApJ*797:95

- Lega E, Morbidelli A, Bitsch B, Crida A Szulágyi J (2015) Outwards migration for planets in stellar irradiated 3D discs. *MNRAS*452(2):1717–1726
- Leinhardt ZM (2008) Terrestrial Planet Formation: A Review and Current Directions. In: Fischer D, Rasio FA, Thorsett SE Wolszczan A (eds) *Extreme Solar Systems*, Astronomical Society of the Pacific Conference Series, vol 398, p 225
- Lesur G, Flock M, Ercolano B et al. (2023) Hydro-, Magnetohydro-, and Dust-Gas Dynamics of Protoplanetary Disks. In: Inutsuka S, Aikawa Y, Muto T, Tomida K Tamura M (eds) *Astronomical Society of the Pacific Conference Series*, Astronomical Society of the Pacific Conference Series, vol 534, p 465
- Levison HF, Morbidelli A, Van Laerhoven C, Gomes R Tsiganis K (2008) Origin of the structure of the Kuiper belt during a dynamical instability in the orbits of Uranus and Neptune. *Icarus*196:258–273
- Levison HF, Thommes E Duncan MJ (2010) Modeling the Formation of Giant Planet Cores. I. Evaluating Key Processes. *AJ*139:1297–1314
- Levison HF, Morbidelli A, Tsiganis K, Nesvorný D Gomes R (2011) Late Orbital Instabilities in the Outer Planets Induced by Interaction with a Self-gravitating Planetesimal Disk. *AJ*142:152
- Levison HF, Duncan MJ Thommes E (2012) A Lagrangian Integrator for Planetary Accretion and Dynamics (LIPAD). *AJ*144:119
- Levison HF, Kretke KA Duncan MJ (2015a) Growing the gas-giant planets by the gradual accumulation of pebbles. *Nature*524:322–324
- Levison HF, Kretke KA, Walsh KJ Bottke WF (2015b) Growing the terrestrial planets from the gradual accumulation of sub-meter sized objects. *Proceedings of the National Academy of Science* 112:14,180–14,185
- Lichtenberg T, Golabek GJ, Dullemond CP et al. (2017) Impact splash chondrule formation during planetesimal recycling. *ArXiv e-prints*
- Lichtenberg T, Drazkowska J, Schönbächler M, Golabek GJ Hands TO (2021) Bifurcation of planetary building blocks during Solar System formation. *Science* 371(6527):365–370
- Lin DNC Ida S (1997) On the Origin of Massive Eccentric Planets. *ApJ*477:781–+
- Lin DNC Papaloizou J (1986) On the tidal interaction between protoplanets and the protoplanetary disk. III - Orbital migration of protoplanets. *ApJ*309:846–857
- Lin DNC, Bodenheimer P Richardson DC (1996) Orbital migration of the planetary companion of 51 Pegasi to its present location. *Nature*380:606–607
- Lin MK Youdin AN (2015) Cooling Requirements for the Vertical Shear Instability in Protoplanetary Disks. *ApJ*811:17
- Lineweaver CH, Fenner Y Gibson BK (2004) The Galactic Habitable Zone and the Age Distribution of Complex Life in the Milky Way. *Science* 303:59–62
- Lissauer JJ (1987) Timescales for planetary accretion and the structure of the protoplanetary disk. *Icarus*69:249–265
- Lissauer JJ (1993) Planet formation. *ARA&A*31:129–174
- Lissauer JJ (2007) Planets Formed in Habitable Zones of M Dwarf Stars Probably Are Deficient in Volatiles. *ApJ*660:L149–L152
- Lissauer JJ, Fabrycky DC, Ford EB et al. (2011a) A closely packed system of low-mass, low-density planets transiting Kepler-11. *Nature*470:53–58
- Lissauer JJ, Ragozzine D, Fabrycky DC et al. (2011b) Architecture and Dynamics of Kepler’s Candidate Multiple Transiting Planet Systems. *ApJS*197:8
- Lissauer JJ, Jontof-Hutter D, Rowe JF et al. (2013) All Six Planets Known to Orbit Kepler-11 Have Low Densities. *ApJ*770:131
- Liu B, Raymond SN Jacobson SA (2022) Early Solar System instability triggered by dispersal of the gaseous disk. *Nature*604(7907):643–646
- Liu D, Jolliff BL, Zeigler RA et al. (2012) Comparative zircon U-Pb geochronology of impact melt breccias from Apollo 12 and lunar meteorite SaU 169, and implications for the age of the Imbrium impact. *Earth and Planetary Science Letters* 319:277–286
- Lodders K (2003) Solar System Abundances and Condensation Temperatures of the Elements. *ApJ*591:1220–1247

- Lopez ED (2017) Born dry in the photoevaporation desert: Kepler's ultra-short-period planets formed water-poor. *MNRAS*472:245–253
- Lopez ED Fortney JJ (2014) Understanding the Mass-Radius Relation for Sub-neptunes: Radius as a Proxy for Composition. *ApJ*792:1
- Lopez ED Rice K (2016) Predictions for the Period Dependence of the Transition Between Rocky Super-Earths and Gaseous Sub-Neptunes and Implications for η - \oplus . ArXiv e-prints
- Lümmen N Kraska T (2005) Homogeneous nucleation of iron from supersaturated vapor investigated by molecular dynamics simulation. *Journal of Aerosol Science* 36(12):1409–1426
- Luque R Pallé E (2022) Density, not radius, separates rocky and water-rich small planets orbiting M dwarf stars. *Science* 377(6611):1211–1214
- Lykawka PS Ito T (2013) Terrestrial Planet Formation during the Migration and Resonance Crossings of the Giant Planets. *ApJ*773:65
- Lykawka PS Ito T (2017) Terrestrial Planet Formation: Constraining the Formation of Mercury. *ApJ*838:106
- Lykawka PS Ito T (2019) Constraining the Formation of the Four Terrestrial Planets in the Solar System. *ApJ*883(2):130
- Lykawka PS Ito T (2023) Terrestrial planet and asteroid belt formation by Jupiter-Saturn chaotic excitation. *Scientific Reports* 13:4708
- Lyra W Klahr H (2011) The baroclinic instability in the context of layered accretion. Self-sustained vortices and their magnetic stability in local compressible unstratified models of protoplanetary disks. *A&A*527:A138
- Lyra W, Johansen A, Klahr H Piskunov N (2008a) Embryos grown in the dead zone. Assembling the first protoplanetary cores in low mass self-gravitating circumstellar disks of gas and solids. *A&A*491:L41–L44
- Lyra W, Johansen A, Klahr H Piskunov N (2008b) Global magnetohydrodynamical models of turbulence in protoplanetary disks. I. A cylindrical potential on a Cartesian grid and transport of solids. *A&A*479:883–901
- Lyra W, Johansen A, Klahr H Piskunov N (2009) Standing on the shoulders of giants. Trojan Earths and vortex trapping in low mass self-gravitating protoplanetary disks of gas and solids. *A&A*493:1125–1139
- Lyra W, Paardekooper SJ Mac Low MM (2010) Orbital Migration of Low-mass Planets in Evolutionary Radiative Models: Avoiding Catastrophic Infall. *ApJ*715:L68–L73
- Magnan N, Heinemann T Latter HN (2024) A physical picture for the acoustic resonant drag instability. *MNRAS*529(1):688–701
- Mah J Bitsch B (2023) Forming super-Mercuries: Role of stellar abundances. *A&A*673:A17
- Malhotra R (1993) The origin of Pluto's peculiar orbit. *Nature*365(6449):819–821
- Mamajek EE (2009) Initial Conditions of Planet Formation: Lifetimes of Primordial Disks. In: Usuda T, Tamura M Ishii M (eds) American Institute of Physics Conference Series, American Institute of Physics Conference Series, vol 1158, pp 3–10, DOI 10.1063/1.3215910
- Mandell AM, Raymond SN Sigurdsson S (2007) Formation of Earth-like Planets During and After Giant Planet Migration. *ApJ*660:823–844
- Marcy GW, Isaacson H, Howard AW et al. (2014) Masses, Radii, and Orbits of Small Kepler Planets: The Transition from Gaseous to Rocky Planets. *ApJS*210:20
- Margot JL, Gladman B Yang T (2024) Quantitative Criteria for Defining Planets. *PSJ*5(7):159
- Martin RG Livio M (2012) On the evolution of the snow line in protoplanetary discs. *MNRAS*425:L6–L9
- Martin RG Livio M (2015) The Solar System as an Exoplanetary System. *ApJ*810:105
- Martins R, Kuthning S, Coles BJ, Kreissig K Rehkämper M (2023) Nucleosynthetic isotope anomalies of zinc in meteorites constrain the origin of Earth's volatiles. *Science* 379(6630):369–372
- Marty B (2012) The origins and concentrations of water, carbon, nitrogen and noble gases on Earth. *Earth and Planetary Science Letters* 313:56–66
- Marty B Yokochi R (2006) Water in the early earth. *Reviews in Mineralogy and Geochemistry* 62(1):421, URL [+http://dx.doi.org/10.2138/rmg.2006.62.18](http://dx.doi.org/10.2138/rmg.2006.62.18)

- Marty B, Avive G, Sano Y et al. (2016) Origins of volatile elements (H, C, N, noble gases) on Earth and Mars in light of recent results from the ROSETTA cometary mission. *Earth and Planetary Science Letters* 441:91–102
- Marty B, Altwegg K, Balsiger H et al. (2017) Xenon isotopes in 67P/Churyumov-Gerasimenko show that comets contributed to Earth's atmosphere. *Science* 356:1069–1072
- Marzari F (2014) Impact of planet-planet scattering on the formation and survival of debris discs. *MNRAS*444:1419–1424
- Masset F Snellgrove M (2001) Reversing type II migration: resonance trapping of a lighter giant protoplanet. *MNRAS*320:L55–L59
- Masset FS, Morbidelli A, Crida A Ferreira J (2006) Disk Surface Density Transitions as Protoplanet Traps. *ApJ*642:478–487
- Matsumura S, Ida S Nagasawa M (2013) Effects of Dynamical Evolution of Giant Planets on Survival of Terrestrial Planets. *ApJ*767:129
- Mayor M, Marmier M, Lovis C et al. (2011a) The HARPS search for southern extra-solar planets XXXIV. Occurrence, mass distribution and orbital properties of super-Earths and Neptune-mass planets. ArXiv e-prints
- Mayor M, Marmier M, Lovis C et al. (2011b) The HARPS search for southern extra-solar planets XXXIV. Occurrence, mass distribution and orbital properties of super-Earths and Neptune-mass planets. arXiv:11092497
- McKee CF Ostriker EC (2007) Theory of Star Formation. *ARA&A*45:565–687
- McNeil DS Nelson RP (2010) On the formation of hot Neptunes and super-Earths. *MNRAS*401:1691–1708
- Meech K Raymond SN (2020) Origin of Earth's Water: Sources and Constraints. In: Meadows VS, Arney GN, Schmidt BE Des Marais DJ (eds) *Planetary Astrobiology*, p 325, DOI 10.2458/azu_uapress_9780816540068
- Melis C, Zuckerman B, Rhee JH et al. (2012) Rapid disappearance of a warm, dusty circumstellar disk. *Nature*487(7405):74–76
- Menon H, Wesolowski L, Zheng G et al. (2015) Adaptive techniques for clustered N-body cosmological simulations. *Computational Astrophysics and Cosmology* 2:1
- Mercer CM, Young KE, Weirich JR et al. (2015) Refining lunar impact chronology through high spatial resolution 40Ar/39Ar dating of impact melts. *Science Advances* 1(1):e1400,050–e1400,050
- Merle RE, Nemchin AA, Grange ML, Whitehouse MJ Pidgeon RT (2014) High resolution U-Pb ages of Ca-phosphates in Apollo 14 breccias: Implications for the age of the Imbrium impact. *Meteoritics and Planetary Science* 49(12):2241–2251
- Michel P Froeschlé C (1997) The Location of Linear Secular Resonances for Semimajor Axes Smaller Than 2 AU. *Icarus*128(1):230–240
- Millholland S, Wang S Laughlin G (2017) Kepler Multi-planet Systems Exhibit Unexpected Intra-system Uniformity in Mass and Radius. *ApJ*849(2):L33
- Mills SM, Fabrycky DC, Migaszewski C et al. (2016) A resonant chain of four transiting, sub-Neptune planets. *Nature*533:509–512
- Minton DA Malhotra R (2010) Dynamical erosion of the asteroid belt and implications for large impacts in the inner Solar System. *Icarus*207:744–757
- Minton DA Malhotra R (2011) Secular Resonance Sweeping of the Main Asteroid Belt During Planet Migration. *ApJ*732:53
- Mizuno H (1980) Formation of the Giant Planets. *Progress of Theoretical Physics* 64:544–557
- Moorhead AV Adams FC (2005) Giant planet migration through the action of disk torques and planet planet scattering. *Icarus* 178:517–539
- Morbidelli A Crida A (2007) The dynamics of Jupiter and Saturn in the gaseous protoplanetary disk. *Icarus*191:158–171
- Morbidelli A Nesvorný D (2012) Dynamics of pebbles in the vicinity of a growing planetary embryo: hydro-dynamical simulations. *A&A*546:A18
- Morbidelli A Raymond SN (2016) Challenges in planet formation. *Journal of Geophysical Research (Planets)* 121:1962–1980

- Morbidelli A, Chambers J, Lunine JI et al. (2000) Source regions and time scales for the delivery of water to Earth. *Meteoritics and Planetary Science* 35:1309–1320
- Morbidelli A, Levison HF, Tsiganis K, Gomes R (2005) Chaotic capture of Jupiter's Trojan asteroids in the early Solar System. *Nature* 435:462–465
- Morbidelli A, Bottke WF, Nesvorný D, Levison HF (2009a) Asteroids were born big. *Icarus* 204:558–573
- Morbidelli A, Brasser R, Tsiganis K, Gomes R, Levison HF (2009b) Constructing the secular architecture of the solar system. I. The giant planets. *A&A* 507:1041–1052
- Morbidelli A, Lunine JI, O'Brien DP, Raymond SN, Walsh KJ (2012) Building Terrestrial Planets. *Annual Review of Earth and Planetary Sciences* 40:251–275
- Morbidelli A, Lambrechts M, Jacobson S, Bitsch B (2015a) The great dichotomy of the Solar System: Small terrestrial embryos and massive giant planet cores. *Icarus* 258:418–429
- Morbidelli A, Lambrechts M, Jacobson S, Bitsch B (2015b) The great dichotomy of the Solar System: Small terrestrial embryos and massive giant planet cores. *Icarus* 258:418–429
- Morbidelli A, Walsh KJ, O'Brien DP, Minton DA, Bottke WF (2015c) The Dynamical Evolution of the Asteroid Belt, pp 493–507. DOI 10.2458/azu_uapress_9780816532131-ch026
- Morbidelli A, Bitsch B, Crida A et al. (2016) Fossilized condensation lines in the Solar System protoplanetary disk. *Icarus* 267:368–376
- Morbidelli A, Nesvorný D, Laurenz V et al. (2018) The timeline of the lunar bombardment: Revisited. *Icarus* 305:262–276
- Morbidelli A, Baillié K, Batygin K et al. (2021) Contemporary formation of early Solar System planetesimals at two distinct radial locations. *Nature Astronomy*
- Morgan JW, Anders E (1980) Chemical Composition of Earth, Venus, and Mercury. *Proceedings of the National Academy of Science* 77(12):6973–6977
- Moriarty J, Fischer D (2015) Building Massive Compact Planetesimal Disks from the Accretion of Pebbles. *ApJ* 809:94
- Moriarty J, Madhusudhan N, Fischer D (2014) Chemistry in an Evolving Protoplanetary Disk: Effects on Terrestrial Planet Composition. *ApJ* 787(1):81
- Morishima R (2015) A particle-based hybrid code for planet formation. *Icarus* 260:368–395
- Morishima R (2017) Onset of oligarchic growth and implication for accretion histories of dwarf planets. *Icarus* 281:459–475
- Morishima R, Schmidt MW, Stadel J, Moore B (2008) Formation and Accretion History of Terrestrial Planets from Runaway Growth through to Late Time: Implications for Orbital Eccentricity. *ApJ* 685:1247–1261
- Morishima R, Stadel J, Moore B (2010) From planetesimals to terrestrial planets: N-body simulations including the effects of nebular gas and giant planets. *Icarus* 207:517–535
- Morris MA, Desch SJ (2010) Thermal Histories of Chondrules in Solar Nebula Shocks. *ApJ* 722:1474–1494
- Mulders GD, Pascucci I, Apai D (2015) An Increase in the Mass of Planetary Systems around Lower-mass Stars. *ApJ* 814:130
- Müller J, Savvidou S, Bitsch B (2021) The water-ice line as a birthplace of planets: implications of a species-dependent dust fragmentation threshold. *A&A* 650:A185
- Nagasawa M, Lin DNC, Thommes E (2005) Dynamical Shake-up of Planetary Systems. I. Embryo Trapping and Induced Collisions by the Sweeping Secular Resonance and Embryo-Disk Tidal Interaction. *ApJ* 635(1):578–598
- Nagasawa M, Ida S, Bessho T (2008) Formation of Hot Planets by a Combination of Planet Scattering, Tidal Circularization, and the Kozai Mechanism. *ApJ* 678:498–508
- Najita JR, Carr JS, Glassgold AE, Valenti JA (2007) Gaseous Inner Disks. *Protostars and Planets V* pp 507–522
- Nakagawa Y, Sekiya M, Hayashi C (1986) Settling and growth of dust particles in a laminar phase of a low-mass solar nebula. *Icarus* 67:375–390
- Natta A, Testi L, Calvet N et al. (2007) Dust in Protoplanetary Disks: Properties and Evolution. *Protostars and Planets V* pp 767–781

- Nelson RP, Gressel O Umurhan OM (2013) Linear and non-linear evolution of the vertical shear instability in accretion discs. *MNRAS*435:2610–2632
- Nesvorný D (2011) Young Solar System's Fifth Giant Planet? *ApJ*742:L22
- Nesvorný D (2015a) Evidence for Slow Migration of Neptune from the Inclination Distribution of Kuiper Belt Objects. *AJ*150:73
- Nesvorný D (2015b) Jumping Neptune Can Explain the Kuiper Belt Kernel. *AJ*150:68
- Nesvorný D (2021) Eccentric Early Migration of Neptune. *ApJ*908(2):L47
- Nesvorný D Morbidelli A (2012) Statistical Study of the Early Solar System's Instability with Four, Five, and Six Giant Planets. *AJ*144:117
- Nesvorný D Vokrouhlický D (2016) Neptune's Orbital Migration Was Grainy, Not Smooth. *ApJ*825(2):94
- Nesvorný D, Vokrouhlický D Morbidelli A (2007) Capture of Irregular Satellites during Planetary Encounters. *AJ*133(5):1962–1976
- Nesvorný D, Vokrouhlický D Morbidelli A (2013) Capture of Trojans by Jumping Jupiter. *ApJ*768:45
- Nesvorný D, Vokrouhlický D Deienno R (2014) Capture of Irregular Satellites at Jupiter. *ApJ*784(1):22
- Nesvorný D, Vokrouhlický D, Bottke WF Levison HF (2018) Evidence for very early migration of the Solar System planets from the Patroclus-Menoetius binary Jupiter Trojan. *Nature Astronomy* 2:878–882
- Nesvorný D, Roig FV Deienno R (2021) The Role of Early Giant-planet Instability in Terrestrial Planet Formation. *AJ*161(2):50
- Nesvorný D, Roig FV, Vokrouhlický D et al. (2023) Early bombardment of the moon: Connecting the lunar crater record to the terrestrial planet formation. *Icarus*399:115545
- Nimmo F Kleine T (2007) How rapidly did Mars accrete? Uncertainties in the Hf W timing of core formation. *Icarus*191:497–504
- Nomura H, Tsukagoshi T, Kawabe R et al. (2016) ALMA Observations of a Gap and a Ring in the Protoplanetary Disk around TW Hya. *ApJ*819:L7
- Nomura R, Hirose K, Uesugi K et al. (2014) Low Core-Mantle Boundary Temperature Inferred from the Solidus of Pyrolyte. *Science* 343:522–525
- Norman MD, Duncan RA Huard JJ (2006) Identifying impact events within the lunar cataclysm from ^{40}Ar - ^{39}Ar ages and compositions of Apollo 16 impact melt rocks. *Geochim Cosmochim Acta*70(24):6032–6049
- Öberg KI, Guzmán VV, Walsh C et al. (2021) Molecules with ALMA at Planet-forming Scales (MAPS). I. Program Overview and Highlights. *ApJS*257(1):1
- O'Brien DP Sykes MV (2011) The Origin and Evolution of the Asteroid Belt Implications for Vesta and Ceres. *Space Sci Rev*163:41–61
- O'Brien DP, Morbidelli A Levison HF (2006) Terrestrial planet formation with strong dynamical friction. *Icarus*184:39–58
- O'Brien DP, Walsh KJ, Morbidelli A, Raymond SN Mandell AM (2014) Water delivery and giant impacts in the 'Grand Tack' scenario. *Icarus*239:74–84
- O'Brien DP, Izidoro A, Jacobson SA, Raymond SN Rubie DC (2018) The Delivery of Water During Terrestrial Planet Formation. *ArXiv e-prints*
- O'dell CR Wen Z (1994) Postrefurbishment mission Hubble Space Telescope images of the core of the Orion Nebula: Proplyds, Herbig-Haro objects, and measurements of a circumstellar disk. *ApJ*436:194–202
- Ogihara M Ida S (2009) N-Body Simulations of Planetary Accretion Around M Dwarf Stars. *ApJ*699:824–838
- Ogihara M, Morbidelli A Guillot T (2015) A reassessment of the in situ formation of close-in super-Earths. *A&A*578:A36
- Ogihara M, Genda H Sekine Y (2023) Early Water Delivery to Terrestrial Planet Regions during the Stages of Jupiter's Formation and Migration in the Grand Tack Model. *PSJ*4(2):32
- Okuzumi S (2009) Electric Charging of Dust Aggregates and its Effect on Dust Coagulation in Protoplanetary Disks. *ApJ*698:1122–1135

- Ormel CW Cuzzi JN (2007) Closed-form expressions for particle relative velocities induced by turbulence. *A&A*466(2):413–420
- Ormel CW Klahr HH (2010) The effect of gas drag on the growth of protoplanets. Analytical expressions for the accretion of small bodies in laminar disks. *A&A*520:A43
- Ormel CW, Spaans M Tielens AGGM (2007) Dust coagulation in protoplanetary disks: porosity matters. *A&A*461:215–232
- Ormel CW, Dullemond CP Spaans M (2010a) A New Condition for the Transition from Runaway to Oligarchic Growth. *ApJ*714:L103–L107
- Ormel CW, Dullemond CP Spaans M (2010b) Accretion among preplanetary bodies: The many faces of runaway growth. *Icarus*210:507–538
- Owen JE Wu Y (2013) Kepler Planets: A Tale of Evaporation. *ApJ*775:105
- Owen JE Wu Y (2017) The Evaporation Valley in the Kepler Planets. *ApJ*847:29
- Owen T, Maillard JP, de Bergh C Lutz BL (1988) Deuterium on Mars - The abundance of HDO and the value of D/H. *Science* 240:1767–1770
- Ozawa S, Takahashi S, Fukuyama H Watanabe M (2011) Temperature dependence of surface tension of molten iron under reducing gas atmosphere. *Journal of Physics: Conference Series* 327(1):012,020, URL <https://dx.doi.org/10.1088/1742-6596/327/1/012020>
- Paardekooper SJ Mellema G (2006) Halting type I planet migration in non-isothermal disks. *A&A*459:L17–L20
- Paardekooper SJ, Baruteau C Kley W (2011) A torque formula for non-isothermal Type I planetary migration - II. Effects of diffusion. *MNRAS*410:293–303
- Papaloizou JCB Larwood JD (2000) On the orbital evolution and growth of protoplanets embedded in a gaseous disc. *MNRAS*315:823–833
- Papaloizou JCB Lin DNC (1995) Theory Of Accretion Disks I: Angular Momentum Transport Processes. *ARA&A*33:505–540
- Peterson LD, Newcombe ME, Alexander CMO et al. (2023) The H₂O content of the ureilite parent body. *Geochim Cosmochim Acta*340:141–157
- Petigura EA, Howard AW Marcy GW (2013a) Prevalence of Earth-size planets orbiting Sun-like stars. *Proceedings of the National Academy of Science* 110:19,273–19,278
- Petigura EA, Howard AW Marcy GW (2013b) Prevalence of Earth-size planets orbiting Sun-like stars. *Proceedings of the National Academy of Science* 110:19,273–19,278
- Petigura EA, Marcy GW, Winn JN et al. (2018) The California-Kepler Survey. IV. Metal-rich Stars Host a Greater Diversity of Planets. *AJ*155(2):89
- Petit JM, Morbidelli A Chambers J (2001) The Primordial Excitation and Clearing of the Asteroid Belt. *Icarus*153:338–347
- Petit JM, Chambers J, Franklin F Nagasawa M (2002) Primordial Excitation and Depletion of the Main Belt, pp 711–723
- Piani L, Marrocchi Y, Rigaudier T et al. (2020) Earth's water may have been inherited from material similar to enstatite chondrite meteorites. *Science* 369(6507):1110–1113
- Pierens A Nelson RP (2008) On the formation and migration of giant planets in circumbinary discs. *A&A*483:633–642
- Pierens A Raymond SN (2011) Two phase, inward-then-outward migration of Jupiter and Saturn in the gaseous solar nebula. *A&A*533:A131
- Pierens A, Raymond SN, Nesvorný D Morbidelli A (2014) Outward Migration of Jupiter and Saturn in 3:2 or 2:1 Resonance in Radiative Disks: Implications for the Grand Tack and Nice models. *ApJ*795:L11
- Piétu V, Dutrey A Guilloteau S (2007) Probing the structure of protoplanetary disks: a comparative study of DM Tau, LkCa 15, and MWC 480. *A&A*467(1):163–178
- Pignatale FC, Liffman K, Maddison ST Brooks G (2016) 2D condensation model for the inner Solar Nebula: an enstatite-rich environment. *MNRAS*457(2):1359–1370
- Pinilla P, Lenz CT Stammer SM (2021) Growing and trapping pebbles with fragile collisions of particles in protoplanetary disks. *A&A*645:A70

- Pollack JB, Hubickyj O, Bodenheimer P et al. (1996) Formation of the Giant Planets by Concurrent Accretion of Solids and Gas. *Icarus*124:62–85
- Poppe T, Blum J Henning T (2000) Experiments on Collisional Grain Charging of Micron-sized Preplanetary Dust. *ApJ*533:472–480
- Qi C, D’Alessio P, Öberg KI et al. (2011) Resolving the CO Snow Line in the Disk around HD 163296. *ApJ*740(2):84
- Quarles B Kaib N (2019) Instabilities in the Early Solar System Due to a Self-gravitating Disk. *AJ*157:67
- Raettig N, Lyra W Klahr H (2013) A Parameter Study for Baroclinic Vortex Amplification. *ApJ*765:115
- Rafikov RR (2003a) Planetesimal Disk Evolution Driven by Embryo-Planetesimal Gravitational Scattering. *AJ*125:922–941
- Rafikov RR (2003b) Planetesimal Disk Evolution Driven by Planetesimal-Planetesimal Gravitational Scattering. *AJ*125:906–921
- Rafikov RR (2003c) The Growth of Planetary Embryos: Orderly, Runaway, or Oligarchic? *AJ*125:942–961
- Rasio FA Ford EB (1996) Dynamical instabilities and the formation of extrasolar planetary systems. *Science* 274:954–956
- Raymond SN Cossou C (2014) No universal minimum-mass extrasolar nebula: evidence against in situ accretion of systems of hot super-Earths. *MNRAS*440:L11–L15
- Raymond SN Izidoro A (2017a) Origin of water in the inner Solar System: Planetesimals scattered inward during Jupiter and Saturn’s rapid gas accretion. *Icarus*297:134–148
- Raymond SN Izidoro A (2017b) The empty primordial asteroid belt. *Science Advances* 3:e1701.138
- Raymond SN Morbidelli A (2014) The Grand Tack model: a critical review. In: *Complex Planetary Systems, Proceedings of the International Astronomical Union, IAU Symposium, vol 310*, pp 194–203, DOI 10.1017/S1743921314008254
- Raymond SN, Quinn T Lunine JI (2004) Making other earths: dynamical simulations of terrestrial planet formation and water delivery. *Icarus*168:1–17
- Raymond SN, Quinn T Lunine JI (2005) Terrestrial Planet Formation in Disks with Varying Surface Density Profiles. *ApJ*632:670–676
- Raymond SN, Mandell AM Sigurdsson S (2006a) Exotic Earths: Forming Habitable Worlds with Giant Planet Migration. *Science* 313:1413–1416
- Raymond SN, Quinn T Lunine JI (2006b) High-resolution simulations of the final assembly of Earth-like planets I. Terrestrial accretion and dynamics. *Icarus*183:265–282
- Raymond SN, Quinn T Lunine JI (2007a) High-Resolution Simulations of The Final Assembly of Earth-Like Planets. 2. Water Delivery And Planetary Habitability. *Astrobiology* 7:66–84
- Raymond SN, Scalo J Meadows VS (2007b) A Decreased Probability of Habitable Planet Formation around Low-Mass Stars. *ApJ*669:606–614
- Raymond SN, Barnes R Mandell AM (2008) Observable consequences of planet formation models in systems with close-in terrestrial planets. *MNRAS*384:663–674
- Raymond SN, O’Brien DP, Morbidelli A Kaib NA (2009) Building the terrestrial planets: Constrained accretion in the inner Solar System. *Icarus*203:644–662
- Raymond SN, Armitage PJ Gorelick N (2010a) Planet-Planet Scattering in Planetesimal Disks. II. Predictions for Outer Extrasolar Planetary Systems. *ApJ*711:772–795
- Raymond SN, Armitage PJ Gorelick N (2010b) Planet-Planet Scattering in Planetesimal Disks. II. Predictions for Outer Extrasolar Planetary Systems. *ApJ*711:772–795
- Raymond SN, Armitage PJ, Moro-Martín A et al. (2011) Debris disks as signposts of terrestrial planet formation. *A&A*530:A62
- Raymond SN, Armitage PJ, Moro-Martín A et al. (2012) Debris disks as signposts of terrestrial planet formation. II. Dependence of exoplanet architectures on giant planet and disk properties. *A&A*541:A11
- Raymond SN, Kokubo E, Morbidelli A, Morishima R Walsh KJ (2014) Terrestrial Planet Formation at Home and Abroad. *Protostars and Planets VI* pp 595–618

- Raymond SN, Izidoro A, Bitsch B, Jacobson SA (2016a) Did Jupiter's core form in the innermost parts of the Sun's protoplanetary disc? *MNRAS*458(3):2962–2972
- Raymond SN, Izidoro A, Bitsch B, Jacobson SA (2016b) Did Jupiter's core form in the innermost parts of the Sun's protoplanetary disc? *MNRAS*458:2962–2972
- Raymond SN, Armitage PJ, Veras D, Quintana EV, Barclay T (2017) Implications of the interstellar object 1I/Oumuamua for planetary dynamics and planetesimal formation. *ArXiv e-prints*
- Raymond SN, Izidoro A, Morbidelli A (2020) Solar System Formation in the Context of Extrasolar Planets. In: Meadows VS, Arney GN, Schmidt BE, Des Marais DJ (eds) *Planetary Astrobiology*, p 287, DOI 10.2458/azu_uapress.9780816540068
- Rein H, Spiegel DS (2015) IAS15: a fast, adaptive, high-order integrator for gravitational dynamics, accurate to machine precision over a billion orbits. *MNRAS*446:1424–1437
- Rein H, Tamayo D (2015) WHFAST: a fast and unbiased implementation of a symplectic Wisdom-Holman integrator for long-term gravitational simulations. *MNRAS*452:376–388
- Rein H, Brown G, Tamayo D (2019) On the accuracy of symplectic integrators for secularly evolving planetary systems. *MNRAS*490(4):5122–5133
- Ribeiro RdS, Morbidelli A, Raymond SN et al. (2020) Dynamical evidence for an early giant planet instability. *Icarus*339:113605
- Ricci L, Testi L, Natta A et al. (2010) Dust properties of protoplanetary disks in the Taurus-Auriga star forming region from millimeter wavelengths. *A&A*512:A15
- Richardson DC, Quinn T, Stadel J, Lake G (2000) Direct Large-Scale N-Body Simulations of Planetsimal Dynamics. *Icarus*143:45–59
- Ricker GR, Winn JN, Vanderspek R et al. (2015) Transiting Exoplanet Survey Satellite (TESS). *Journal of Astronomical Telescopes, Instruments, and Systems* 1:014003
- Rodmann J, Henning T, Chandler CJ, Mundy LG, Wilner DJ (2006) Large dust particles in disks around T Tauri stars. *A&A*446:211–221
- Rodríguez Martínez R, Gaudi BS, Schulze JG et al. (2023) A Reanalysis of the Composition of K2-106b: An Ultra-short-period Super-Mercury Candidate. *AJ*165(3):97
- Rogers LA (2015) Most 1.6 Earth-radius Planets are Not Rocky. *ApJ*801:41
- Roig F, Nesvorný D (2015) The Evolution of Asteroids in the Jumping-Jupiter Migration Model. *AJ*150:186
- Roig F, Nesvorný D, DeSouza SR (2016) Jumping Jupiter Can Explain Mercury's Orbit. *ApJ*820:L30
- Romanova MM, Ustyugova GV, Koldoba AV, Wick JV, Lovelace RVE (2003) Three-dimensional Simulations of Disk Accretion to an Inclined Dipole. I. Magnetospheric Flows at Different Θ . *ApJ*595:1009–1031
- Romanova MM, Ustyugova GV, Koldoba AV, Lovelace RVE (2004) Three-dimensional Simulations of Disk Accretion to an Inclined Dipole. II. Hot Spots and Variability. *ApJ*610:920–932
- Rowan D, Meschiari S, Laughlin G et al. (2016) The Lick-Carnegie Exoplanet Survey: HD 32963 — A New Jupiter Analog Orbiting a Sun-like Star. *ApJ*817:104
- Rubie DC, Jacobson SA, Morbidelli A et al. (2015) Accretion and differentiation of the terrestrial planets with implications for the compositions of early-formed Solar System bodies and accretion of water. *Icarus*248:89–108
- Rubie DC, Laurenz V, Jacobson SA et al. (2016) Highly siderophile elements were stripped from Earth's mantle by iron sulfide segregation. *Science* 353(6304):1141–1144
- Rudge JF, Kleine T, Bourdon B (2010) Broad bounds on Earth's accretion and core formation constrained by geochemical models. *Nature Geoscience* 3(6):439–443
- Safronov VS (1972) Evolution of the protoplanetary cloud and formation of the earth and planets.
- Saha P, Tremaine S (1994) Long-term planetary integration with individual time steps. *AJ*108:1962–1969
- Sato T, Okuzumi S, Ida S (2016) On the water delivery to terrestrial embryos by ice pebble accretion. *A&A*589:A15
- Savage PS, Moynier F, Boyet M (2022) Zinc isotope anomalies in primitive meteorites identify the outer solar system as an important source of Earth's volatile inventory. *Icarus*386:115172

- Schäfer U, Yang CC, Johansen A (2017) Initial mass function of planetesimals formed by the streaming instability. *A&A*597:A69
- Schlaufman KC (2014) Tests of in situ Formation Scenarios for Compact Multiplanet Systems. *ApJ*790:91
- Schlichting HE (2014) Formation of Close in Super-Earths and Mini-Neptunes: Required Disk Masses and their Implications. *ApJ*795:L15
- Schlichting HE, Sari R (2011) Runaway Growth During Planet Formation: Explaining the Size Distribution of Large Kuiper Belt Objects. *ApJ*728:68
- Schlichting HE, Fuentes CI, Trilling DE (2013) Initial Planetesimal Sizes and the Size Distribution of Small Kuiper Belt Objects. *AJ*146:36
- Schneider G, Smith BA, Becklin EE et al. (1999) NICMOS Imaging of the HR 4796A Circumstellar Disk. *ApJ*513:L127–L130
- Schräpler RR, Landeck WA, Blum J (2022) Collisional properties of cm-sized high-porosity ice and dust aggregates and their applications to early planet formation. *MNRAS*509(4):5641–5656
- Scott ERD (2007) Chondrites and the Protoplanetary Disk. *Annual Review of Earth and Planetary Sciences* 35:577–620
- Scott ERD, Krot AN (2014) Chondrites and Their Components, pp 65–137
- Scott ERD, Taylor GJ (1983) Chondrules and other components in C, O, and E chondrites: similarities in their properties and origins. *J Geophys Res*88:B275–B286
- Selsis F, Chazelas B, Bordé P et al. (2007) Could we identify hot ocean-planets with CoRoT, Kepler and Doppler velocimetry? *Icarus* 191:453–468
- Shu FH, Adams FC, Lizano S (1987) Star formation in molecular clouds - Observation and theory. *ARA&A*25:23–81
- Shu FH, Shang H, Gounelle M, Glassgold AE, Lee T (2001) The Origin of Chondrules and Refractory Inclusions in Chondritic Meteorites. *ApJ*548:1029–1050
- Simon JB, Armitage PJ, Li R, Youdin AN (2016) The Mass and Size Distribution of Planetesimals Formed by the Streaming Instability. I. The Role of Self-gravity. *ApJ*822:55
- Sirono Si (2011) Planetesimal Formation Induced by Sintering. *ApJ*733:L41
- Smith BA, Terrile RJ (1984) A circumstellar disk around Beta Pictoris. *Science* 226:1421–1424
- Spalding C, Adams FC (2020) The Solar Wind Prevents Reaccretion of Debris after Mercury's Giant Impact. *The Planetary Science Journal* 1(1):7
- Spaute D, Weidenschilling SJ, Davis DR, Marzari F (1991) Accretional evolution of a planetesimal swarm. I - A new simulation. *Icarus*92:147–164
- Spitzer F, Burkhardt C, Nimmo F, Kleine T (2021) Nucleosynthetic Pt isotope anomalies and the Hf-W chronology of core formation in inner and outer solar system planetesimals. *Earth and Planetary Science Letters* 576:117211
- Spitzer F, Burkhardt C, Pape J, Kleine T (2022) Collisional mixing between inner and outer solar system planetesimals inferred from the Nedagolla iron meteorite. *MaPS*57(2):261–276
- Spudis PD, Wilhelms DE, Robinson MS (2011) The Sculptured Hills of the Taurus Highlands: Implications for the relative age of Serenitatis, basin chronologies and the cratering history of the Moon. *Journal of Geophysical Research (Planets)* 116:E00H03
- Squire J, Hopkins PF (2017) Resonant Drag Instabilities in protoplanetary disks: the streaming instability and new, faster-growing instabilities. *ArXiv e-prints*
- Stadel JG (2001) Cosmological N-body simulations and their analysis. PhD thesis, University of Washington, Seattle
- Steffen JH, Ragozzine D, Fabrycky DC et al. (2012) Kepler constraints on planets near hot Jupiters. *Proceedings of the National Academy of Science* 109:7982–7987
- Steller T, Burkhardt C, Yang C, Kleine T (2022) Nucleosynthetic zinc isotope anomalies reveal a dual origin of terrestrial volatiles. *Icarus*386:115171
- Stoll MHR, Kley W (2016) Particle dynamics in discs with turbulence generated by the vertical shear instability. *A&A*594:A57
- Takeuchi T, Artymowicz P (2001) Dust Migration and Morphology in Optically Thin Circumstellar Gas Disks. *ApJ*557:990–1006

- Tamayo D, Rein H, Shi P, Hernandez DM (2020) REBOUNDx: a library for adding conservative and dissipative forces to otherwise symplectic N-body integrations. *MNRAS*491(2):2885–2901
- Tanaka H, Ida S (1997) Distribution of Planetesimals around a Protoplanet in the Nebula Gas. *Icarus*125:302–316
- Tanaka H, Ida S (1999) Growth of a Migrating Protoplanet. *Icarus* 139:350–366
- Tanaka H, Ward WR (2004) Three-dimensional Interaction between a Planet and an Isothermal Gaseous Disk. II. Eccentricity Waves and Bending Waves. *ApJ*602:388–395
- Tanaka H, Takeuchi T, Ward WR (2002) Three-Dimensional Interaction between a Planet and an Isothermal Gaseous Disk. I. Corotation and Lindblad Torques and Planet Migration. *ApJ*565:1257–1274
- Tang H, Dauphas N (2014) ^{60}Fe - ^{60}Ni chronology of core formation in Mars. *Earth and Planetary Science Letters* 390:264–274
- Tazaki R, Tanaka H, Kataoka A, Okuzumi S, Muto T (2019) Unveiling Dust Aggregate Structure in Protoplanetary Disks by Millimeter-wave Scattering Polarization. *ApJ*885(1):52
- Tera F, Papanastassiou DA, Wasserburg GJ (1974) Isotopic evidence for a terminal lunar cataclysm. *Earth and Planetary Science Letters* 22(1):1–21
- Terquem C, Papaloizou JCB (2007) Migration and the Formation of Systems of Hot Super-Earths and Neptunes. *ApJ*654:1110–1120
- Testi L, Natta A, Shepherd DS, Wilner DJ (2003) Large grains in the disk of CQ Tau. *A&A*403:323–328
- Testi L, Birnstiel T, Ricci L et al. (2014) Dust Evolution in Protoplanetary Disks. *Protostars and Planets VI* pp 339–361
- Thommes E, Nagasawa M, Lin DNC (2008) Dynamical Shake-up of Planetary Systems. II. N-Body Simulations of Solar System Terrestrial Planet Formation Induced by Secular Resonance Sweeping. *ApJ*676:728–739
- Thommes EW, Duncan MJ, Levison HF (2003) Oligarchic growth of giant planets. *Icarus*161:431–455
- Toliou A, Morbidelli A, Tsiganis K (2016) Magnitude and timing of the giant planet instability: A reassessment from the perspective of the asteroid belt. *A&A*592:A72
- Touboul M, Kleine T, Bourdon B, Palme H, Wieler R (2007) Late formation and prolonged differentiation of the Moon inferred from W isotopes in lunar metals. *Nature*450:1206–1209
- Tremaine S, Dong S (2012) The Statistics of Multi-planet Systems. *AJ*143:94
- Tsiganis K, Gomes R, Morbidelli A, Levison HF (2005) Origin of the orbital architecture of the giant planets of the Solar System. *Nature*435:459–461
- Udry S, Santos NC (2007a) Statistical Properties of Exoplanets. *ARA&A*45:397–439
- Udry S, Santos NC (2007b) Statistical Properties of Exoplanets. *ARA&A*45:397–439
- Umurhan OM, Nelson RP, Gressel O (2016) Linear analysis of the vertical shear instability: outstanding issues and improved solutions. *A&A*586:A33
- van der Marel N, van Dishoeck EF, Bruderer S et al. (2013) A Major Asymmetric Dust Trap in a Transition Disk. *Science* 340:1199–1202
- Veras D, Armitage PJ (2005) The Influence of Massive Planet Scattering on Nascent Terrestrial Planets. *ApJ*620:L111–L114
- Veras D, Armitage PJ (2006) Predictions for the Correlation between Giant and Terrestrial Extrasolar Planets in Dynamically Evolved Systems. *ApJ*645:1509–1515
- Volk K, Gladman B (2015) Consolidating and Crushing Exoplanets: Did It Happen Here? *ApJ*806:L26
- Wada K, Tanaka H, Suyama T, Kimura H, Yamamoto T (2009) Collisional Growth Conditions for Dust Aggregates. *ApJ*702:1490–1501
- Wakita S, Matsumoto Y, Oshino S, Hasegawa Y (2017) Planetesimal Collisions as a Chondrule Forming Event. *ApJ*834:125
- Wallace SC, Quinn TR (2019) N-body simulations of terrestrial planet growth with resonant dynamical friction. *MNRAS* 2217
- Wallace SC, Quinn TR, Boley AC (2021) Collision rates of planetesimals near mean-motion resonances. *MNRAS*503(4):5409–5424

- Walsh KJ Levison HF (2016) Terrestrial Planet Formation from an Annulus. *AJ*152:68
- Walsh KJ Levison HF (2019) Planetesimals to terrestrial planets: Collisional evolution amidst a dissipating gas disk. *Icarus*329:88–100
- Walsh KJ Morbidelli A (2011) The effect of an early planetesimal-driven migration of the giant planets on terrestrial planet formation. *A&A*526:A126
- Walsh KJ, Morbidelli A, Raymond SN, O’Brien DP Mandell AM (2011) A low mass for Mars from Jupiter’s early gas-driven migration. *Nature*475:206–209
- Walsh KJ, Morbidelli A, Raymond SN, O’Brien DP Mandell AM (2012) Populating the asteroid belt from two parent source regions due to the migration of giant planets –“The Grand Tack”. *Meteoritics and Planetary Science* 47:1941–1947
- Ward WR (1986) Density waves in the solar nebula - Differential Lindblad torque. *Icarus* 67:164–180
- Ward WR (1997) Protoplanet Migration by Nebula Tides. *Icarus* 126:261–281
- Weidenschilling SJ (1977) The distribution of mass in the planetary system and solar nebula. *Ap&SS*51:153–158
- Weidenschilling SJ (1980) Dust to planetesimals - Settling and coagulation in the solar nebula. *Icarus*44:172–189
- Weidenschilling SJ Marzari F (1996) Gravitational scattering as a possible origin for giant planets at small stellar distances. *Nature*384:619–621
- Weidenschilling SJ, Spaute D, Davis DR, Marzari F Ohtsuki K (1997) Accretional Evolution of a Planetesimal Swarm. *Icarus*128:429–455
- Weider SZ, Nittler LR, Starr RD et al. (2015) Evidence for geochemical terranes on Mercury: Global mapping of major elements with MESSENGER’s X-Ray Spectrometer. *Earth and Planetary Science Letters* 416:109–120
- Weiss LM Marcy GW (2014) The Mass-Radius Relation for 65 Exoplanets Smaller than 4 Earth Radii. *ApJ*783:L6
- Weiss LM, Marcy GW, Rowe JF et al. (2013) The Mass of KOI-94d and a Relation for Planet Radius, Mass, and Incident Flux. *ApJ*768:14
- Weiss LM, Marcy GW, Petigura EA et al. (2018) The California-Kepler Survey. V. Peas in a Pod: Planets in a Kepler Multi-planet System Are Similar in Size and Regularly Spaced. *AJ*155:48
- Wetherill GW (1978) Accumulation of the terrestrial planets. In: Gehrels T (ed) *IAU Colloq. 52: Protostars and Planets*, pp 565–598
- Wetherill GW (1986) Accumulation of the terrestrial planets and implications concerning lunar origin. In: Hartmann WK, Phillips RJ Taylor GJ (eds) *Origin of the Moon*, pp 519–550
- Wetherill GW (1990) Formation of the earth. *Annual Review of Earth and Planetary Sciences* 18:205–256
- Wetherill GW (1996) The Formation and Habitability of Extra-Solar Planets. *Icarus*119:219–238
- Wetherill GW Stewart GR (1989) Accumulation of a swarm of small planetesimals. *Icarus*77:330–357
- Whipple FL (1972) On certain aerodynamic processes for asteroids and comets. In: Elvius A (ed) *From Plasma to Planet*, p 211
- Williams JP Cieza LA (2011) Protoplanetary Disks and Their Evolution. *ARA&A*49:67–117
- Wilner DJ, D’Alessio P, Calvet N, Claussen MJ Hartmann L (2005) Toward Planetesimals in the Disk around TW Hydrae: 3.5 Centimeter Dust Emission. *ApJ*626:L109–L112
- Wisdom J Holman M (1991) Symplectic maps for the n-body problem. *AJ*102:1528–1538
- Wittenmyer RA, Butler RP, Tinney CG et al. (2016) The Anglo-Australian Planet Search XXIV: The Frequency of Jupiter Analogs. *ApJ*819:28
- Wolfgang A, Rogers LA Ford EB (2016) Probabilistic Mass-Radius Relationship for Sub-Neptune-Sized Planets. *ApJ*825:19
- Woo JMY, Grimm S, Brasser R Stadel J (2021a) Growing Mars fast: High-resolution GPU simulations of embryo formation. *Icarus*359:114305
- Woo JMY, Stadel J, Grimm S Brasser R (2021b) Mars’ Formation Can Constrain the Primordial Orbits of the Gas Giants. *ApJ*910(2):L16

- Woo JMY, Brasser R, Grimm SL, Timpe ML, Stadel J (2022) The terrestrial planet formation paradox inferred from high-resolution N-body simulations. *Icarus* 371:114692
- Wright JT, Marcy GW, Howard AW et al. (2012) The Frequency of Hot Jupiters Orbiting nearby Solar-type Stars. *ApJ* 753:160
- Wurm G, Trialet M, Rauer H (2013) Photophoretic Separation of Metals and Silicates: The Formation of Mercury-like Planets and Metal Depletion in Chondrites. *ApJ* 769(1):78
- Xu Z, Bai XN, Murray-Clay RA (2017) Pebble Accretion in Turbulent Protoplanetary Disks. *ApJ* 847:52
- Yang CC, Zhu Z (2021) Streaming instability with multiple dust species - II. Turbulence and dust-gas dynamics at non-linear saturation. *MNRAS* 508(4):5538–5553
- Yang CC, Johansen A, Carrera D (2017) Concentrating small particles in protoplanetary disks through the streaming instability. *A&A* 606:A80
- Yin Q, Jacobsen SB, Yamashita K et al. (2002) A short timescale for terrestrial planet formation from Hf-W chronometry of meteorites. *Nature* 418:949–952
- Youdin AN, Goodman J (2005) Streaming Instabilities in Protoplanetary Disks. *ApJ* 620:459–469
- Youdin AN, Shu FH (2002) Planetesimal Formation by Gravitational Instability. *ApJ* 580:494–505
- Yurimoto H, Abe M, Abe M et al. (2011) Oxygen Isotopic Compositions of Asteroidal Materials Returned from Itokawa by the Hayabusa Mission. *Science* 333(6046):1116
- Zhang H, Zhou JL (2010) On the Orbital Evolution of a Giant Planet Pair Embedded in a Gaseous Disk. I. Jupiter-Saturn Configuration. *ApJ* 714:532–548
- Zhang Z, Bercovici D, Jordan JS (2021) A Two Phase Model for the Evolution of Planetary Embryos With Implications for the Formation of Mars. *Journal of Geophysical Research (Planets)* 126(4):e06754
- Zhu W, Petrovich C, Wu Y, Dong S, Xie J (2018) About 30% of Sun-like Stars Have Kepler-like Planetary Systems: A Study of Their Intrinsic Architecture. *ApJ* 860(2):101
- Zsom A, Ormel CW, Güttler C, Blum J, Dullemond CP (2010) The outcome of protoplanetary dust growth: pebbles, boulders, or planetesimals? II. Introducing the bouncing barrier. *A&A* 513:A57
- Zube NG, Nimmo F, Fischer RA, Jacobson SA (2019) Constraints on terrestrial planet formation timescales and equilibration processes in the Grand Tack scenario from Hf-W isotopic evolution. *Earth and Planetary Science Letters* 522:210–218